

**A NUMERICAL STUDY ON THE BEHAVIOUR OF
REINFORCED CONCRETE SLAB STRENGTHENED WITH
FRP LAMINATES USING FINITE ELEMENT APPROACH**

A THESIS SUBMITTED

IN PARTIAL FULFILLMENT OF THE REQUIREMENTS FOR THE DEGREE OF
MASTER OF ENGINEERING IN CIVIL ENGINEERING
(SPECIALIZATION: STRUCTURAL ENGINEERING)

BY

FALGUNI SHIT

CLASS ROLL NO: 001410402015

EXAMINATION ROLL NO: M4CIV1606

REGISTRATION NO: 128866 of 2014-15

UNDER THE GUIDANCE OF

DR. SUBHASHISH ROY CHOWDHURY

AT THE

DEPARTMENT OF CIVIL ENGINEERING

FACULTY OF ENGINEERING AND TECHNOLOGY

JADAVPUR UNIVERSITY

KOLKATA – 700 032

INDIA

MAY, 2016

CERTIFICATE OF RECOMMENDATION

This is to certify that **Falguni Shit** (Class Roll No. - 001410402015, Examination Roll No. - M4CIV1606 Registration No. - 128866 of 2014-15) has carried out the thesis work entitled, **“A NUMERICAL STUDY ON THE BEHAVIOUR OF REINFORCED CONCRETE SLAB STRENGTHENED WITH FRP LAMINATES USING FINITE ELEMENT APPROACH”**, under my direct supervision & guidance. He carried out this work independently. I hereby recommend that the thesis be accepted in partial fulfillment of the requirements for awarding the degree of **“MASTER OF ENGINEERING IN CIVIL ENGINEERING (SPECIALIZATION: STRUCTURAL ENGINEERING)”**

.....
DR. SUBHASHISH ROY CHOWDHURY

Asst. Professor
Department of Civil Engineering
Jadavpur University
Kolkata-700 032

Date:.....

Countersigned by....

.....
Prof.Dr. Sivaji Bandyopadhyay

Dean
Faculty of Engineering and Technology
Jadavpur University
Kolkata-700 032

Date:.....

.....
Prof.Dr. R.B. Sahu

Head of the Department
Department of Civil Engineering
Jadavpur University
Kolkata-700032

Date:.....

CERTIFICATE OF APPROVAL

This foregoing thesis entitled “**A numerical study on the behaviour of reinforced concrete slab strengthened with FRP laminates using finite element approach**” submitted by **Falguni Shit** is hereby approved as credible study on an Engineering subject carried out and presented in a manner satisfactory to warrant its acceptance as a prerequisite to the degree of **Master of engineering in Civil Engineering (Specialization: Structural Engineering)** for which it has been submitted. It is understood that by this approval the undersigned do not necessarily endorse or approve any statement made, opinion expressed or conclusion drawn therein, but approve the thesis only for the purpose for which it is submitted.

Committee on final examination for evaluation of the thesis.

.....

.....

.....

(Signature of the Examiners)

DECLARATION

I, Falguni Shit, a student of Master of Engineering in Civil Engineering (Structural Engineering), Jadavpur University, Faculty of Engineering & Technology, hereby declare that the work being presented in the thesis work entitled, “**A numerical study on the behaviour of reinforced concrete slab strengthened with FRP laminates using finite element approach**”, is authentic record of work that has been carried out at the Department of Civil Engineering, Jadavpur University, under the guidance of Dr. Subhashish Roy Chowdhury, Asst. Professor, Department of Civil Engineering, Jadavpur University.

The work contained in the thesis has not yet been submitted in part or full to any other university or institution or professional body for award of any degree or diploma or any fellowship.

Date:.....

Place: Jadavpur University, Kolkata

.....
(FALGUNI SHIT)
Class Roll no.-001410402015
Registration no. - 128866 of 2014-2015
Exam Roll no.:- M4CIV1606
Jadavpur University

ACKNOWLEDGEMENTS

I would like to express my sincere gratitude and thanks to my guide, Dr Subhashish Roychowdhury, for his guidance, constant encouragement and support during the course of my work in the last one year. I truly appreciate and value his esteemed guidance and encouragement from the beginning to the end of the thesis. His knowledge and company at the time of crises would be remembered lifelong.

I would also like to offer my sincere thanks to all faculty member, teaching and non-teaching staff of Civil Engineering Department of Jadavpur University for their assistance.

I am also thankful to my fellow postgraduate colleagues Mr. Sougata Das, Likhan Biswas, Subhankar Paramanik, Bibekananda Mandal, Sourav Chanda for supported me extensively throughout my studies. My special thanks to Mr. Habibulla Sheikh and Mr. Mrinmoy Baidya for supporting and solving some problems occurred in the software ANSYS used in this thesis work.

I would also like to express my gratitude to my family, for their unconditional support and prayers at all times and constant encouragement during the entire course of my thesis work.

Date:.....

Place: Jadavpur University, Kolkata

.....
(FALGUNI SHIT)

ABSTRACT

Strengthening of reinforced concrete (RC) structures is frequently required due to inadequate maintenance, excessive loading, change in use or in code of practice and exposure to adverse environmental conditions. Many structure are damaged due to increasing load, earthquake and many other natural disaster. To rectify those structures, repair and rehabilitation has become an important challenge for the reinforced concrete structure. Recently retrofitting concrete structures with bonded fiber reinforced polymer (FRP) has grown to be a widely used method throughout the world. External wrapping with fiber reinforced polymer (FRP) is a promising solution for retrofitting due to various advantages such as high strength-weight ratio, corrosion resistance, ease of application, low labour costs and no significant increase in member size over other strengthening techniques. As the slab is a very important part of the reinforced concrete framed structures as well as brick masonry structures, the repair and strengthening of the slab elements are also very important in addition to the repair of beams, columns etc. In particular, the flexural strength of a slab can be significantly increased by application of FRP sheets adhesively bonded to the tension face of the slab.

Now a days various types of fiber reinforced polymer sheet used such as carbon fiber reinforced polymer (CFRP), glass fiber reinforced polymer (GFRP) and aramid fiber reinforced polymer (AFRP) sheets to strengthen the RC slab. The retrofitting can be applied economically, as there is no need for mechanical fixing or surface preparation. Moreover the strengthening system with FRP can be easily maintained.

It has been tried in the present work to study the behavior of reinforced concrete slab strengthened with fibre reinforced polymer (FRP) laminates following the finite element approach using the software ANSYS. Previous research work based on the experimental observation reveals the fact that the extent of repair or strengthening of reinforced concrete slab with FRP laminates in terms of the load carrying capacity or deformation under service load depends on different parameters. As the experimental study is an expensive and time-consuming approach, the numerical analysis based on finite element technique has been chosen in the present work to assess the extent of the effect of these parameters on the load deformation response of the reinforced concrete slab strengthened with FRP laminates. The finite element

package ANSYS 15.0 is used to develop the finite element model of un-retrofitted as well as retrofitted reinforced concrete slabs and to analyze these in the linear as well as in the nonlinear range. Firstly control slab or un-retrofitted slabs with simply supported boundary condition is analyzed and the results obtained are compared with the same obtained by the previous researchers in their experimental and numerical study for the purpose of validation.

The RC slab specimen is retrofitted with externally bonded glass-fiber-reinforced polymer (GFRP) sheets with different retrofitting position of the slab and analyzed. The variation with respect to the location of FRP laminate, the width of the FRP strips, thickness of the FRP, number of layers in FRP and orientation of fibers in FRP have been taken in the parametric study for both simply supported slab and fixed slab. Total 54 numbers of slabs have been modeled and analyzed using ANSYS. The results from the retrofitted RC slabs are then compared with the results of the control slab. From the analysis it has been observed that the structural behavior of retrofitted RC slab improves significantly compared to the control RC slab. It has also been discussed here the most suitable and effective retrofitting mode among the different retrofitting position for both simply supported and fixed boundary condition.

TABLE OF CONTENTS

DECLARATION	III
ACKNOWLEDGEMENT	IV
ABSTRACT	V-VI
CONTENTS	VII-X
LIST OF TABLES	XI
LIST OF FIGURES	XII-XIX
CHAPTER 1 - INTRODUCTION.....	1-9
1.1: General.....	1-2
1.2: Types of slab.....	2
1.3 Necessity of Strengthening Reinforced Concrete slab.....	3
1.4 Retrofitting using Fiber Reinforced Polymers (FRP).....	3-7
1.4.1 Carbon Fiber Reinforced Polymer.....	5-6
1.4.2 Glass Fiber Reinforced Polymer.....	6-7
1.4.3 Failure Mode of FRP Material.....	7
1.5 Analysis Tools – ANSYS	7-8
1.6 Objectives.....	8
1.7 Present Scope of the Work.....	8-9
CHAPTER 2 – LITERATURE REVIEW.....	10-19
2.1 General.....	10
2.2 Finite Element Modelling and the Strengthening of RC Slab.....	10-19
CHAPTER 3 – FINITE ELEMENT MODELLING OF RC SLAB USING ANSYS.....	20-43
3.1 Introduction.....	20
3.2 Numerical Embodiment.....	20-21
3.3 Model of RC Slab Structure.....	21-22

3.4 Elements used in ANSYS to Model Un-retrofitted and Retrofitted RC Slab...	23-26
3.4.1 Element Types.....	23-25
3.4.1.1 SOLID65.....	23
3.4.1.2 LINK180.....	24
3.4.1.3 SOLID185.....	24-25
3.4.2 Real Constants.....	25-26
3.5 Modelling of Material Behavior	26-33
3.5.1 Concrete.....	27-28
3.5.1.1 Concrete Models.....	27
3.5.1.2 Failure Criteria for Concrete.....	28
3.5.2 Finite Element Modeling Reinforcing Steel.....	29
3.5.3 Material Properties.....	30-33
3.6 Details of present Finite Element Model.....	33-39
3.6.1 Meshing.....	35
3.6.2 Loading & Boundary Condition.....	36
3.6.3 Solution Control for Non-Linear Solution.....	37-39
3.7 Steps for the Development of the Model with or without FRP.....	40-41
3.8 Model of Retrofitted Material under Different Retrofitted Setup.....	42-43
Setup 1 (By Varying the FRP Location at the Bottom of the RC Slab)	41-42
Setup 2 (By Increasing the FRP area at different locations of the RC Slab)...	42
Setup 3 (By Varying the numbers of FRP layers of RC slab).....	43
Setup 4 (By Varying FRP layer thickness of RC slab)	43
Setup 5 (By Varying the orientation of FRP layers of the RC Slab)	43
CHAPTER 4 – RESULTS & DISCUSSIONS.....	44-96
4.1 Introduction.....	44
4.2 Validation of proposed model.....	44-47
4.3 Parametric study.....	48-96
4.3.1 Support Conditions.....	50
Part A: Simply Supported Slab	
4.3.2 Discretization or Mesh Size.....	50-52
4.3.3 Location of FRP in simply supported slab.....	52-60

Contour plot of Nodal Solution in slabs SS1, SS2, SS3 and SS4....	54-56
Crack pattern in slabs SS1, SS2, SS3 & SS4.....	57-60
4.3.4 Width of FRP in the simply supported slab.....	60-66
4.3.4.1 FRP along the support edge of the simply supported slab.....	60-61
4.3.4.2 FRP along the continuous edge of the simply supported slab.....	62-63
4.3.4.3 FRP along the diagonal of the simply supported slab.....	63-67
4.3.5 Layers of FRP in simply supported slab.....	67-68
4.3.6 Thickness of FRP in simply supported slab.....	68-70
4.3.7 Orientation of FRP in simply supported slab.....	70-72

Part B: Fixed Slab

4.3.8 Discretization of the fixed control slab.....	73-78
4.3.9 Location of FRP in fixed slab.....	75-83
Contour plot of Nodal Solution (FS1, FS2, FS3 and FS4).....	77-80
Crack pattern (FS1, FS2, FS3 and FS4).....	80-83
4.3.10 Width of FRP in the fixed slab.....	83-90
4.3.10.1 FRP along the support edge of the fixed slab.....	84-85
4.3.9.2 FRP along the continuous edge of the fixed slab.....	86-87
4.3.9.3 FRP along the diagonal of the fixed slab	88-90
4.3.11 Layers of FRP in Fixed slab.....	91-92
4.3.12 Thickness of FRP in fixed slab	93-95
4.3.13 Orientation of FRP in fixed slab.....	95-96

CHAPTER 5 – CONCLUSION.....97-100

5.1 Introduction.....	97
5.2 Validation	97
5.3 Parametric Study	97
5.3.1 Location of FRP.....	98
5.3.2 Area covered by FRP.....	99
5.3.3 Number of layers in FRP.....	99
5.3.4 Thickness of FRP.....	99

5.3.5 Orientation of the fibers in FRP.....	100
5.6 Final Remarks.....	100
5.7 Future scope of study.....	100
REFERENCES.....	101-103

LIST OF TABLES

Table 1.1: Properties of CFRP material [7].....	5
Table 1.2: Typical properties of glass fibers [26].....	6
Table 3.1: Element Types used in present F.E. model.....	23
Table 3.2: Real Constants for Present Model.....	25
Table 3.3: Material Properties for Present Model.....	30-31
Table 3.4: Dimensions for concrete volume.....	34
Table 3.5: Mesh Attributes for the Model.....	35
Table 3.6: Commands used to Control Nonlinear Analysis.....	38
Table 3.7: Commands Used to Control Output.....	38
Table 3.8: Nonlinear Algorithm and Convergence Criteria Parameters.....	39
Table 3.9: Advanced Nonlinear Control Settings Used.....	39
Table 4.1: Material Properties for Concrete and Steel [8].....	46
Table 4.2a: Notation used for different variable parameters.....	48
Table 4.2b: Details of parameters used in different slabs.....	49
Table 4.3: Comparison of deflection at load 96KN due to change in mesh.....	52
Table 4.4: Change of load carrying capacity of simply supported RC slab retrofitted with FRP.....	66
Table 4.5: Change of deformation at ultimate load of simply supported RC slab retrofitted with FRP.....	66
Table 4.6: Comparison of deflection at load 575 KN due to change in mesh.....	72
Table 4.7: Change of load carrying capacity of fixed RC slab retrofitted with FRP.....	75
Table 4.8: Change of deformation at ultimate load of fixed RC slab retrofitted with FRP.....	75

LIST OF FIGURES

Figure 1.1: Types of RC slabs (one way & two way slab).....	2
Figure 1.2: Formation of FRP composite.....	4
Figure 1.3: Fiber wrapping of the slab [15].....	5
Figure 2.1: Typical layout of GFRP and CFRP strengthened specimens at failure [11].....	11
Figure 2.2: Relative vertical displacement between two sides of a flexural-shear crack [12].	12
Figure 2.3: Details of Yao et al.'s (2002) test slabs [13].....	13
Figure 2.4: RC slab specimen and test configuration [18].....	14
Figure 2.5: photograph of failed specimen control specimen and externally bounded FRP specimen [18].....	14
Figure 2.6: photograph of failed specimen control specimen and mechanically fastened FRP specimen [18].....	14
Figure 2.7: Typical stress strain relationship of FRP composite and mild steel [20].....	16
Figure 2.8: Slab loading pattern [21].....	17
Figure 2.9: Slab cross-section with different CFRP position [21].....	17
Figure 2.10: Load-deflection curve for strengthened slab mild reinforcement [21].....	17
Figure 2.11: Shear strengthening of Reinforced concrete using CFRP laminate [22].....	18
Figure 2.12: Plan and cross section details of the slab model, dimensions in meter [25].....	19
Figure 2.13: 3D and elevation of ANSYS model [25].....	19
Figure 3.1: Plan and Cross section of RC slab and its FE representation.....	22
Figure.3.2 SOLID65 element [27].....	23
Figure 3.3: LINK180 Geometry [27].....	24
Figure 3.4: SOLID185 Layered Structural Solid Geometry. [27].....	25
Figure 3.5: Typical load-displacement response of RC element.....	26
Figure 3.6: Dimension failure surface for concrete.....	28
Figure 3.7: Models for Reinforcement in Reinforced Concrete (Tavarez 2001); (a) Discrete; (b) embedded; and (c) smeared [1].....	29
Figure 3.8: Uniaxial Stress-strain curve for concrete.....	32
Figure 3.9: Post cracking model of concrete in tension [26].....	32
Fig.3.10: Stress-strain curve for steel reinforcement [4].....	33

Figure 3.11: Volume created in ANSYS.....	34
Figure 3.12: Element connectivity: (a) Concrete solid element and link element; (b) Concrete solid element and FRP layered elements.....	35
Figure 3.13: Mesh of the quarter volume of RC beam with rebar arrangement.....	35
Figure 3.14: Application of loading and boundary condition on the RC slab model.....	36
Figure 3.15: modelling of reinforcement bars.....	36
Figure 3.16: nonlinear solutions as Newton-Raphson approach.....	37
Figure 3.17: Locations of FRP at the bottom of the slab.....	42
Figure 3.18: Increasing the FRP area along support edge.....	42
Figure 3.19: Increasing the FRP area along continuous edge.....	42
Figure 3.20: Increasing the FRP area along diagonal.....	42
Figure 3.21: Increasing no of layers of the FRP.....	43
Figure 3.22: Changing the orientation of the FRP layers.....	43
Figure: 4.1: Details of RC slab and its finite element representation [8].....	45
Figure: 4.2: a) Discretization of quarter RC slab in X-Z plane with (3 x 3) mesh of 9 elements b) modelling of reinforcement bars.....	46
Figure 4.3: Comparision of load deflection curve of the present ANSYS model with the same obtained by other previous researchers.....	47
Figure 4.4a: Discretization of quarter RC slab in X-Z plane with (6 x 6) mesh of 36 Elements.....	50
Figure 4.4b: Discretization of quarter RC slab in X-Z plane with (9 x 9) mesh of 81 elements.....	51
Figure 4.4c: Discretization of quarter RC slab in X-Z plane with (12 x 12) mesh of 144 elements.....	51
Figure 4.4d: Variation of load-deflection plot due to change in mesh size.....	51
Figure 4.5a: FRP along support edge in Slab SS2.....	52
Figure 4.5b: FRP along continuous edge in Slab SS3.....	53
Figure 4.6: Variation of load deflection curve of the slab S2, S3, S4 (retrofitted) with S1 (control slab).....	53
Figure 4.7a: Contour of x-component stress in slab SS1.....	54
Figure 4.7b: Contour of y-component stress in slab SS1.....	54
Figure 4.7c: Contour of -Z component stress in slab SS1.....	54

Figure 4.7d: Contour of y-component deflection in slab SS1.....	54
Figure 4.8a: Contour of x-component stress in slab SS2.....	55
Figure 4.8b: Contour of y-component stress in slab SS2.....	55
Figure 4.8c: Contour of z-component stress in slab SS2.....	55
Figure 4.8d: Contour of Y-component deflection in slab SS2.....	55
Figure 4.9a: Contour of x-component stress in slab SS3.....	55
Figure 4.9b: Contour of y-component stress in slab SS3.....	55
Figure 4.9c: Contour of z-component stress in slab SS3.....	56
Figure 4.9d: Contour of y-component deformation in slab SS3.....	56
Figure 4.10a: contour of x-component stress in slab SS4.....	56
Figure 4.10b: contour of y-component stress in slab SS4.....	56
Figure 4.10c: Contour of z-component stress in slab SS4.....	56
Figure 4.10d: Contour of y-component deflection in slab SS4.....	56
Figure 4.11 a: Pattern of 1 st crack in slab SS1.....	57
Figure 4.11b: Pattern of 1 st crack in slab SS2.....	57
Figure 4.11c: Pattern of 1 st crack in slab SS3.....	58
Figure 4.11d: Pattern of 1 st crack in slab SS4.....	58
Figure 4.12a: Pattern of 2 nd crack in slab SS1.....	58
Figure 4.12b: Pattern of 2 nd crack in slab SS2.....	58
Figure 4.12c: Pattern of 2 nd crack in slab SS3.....	58
Figure 4.12d: Pattern of 2 nd crack in slab SS4.....	58
Figure 4.13a: Pattern of 3 rd crack in slab SS1.....	59
Figure 4.13b: Pattern of 3 rd crack in slab SS2.....	59
Figure 4.13c: Pattern of 3 rd crack in slab SS3.....	59

Figure 4.13d: Pattern of 3 rd crack in slab SS4.....	59
Figure 4.14a: Pattern of all cracks in slab SS1.....	59
Figure 4.14b: Pattern of all cracks in slab SS2.....	59
Figure 4.14c: Pattern of all cracks in slab SS3.....	60
Figure 4.14d: Pattern of all cracks in slab SS4.....	60
Figure 4.15: Location of FRP along support edge in the full model of simply supported retrofitted slab.....	61
Figure 4.16: Variation of load deformation behavior of retrofitted simply supported RC slab due to change in the area covered with FRP along support edge.....	61
Figure 4.17: Location of FRP along continuous edge in the full model of simply supported retrofitted slab.....	62
Figure 4.18: Variation of load deformation behavior of retrofitted simply supported RC slab due to change in the area covered with FRP along continuous edge.....	63
Figure 4.19: Location of FRP along diagonal in the full model of simply supported retrofitted slab.....	64
Figure 4.20: Variation of load deformation behavior of retrofitted simply supported RC slab due to change in the area covered with FRP along both the diagonals.....	65
Figure 4.21a: Variation of load deformation behavior of retrofitted simply supported RC slab due to change in number of layers in FRP along support edge.....	67
Figure 4.21b: Variation of load deformation behavior of retrofitted simply supported RC slab due to change in number of layers in FRP along continuous edge.....	68
Figure 4.21c: Variation of load deformation behavior of retrofitted simply supported RC slab due to change in number of layers in FRP along diagonal position.....	68
Figure 4.22a: Finite element model of slab SS12.....	69
Figure 4.22b: Variation of load deformation behavior of retrofitted simply supported RC slab due to change in thickness of FRP along support edge for slab SS12.....	69
4.23a: Finite element model of slab SS13.....	69
Figure 4.23b: Variation of load deformation behavior of retrofitted simply supported RC slab due to change in thickness of FRP along continuous edge for slab SS13.....	69

Figure 4.24a: Finite element model of slab SS14.....	70
Figure 4.24b: Variation of load deformation behavior of retrofitted simply supported RC slab due to change in thickness of FRP along diagonal for slab SS14.....	70
Figure 4.25: Variation of load deformation behavior of retrofitted simply supported RC slab due to change in the orientation of FRP along support edge.....	71
Figure 4.26: Variation of load deformation behavior of retrofitted simply supported RC slab due to change in the orientation of FRP along continuous edge.....	71
Figure 4.27: Variation of load deformation behavior of retrofitted simply supported RC slab due to change in the orientation of FRP along diagonal.....	72
Figure 4.28a: Discretization of quarter RC slab in X-Z plane with (6 x 6) mesh of 36 elements.....	73
Figure 4.28b: Discretization of quarter RC slab in X-Z plane with (9 x 9) mesh of 81 elements.....	73
Figure 4.28c: Discretization of quarter RC slab in X-Z plane with (12 x 12) mesh of 144 element.....	73
Figure 4.29a: Modelling of reinforcing bars with (6 x 6) mesh of 36 elements.....	74
Figure 4.29b: Modelling of reinforcing bars with (9 x 9) mesh of 81 elements.....	74
Figure 4.29c: Modelling of reinforcing bars with (12 x 12) mesh of 144 elements.....	74
Figure 4.30: Variation of load-deflection plot due to change in mesh size in fixed slab.....	75
Figure 4.31a: FRP along support edge in slab FS2	76
Figure 4.31b: FRP along continuous edge in the slab FS3.....	76
Figure 4.31c: FRP along diagonal in the slab FS4.....	77
Figure 4.32: Variation of load deflection curve of the slab FS2, FS3, FS4 (retrofitted) with FS1 (control slab).....	77
Figure 4.33a: Contour of x-component stress in slab FS1.....	78
Figure 4.33b: Contour of y-component stress in slab FS1.....	78
Figure 4.33c: Contour of z-component stress in slab FS1.....	78
Figure 4.33d: Contour of y-component deformation in slab FS1.....	78
Figure 4.34a: Contour of x-component stress in slab FS2.....	78

Figure 4.34b: Contour of y-component stress in slab FS2.....	78
Figure 4.34c: Contour of z-component stress in slab FS2.....	79
Figure 4.34d: Contour of y-component deformation in slab FS2.....	79
Figure 4.35a: Contour of x-component stress in slab FS3.....	79
Figure 4.35b: Contour of y-component stress in slab FS3.....	79
Figure 4.35c: Contour of z-component stress in slab FS3.....	79
Figure 4.35d: Contour of y-component deflection in slab FS3.....	79
Figure 4.36a: Contour of x-component stress in slab FS4.....	80
Figure 4.36b: Contour of y-component stress in slab FS4.....	80
Figure 4.36c: Contour of z-component stress in slab FS4.....	80
Figure 4.36d: Contour of y-component deflection in slab FS4.....	80
Figure 4.37a: Pattern of 1 st crack in slab FS1.....	81
Figure 4.37b: Pattern of 1 st crack in slab FS2.....	81
Figure 4.37c: Pattern of 1 st crack in slab FS3.....	81
Figure 4.37d: Pattern of 1 st crack in slab FS4.....	81
Figure 4.38a: Pattern of 2 nd crack in slab FS1.....	81
Figure 4.38b: Pattern of 2 nd crack in slab FS2.....	81
Figure 4.38c: Pattern of 2 nd crack in slab FS3.....	82
Figure 4.38d: Pattern of 2 nd crack in slab FS4.....	82
Figure 4.39a: Pattern of 3 rd crack in slab FS1.....	82
Figure 4.39b: Pattern of 3 rd crack in slab FS2.....	82
Figure 4.39c: Pattern of 3 rd crack in slab FS3.....	82
Figure 4.39d: Pattern of 3 rd crack in slab FS4.....	82
Figure 4.40a: Pattern of all cracks in slab FS1.....	83
Figure 4.40b: Pattern of all cracks in slab FS2.....	83
Figure 4.40c: Pattern of all cracks in slab FS3.....	83
Figure 4.40d: Pattern of all cracks in slab FS4.....	83

Figure 4.41: Variation of FRP width along the support edge.....	85
Figure 4.42: Variation of load deformation behavior of retrofitted fixed supported RC slab due to change in the area covered with FRP along support edge.....	85
Figure 4.43: Variation of FRP width along the continuous edge	87
Figure 4.44: Variation of load deformation behavior of retrofitted fixed supported RC slab due to change in the area covered with FRP along continuous edge.....	87
Figure 4.45: Variation of FRP width along the diagonal.....	89
Figure 4.46: Variation of load deformation behavior of retrofitted fixed supported RC slab due to change in the area covered with FRP along diagonal	89
Figure 4.47a: Variation of load deformation behavior of retrofitted fixed supported RC slab due to change in number of layers in FRP along support edge.....	91
Figure 4.47b: Variation of load deformation behavior of retrofitted fixed supported RC slab due to change in number of layers in FRP along continuous edge.....	92
Figure 4.47c: Variation of load deformation behavior of retrofitted fixed supported RC slab due to change in number of layers in FRP along diagonal.....	92
Figure 4.48a: Finite element model of slab FS12.....	93
Figure 4.48b: Variation of load deformation behavior of retrofitted fixed supported RC slab due to change in thickness of FRP along support edge for FS12.....	93
Figure 4.49a: Finite element model of slab FS13.....	93
Figure 4.49b: Variation of load deformation behavior of retrofitted fixed supported RC slab due to change in thickness of FRP along continuous edge for slab FS13.....	93
Figure 4.50a: Finite element model of slab FS14.....	94
Figure 4.50b: Variation of load deformation behavior of retrofitted fixed supported RC slab due to change in thickness of FRP along diagonal for slab FS14.....	94
Figure 4.51: Variation of load deformation behavior of retrofitted fixed supported RC slab due to change in thickness of FRP along support edge, continuous edge and diagonal.....	94
Figure 4.52: Variation of load deformation behavior of retrofitted fixed supported RC slab due to change in the orientation of FRP along support edge.....	95
Figure 4.53: Variation of load deformation behavior of retrofitted fixed supported RC slab due to change in the orientation of FRP along continuous edge.....	96

Figure 4.54: Variation of load deformation behavior of retrofitted fixed supported RC slab due to change in the orientation of FRP along diagonal.....96

CHAPTER 1

INTRODUCTION

1.1 General

Reinforced concrete (RC) has become one of the most versatile construction materials and is widely used in many types of engineering structures. The economy, the efficiency, the strength and the stiffness of reinforced concrete make it an attractive construction material for a wide range of structural applications.

Many natural disasters, earthquake being the most affecting of all, have produced a need to increase the present safety levels in buildings. The knowledge of understanding of the earthquakes is increasing day by day and therefore the seismic demands imposed on the structures need to be revised. The design methodologies are also changing with the growing research in the area of seismic engineering. So the existing structures may not qualify to the current requirements. As the complete replacement of such deficient structures leads to incurring a huge amount of public money and time, retrofitting has become the acceptable way of improving their load carrying capacity and extending their service lives.

In recent decades fiber reinforced polymers (FRPs) are used for strengthening of RC slab very widely because of the benefits of extremely high ultimate tensile strength and light weight of this materials. FRP material has shown to be applicable to the strengthening of structural members or repairing of damaged structures, such as columns, beams and slab, etc. The FRP can used to improve the flexure and shear capacity and provide the confinement and ductility for various structural members. It is characterized by high strength fiber embedded in polymer resin. According to the previous researchers, the study on the applications of FRP laminates in strengthening of RC slabs has become one of the fastest growing new research area within the structural engineering.

Slabs are plane structural members whose thickness is quite small as compared to its span and width. In reinforced concrete construction, slabs are most frequently used as structural elements forming roof covering, floors and bridges. Slabs may be supported by reinforced concrete beams or directly by columns. It usually carries uniformly distributed gravity load acting normal to its surface and transfers same to the supports by flexure, shear and torsion. Therefore because of its complex behavior it is difficult to decide whether the slab is a structural component, structural element, or structural system in itself.

To model the complex behavior of reinforced concrete analytically specially in its non-linear zone is extremely difficult. Most of the researchers use a number of numerical approach and empirical formulas which were derived from numerous experiments. The Finite Element

method makes it possible to take into account non-linear response of reinforced concrete structure analytically. Moreover, researchers had used commercially-available software package such as ANSYS, ABAQUS, DIANA, ATENA, or SBETA to carry out the FE analysis. Studies regarding the modeling of RC slab structure with FRP materials are relatively limited.

In the present work the Finite Element method is used to develop the model of a two way RC slab. The non-linear response of RC slab under the incremental static load has been carried out using the commercial software package ANSYS version 15.0 with the intension of improvement of such joint under different retrofitting position with FRP laminates.

1.2 Types of Slab

There are two types of RC slab used as structural member with different support conditions can be identified viz. one way and two way as shown in Figure 1.1.

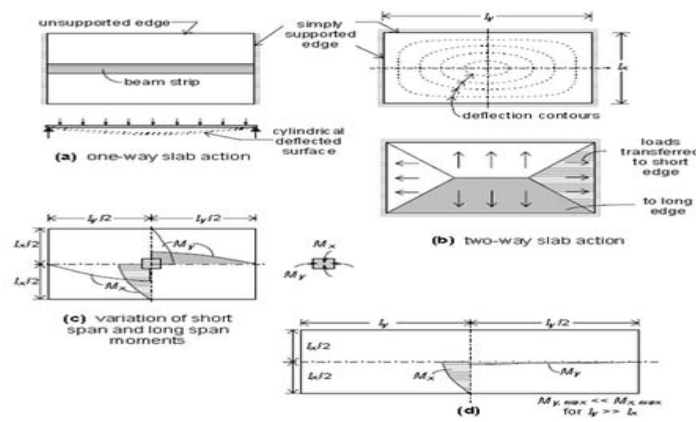


Figure 1.1: Types of RC slabs (one way & two way slab)

Figure 1.1 explain the share of loads on beams in two perpendicular directions depends upon the aspect ratio l_y/l_x of the slab, l_x being the shorter span. For large values of l_y , the triangular area is much less than the trapezoidal area. Hence, the share of loads on beams along shorter span will gradually reduce with increasing ratio of l_y/l_x . In such cases, it may be said that the loads are primarily taken by beams along the longer span. The deflection profiles of the slab along both directions are also shown in the Figure 1.1. The deflection profile is found to be constant along the longer span except near the edges for the slab panel. These slabs are designated as one-way slabs as they span in one direction (shorter one) only for a large part of the slab when $l_y/l_x > 2$. The slabs which are subjected mostly to uniformly distributed load to resist them primarily by bending about both the axis shown in Figure 1.1. In this aspect ratio should be less than 2, it is designed by method of coefficients method given in IS 456-2000 [28]

1.3 Necessity of Strengthening Reinforced Concrete slab

The situations in which the reinforced concrete slabs require the intervention for repairs or strengthening are the following [6]:

- a) Repairing damaged/deteriorated concrete slabs to restore their strength and stiffness.
- b) Corrosion of the reinforcement.
- c) Limiting crack width under increased (design/service) loads or sustained loads.
- d) Retrofitting concrete members to enhance the flexural strength and strain to failure of concrete elements requested by increased loading conditions such as earthquakes or traffic loads.
- e) Rectifying design and construction errors such as undersized reinforcement.
- f) Enhancing the service life of the RC slabs
- g) Shear strengthening around columns for increasing the perimeter of the critical section for punching shear.
- h) Changes in the structural system such as cut-outs in the existing RC slabs.
- i) Changes of the design parameters.
- j) Optimization of structure regarding the reduction of deformations and of the stresses in the reinforcing bars.

1.4 Retrofitting using Fiber Reinforced Polymers (FRP)

Besides the use of different conventional methods used to repair and retrofit the concrete structures like adding of shear wall, jacketing etc., strengthening with the use of fiber reinforced polymer (FRP) is one of the techniques which has wide range of scope and is extensively used these days. Continuing advances in the manufacturing techniques and performance of fiber reinforced polymer (FRP) materials have allowed FRPs to move from playing a secondary role in civil infrastructure to one that is a genuinely feasible construction alternative.

This is a new technique having tremendous potential. FRP is a composite material made by combining two or more materials to give a new combination of properties. FRP composite is a two-phased material and is composed of fiber and polymer matrix, which are bonded at interface as shown in Figure 1.2. The fibers are usually glass, carbon, aramid while the polymer is usually epoxy, vinyl ester. Fibers provide FRP composite with strength and stiffness, while the matrix gives rigidity and environmental protection. Fibers can be used in its two forms: fiber wraps or sheets and fiber laminates.

The technology for external retrofitting was developed primarily in Japan (sheet wrapping) and Europe (laminare bonding). Today there are more than 1000 concrete slab/steel girder bridges in Japan that have been strengthened with sheet bonding to the slabs. Reduced material cost,

coupled with labor savings inherent with its low weight and comparably simpler installation, relatively unlimited material length availability, and immunity to corrosion, make FRP materials an attractive solution for post strengthening, repair, seismic retrofit, and infrastructure security. [3]

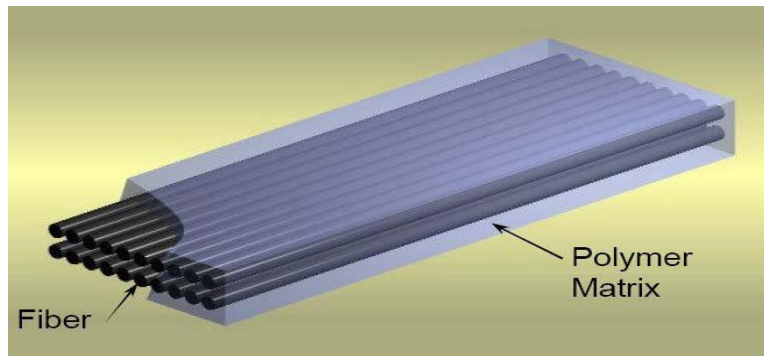


Figure 1.2: Formation of FRP composite

Through retrofitting of concrete beams and columns is quite common these days but nowadays retrofitting of slabs is also coming into picture. The FRP laminates are bonded to the bottom surface of the slab to increase the strength and stiffness of the slab. The delamination of the FRP layer is seen in the slab. This delamination of the FRP layer can be controlled or reduced by anchoring the bonded layer by fiber anchors which in turn also increases the load carrying capacity of the slab. The bond between the concrete substrate and the FRP laminate should be proper for lesser debonding.

The selection of the most appropriate method to use will depend on several factors, such as the amount of strengthening required, the location where strengthening is required, architectural requirements, simplicity and speed of application, and total cost. The fiber wrapping on the slab is done as shown in Figure 1.3.

Fiber reinforced polymers (FRP) have great potential for use in civil infrastructure applications. They offer a number of advantages over conventional materials such as:

- ❖ Superior strength to weight ratio;
- ❖ Superior stiffness to weight ratio;
- ❖ Superior electromagnetic properties;
- ❖ Excellent fatigue damage tolerance;



Figure 1.3: Fiber wrapping of the slab [15]

The finite element method allows complex analysis of the nonlinear response of RC structures. FEM helps in investigating the behavior of the structure, before and after the application of load, its load- deflection behavior and the cracks pattern. The analytical results of finite element models have to be evaluated by comparing them with experiments of full-scale models of structure. The development of reliable analytical models can, however, reduce the number of required test specimens for the solution of a given problem whereas conducting those tests experimentally are time-consuming and costly and they often do not simulate exactly the loading and support conditions of the actual structure.

1.4.1 Carbon Fiber Reinforced Polymer

Carbon fiber–reinforced polymer (CFRP) is an extremely strong and light fiber-reinforced polymer. CFRPs can be expensive to produce but are commonly used wherever high strength to- weight ratio and rigidity are required, such as structural engineering.

Table 1.1: Properties of CFRP material [7]

Fiber material	High strength carbon
Areal Weight	600 gm/m ²
Fabric width	610 mm
Nominal thickness	0.33 mm/ply
Ultimate Tensile Strength	3800 MPa
Tensile Modulus	227 GPa
Ultimate tensile strength per unit weight	1.25 KN/mm/ply
Tensile Modulus per unit width	76 KN/mm/ply
Ultimate Rupture strain	1.25 %

Carbon-fiber-reinforced polymers are composite materials. In this case the composite consists of two parts: a matrix and reinforcement. In CFRP the reinforcement is carbon fiber, which provides the strength. The matrix is usually a polymer resin, such as epoxy, to bind the reinforcements together. [6]. The reinforcement will give the CFRP its strength and rigidity.

Unlike isotropic materials like steel and aluminum, CFRP has directional strength properties. The properties of CFRP depend on the layouts of the carbon fiber and the proportion of the carbon fibers relative to the polymer shown in table 1.1

1.4.2 Glass Fiber Reinforced Polymer

Glass fiber reinforced composites provided the initial scientific and engineering understanding of FRP matrix composites. In case of GFRP vinyl-esters resin is preferred as matrix material than polyesters due to their chemical structure. These resins have fewer cross links and they are more flexible and have higher fracture toughness than polyesters. They also have very good wet-out and good adhesion when reinforced with glass fibers. [27]

The most common glass fibers are made of E-glass and S-glass. E-glass is the least expensive of all glass types and it has a wide application in fiber reinforced plastic industry. S-glass has higher tensile strength and higher modulus than E-glass. [27] However, the higher cost of S-glass fibers makes them less popular than E-glass. The relative properties of these two types of glass fiber are shown in table 1.2.

Table 1.2. Typical properties of glass fibers [26]

Characteristics \ Fibre	E-glass	S-glass
Density(kg/m ³)	2500	2500
Tensile strength (MPa)	3450	4580
Young modulus (GPa)	72.4	85.5
Ultimate tensile strain (%)	2.4	3.3
Thermal exp. coefficient (10 ⁻⁶ / °C)	5	2.9
Poisson's coefficient	0.22	0.22

According to the previous researchers glass fiber reinforced polymers have numerous advantage than other fiber reinforced polymer. The main advantages that enabled the widespread use of glass fibers in composites are. [28]

- ❖ Competitive price, availability, good handle ability and ease of processing.
- ❖ Higher tensile strength up to 4580 MPa.
- ❖ Up to a 60% reduction in weight.
- ❖ Improved surface quality gives higher resistance to aggressive environment.
- ❖ Fibers can be oriented in different direction to against specific stresses, increasing the durability and load carrying capacity.

1.4.3 Failure Mode of FRP Material

Structural failure can occur in FRP materials as per previous researchers when:

- ❖ Tensile forces stretch the matrix more than the fibers, causing the material to shear at the interface between matrix and fibers.
- ❖ Tensile forces near the end of the fibers exceed the tolerances of the matrix, separating the fibers from the matrix
- ❖ Tensile forces can also exceed the tolerances of the fibers causing the fibers themselves to fracture leading to material failure [28].

1.5 Analysis Tools – ANSYS

Nonlinear finite element analysis of reinforced concrete structure can be performed either by developing computer program intended for the specific purpose or by using standard commercial software packages like ANSYS, ABAQUS, DIANA, ATENA, or SBETA etc.

The first approach is very old and being followed by the researchers since the advent of finite element technique. This approach is suitable mainly for the purpose of research where the researcher can upgrade or modify the formulation by choosing different parameters, models, procedures etc. There is an ample scope here to analyze the structure rigorously under different loading conditions, boundary conditions, with different geometry and material modeling.

The second approach is comparatively newer one where the researcher has to use a particular general purpose finite element package with some limitations regarding element choice, material modeling, boundary condition, solution methodology etc. Still the research is going on with this general purpose finite element packages for the analysis of reinforced concrete structures due to different reasons.

Firstly the researchers do not need to develop the program if the research is not involving any investigation regarding the basic element development or modeling material behavior etc. Secondly the most important reason is that these general purpose software packages are commercially available to the designers who will ultimately analyze and design the reinforced concrete structures.

It will meet the requirement if the result coming from this software can be used for economic as well as safe design of the structures. Thus an attempt has been initiated by the researchers to investigate the suitability of these finite element packages for realistic analysis of different civil engineering structures. Out of different software package, ANSYS is one using which the above mentioned research is being performed for last two-three decades. It has large number of options regarding choice of elements to model the composite action of steel and concrete and different types of constitutive relationships of materials i.e. elastic, elasto-plastic, visco-plastic, time dependent as well as time-independent relationships, solution methodologies etc. Thus, in the present research work, ANSYS Graphical User Interface (GUI) is used for the nonlinear analysis of un-retrofitted and retrofitted RC slabs.

1.6 Objectives

The main objective of the present study is to investigate the non-linear response up to failure of un-retrofitted RC slabs and retrofitted RC slabs using FE modelling under incremental loading and is intended to investigate the relative importance of several factors of retrofitting with FRP in non-linear finite element analysis of RC slabs. This includes the variation in the load-displacement graph, the crack patterns, propagation of cracks, the crack width and the effect of non-linear behavior of concrete and steel on the response of control slab and the retrofitted slab with different location, orientation, thickness and layers of FRP.

Keeping the above objective in mind, the entire present study has been divided into the following number of phases:

1. To model the reinforced cement concrete slab called as control slab and the retrofitted slab with FRP at bottom of RC slab at different location like along support edge, continuous edge and diagonal using FEM.
2. To determine analytically the load deflection curve of both control slab and retrofitted slab for both support conditions.
3. To compare the results of control slab and the retrofitted slabs and also to compare the analytical results with the experimental results.
4. To determine analytically the percentage of load carrying capacity of the slab with respect to increment in area of FRP materials.

1.7 Present Scope of the Work

In the first phase of the present study, Finite Element Modelling of the control RC slab under the incremental loads has been analyzed using ANSYS software and the results so obtained have been compared with available experimental results from the work done by Taylor (1966)

[29] and Owen[30]. The size of slab is 1980mm x 1980mm x 51mm with constant rate of increment of uniformly distributed load. The slab is simply supported at 1830mm centre to centre distance. The materials which are used in the modeling are M 35 concrete and Fe 500 reinforced area 281 mm²/m were used as reinforcement [8].

The control slab is analyzed using ANSYS software up to the failure and then gets the load deformation curves, development of stress at three directions and the cracking behavior is monitored. The control slab has been analyzed and results have been compared with the experimental results from Taylor [30] and numerical results from Owen [29].

In the second phase of the present study, FE modelling of the retrofitted RC slabs for two different support condition (simply supported slab and fixed supported slab) are analyzed using ANSYS software and the load- displacement curve, maximum load carrying capacity and the cracking behavior are also obtained analytically.

The following parameters are proposed to be measured:

- 1) The non-linear load deformation behavior and stress at all three directions for control slab.
- 2) The crack pattern for control slab and the all types of retrofitted slabs.
- 3) The deformation at ultimate load for various retrofitted slabs.
- 4) The parametric study of un-retrofitted and retrofitted RC slabs to observe on the ultimate load carrying capacity.

CHAPTER 2

LITERATURE REVIEW

2.1 General

The state of deterioration of the existing civil engineering concrete structures is one of the greatest concerns to the structural engineers worldwide. The renewal strategies applied to existing structures comprise of rehabilitation and complete replacement. The latter involves a huge expenditure and time; hence the rehabilitation is the only option available. Fibre reinforced polymers (FRP) are the promising materials in rehabilitation of the existing structures and strengthening of the new civil engineering structures.

This chapter presents a brief review of the existing literature both numerical and experimental studies in the area of reinforced concrete (RC) slab strengthened with GFRP. This literature review focuses on recent contributions related to retrofitting techniques of the RCC structures, material used for retrofit and past efforts most closely related to the needs of the present work.

2.2 Finite Element Modelling and the Strengthening of RC Slab

U. Ebead, H. Marzouk, and L. M. Lye (2002) examined and study for a finite element analysis of strengthened two-way slabs using FRP laminates and sheets are discussed. In this paper the results of six specimens evaluate the effectiveness of using fibre reinforced plastics as strengthening materials for two way slabs against flexural deficiency. An incremental elastic-plastic concrete model is implemented. In compression, the concrete model is elastic until a yield point is reached after which irrecoverable plastic strain exists. Pre-cracking and post- cracking behavior of concrete are considered in the study with special emphasis on the impact of the presence of FRP materials on the fracture energy and hence on the tension stiffening. In the analysis, a full bond assumption is made between the concrete and both reinforcing steel bars and also between concrete and the strengthening FRP material. A parametric study is also carried out to study the impact of the strengthening material type, strengthening material area ratio, span of the slab, reinforcement ratio, and thickness of the slabs. A face-centered central composite response surface experimental design was then used to develop simple statistical models as replacements for the complex and time consuming finite element model to explain and predict the ultimate load carrying capacity of the slabs. [9]

Ayman S. Mosallam, Khalid M. Mosalam (2003) this paper presents an experimental and analytical investigation for evaluating the ultimate response of unreinforced and reinforced concrete slabs repaired and retrofitted with fibre reinforced polymer (FRP) composite strips. A uniformly distributed pressure was applied to several two-way large-scale slab specimens using a high-pressure water bag. Both carbon/epoxy and E- glass/epoxy composite systems were used in this study. In predicting the behavior of the repaired slabs, the finite element method was used. Comparison between the experimental and the analytical results indicated the

validity of the computational models in capturing the experimentally determined results for both the control and the rehabilitated slabs. For repair applications, test results indicated that both FRP systems were effective in appreciably increasing the strength of the repaired slabs to approximately five times that of the as-built slabs. For retrofitting applications, use of FRP systems resulted in appreciable upgrade of the structural capacity of the as-built slabs up to 500% for unreinforced specimens and 200% for steel reinforced specimens. [10]

Usama Ebead and Hesham Marzouk (2003) this paper is an ACI code verification of FRP externally reinforced two-way slabs is introduced. An implementation of the ACI-318 and the ACI-440 is presented for the purpose of verification against experimental results. In the experimental work, two different types of FRP materials were evaluated; namely carbon FRP (CFRP) strips and glass FRP (GFRP) laminates. The externally reinforced or strengthened slabs had steel reinforcement ratios of 0.35% and 0.5%. Results show that the flexural capacity of two way slabs can be increased to an average of 35.5% over that of the reference (unstrengthened) specimen. An increase of the initial stiffness is achieved; however, an apparent decrease in the overall ductility is evident. In addition, an average decrease in the values of the energy absorption of about 30% is observed. The estimated ultimate load capacity using the ACI code is in an accepted level of agreement with the experimental results. Figure 1.1 shows a typical flexural failure mode of GFRP and CFRP strengthened specimens after failure. It is evident that the FRP materials contributed to an increase of the capacity until the bond between the FRP material and concrete failed. [11]



(a) GFRP strengthened specimen



(b) CFRP strengthened specimen

Figure 2.1: Typical layout of GFRP and CFRP strengthened specimens at failure

J. Yao, J.G. Teng, J.F. Chen (2004) this paper represents the behavior of bond between FRP and concrete is a key factor controlling the behavior of concrete structures strengthened with FRP composites. This article presents an experimental study on the bond shear strength between FRP and concrete using a near-end supported (NES) single-shear pull test. The test results are found to be in close agreement with the predictions of Chen and Teng's [J. Struct. Eng. 127(2001) 784] bond strength model, which mutually verifies the reliability of both the test method and the Chen and Teng model in general. The NES single-shear pull test, given its simplicity and reliability, is therefore a good candidate as a standard bond test. The test results also showed that Chen and Teng's [J. Struct. Eng. 127(2001) 784] bond strength model is slightly conservative when the FRP-to-concrete width ratios are at the two extremes, but this small weakness can be easily removed when more test results of good quality become available. Figure 1.2 represent the flexure shear crack at the flexure zone of RC section. [12]

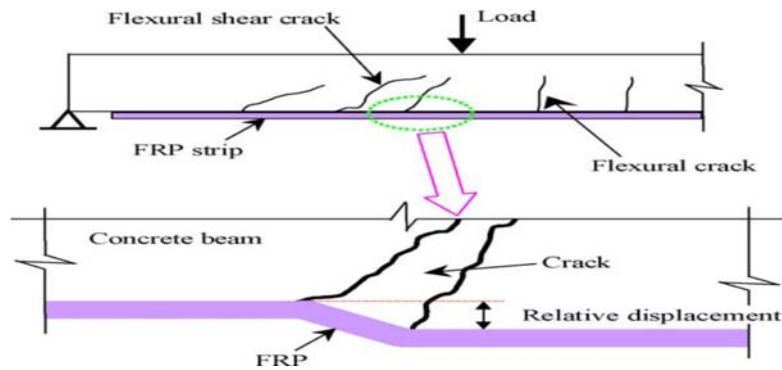


Figure 2.2: Relative vertical displacement between two sides of a flexural-shear crack.

S.T. Smith and R.J. Gravina (2005) the paper attempts reinforced concrete beams and slabs bonded with tension face fibre reinforced polymers (FRP) are susceptible to premature failure by intermediate crack (IC) induced debonding, otherwise known as IC debonding, that originates at a flexural crack. Two key parameters needed in the determination of IC debonding are

(a) The load required to initiate localised debonding near the base of flexural cracks, and (b) the length of debonded plate required to cause complete loss of load carrying capacity of the FRP-strengthened member. These two parameters are investigated in this paper using a local deformation model previously reported by the authors (Gravina and Smith 2004 and 2005). A recently published bond-slip relation for the FRP-to-concrete interface (Lu et al. 2005) is used to determine the onset of debonding while the local deformation model is used to investigate the debonded plate length in FRP-strengthened RC cantilever slabs. The results are compared with Chen and Teng's (2001) effective bond length and then recommendations given. [13]

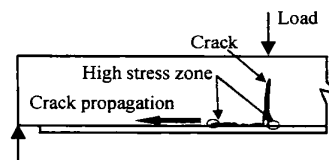


Figure 2.3: IC debonding

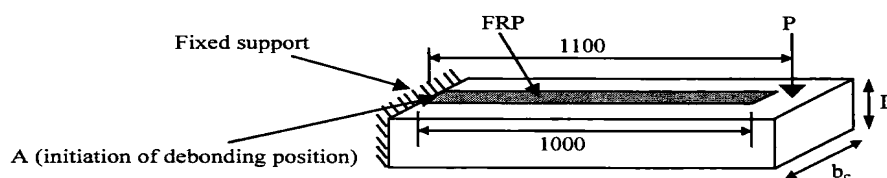


Figure 2.3: Details of Yao et al.'s (2002) test slabs

Khalil Belakhdar (2006) this paper presents an implementation of a rational three-dimensional nonlinear finite element model for evaluating the behavior of reinforced concrete slabs strengthened with shear bolts under transverse load. The concrete was idealized by using eight-noded brick elements. While both flexural reinforcement and the shear bolts were modelled as truss elements, a perfected bond between brick elements and truss elements was assumed. The nonlinear behavior of concrete in compression is simulated by an elasto-plastic work-hardening model, and in tension a suitable post-cracking model based on tension stiffening and shear retention models are employed. The steel was simulated using an elastic-full plastic model. The validity of the theoretical formulations and the program used was verified through comparison with available experimental data, and the agreement has proven to be good. A parametric study has been also carried out to investigate the influence of the shear bolts' diameter and number of bolts' rows around the column-slab connection, on the ductility and ultimate load capacity of slabs. [14]

K.W. Neale (2007) in recent years considerable efforts have been directed towards the numerical modelling of FRP-strengthened reinforced concrete beams, slabs and columns. For beams and slabs, the FRP/concrete interfacial behavior has been a topic of study by a number of researchers, and good progress has been achieved with regard to the development of analytical and modelling approaches for simulating the various debonding phenomena. This paper first focuses on the numerical models for reinforced concrete beams and slabs, and the associated FRP strengthening schemes for flexure and shear. This confirms that the major challenges are the proper simulation of the FRP/concrete interfaces and the complex behavior of concrete in such applications. In the second part of this paper, a brief discussion of the modelling of FRP-confined concrete columns is given. [16]

Ravikant Shrivastava, Uttamasha Gupta, U B Choubey (2009) studied this theoretical approach the engineers throughout the world including India and China have used FRP to solve their structural problems in an efficient and economical manner. In the field of civil engineering, most of the use of FRP is confined to repairing and strengthening of structures. FRPs offer an added advantage over conventional materials and methods of retrofitting. Like other materials, FRP also has its limitations. After presenting a brief review on these dimensions, this paper provides a thorough survey of the research, education and application field of FRP in civil engineering in India and China. The paper also indicates pitfalls in the field and furnishes suggestions for improvement. [17]

A. Napoli, F. Matta, E. Martinelli and A. Nanni (2010) this is an experimental investigation of six one-way RC slabs were tested under four-point bending. Four slabs were strengthened with a mechanically fastened FRP laminate, a counterpart was strengthened with an externally bonded FRP laminate, while an un-strengthened slab was used as the control specimen. The experimental setup of RC slab with two concentrated load is shown in figure 2.4. [18]

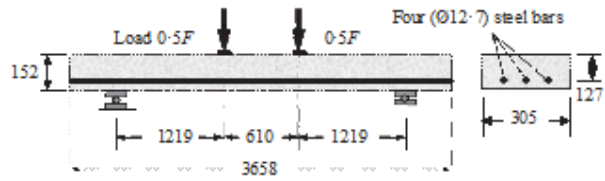


Figure 2.4: RC slab specimen and test configuration



Figure 2.5: photograph of failed specimen control specimen and externally bounded FRP specimen



Figure 2.6: photograph of failed specimen control specimen and mechanically fastened FRP specimen

Figure 2.5 and 2.6 shows photograph of failed specimen control specimen and externally bounded FRP specimen and mechanically fastened FRP specimen.

Kenneth W. Neale, Ahmed Godat and Usama A. Ebead (2011) this paper presents the nonlinear finite element modelling of reinforced concrete members externally strengthened with fiber reinforced polymers (FRPs). Modelling approaches for various applications are reviewed, including the flexural and shear strengthening of beams, as well as the FRP strengthening of two-way slabs. Two types of strengthening methods are considered; namely externally bonded and mechanically fastened FRP strengthening schemes. In all applications, special attention is paid to the implementation of appropriate constitutive models for the FRP/concrete interfaces. To obtain accurate predictions, these models must be capable of properly simulating interfacial stresses and strains, as well as characterizing possible debonding failures. The performance of the various numerical models is assessed through comparisons with appropriate experimental data. It is shown that, with adequate interface

models, the numerical predictions can compare very well with experimental measurements in terms of ultimate load carrying capacities, load-deflection relationships and failure modes. The numerical analyses are shown to provide useful insight into phenomena that are difficult to obtain experimentally (e.g., interfacial stress distributions and interfacial slip profiles). [19]

Chothani D.G. et al. (2012) studied the effect of GFRP sheet on ultimate strength of slab. The structural response of slab was improved due to FRP laminate bonded on the slab. In the experimental work, three identical reinforced concrete slabs (1500x900x50mm) were constructed. All the slabs were reinforced with 4mm diameter steel rods. The steel rods were placed at 150mm center to center in both the directions and were tied by the binding wires with 10mm cover provided to the rods. Out of the three slabs, one slab was taken as control slab i.e. slab without any FRP laminate, second slab was strengthened with a layer of GFRP which was bonded at the bottom with the help of epoxy resin and the third slab was strengthened with a GFRP sheet which was bonded at the bottom as well as anchored to the slab. The grade of concrete used was M25 and the proof stress of the steel rod was 722 MPa and the ultimate stress was 807MPa. All the three slabs were simply supported at 1300mm center to center distance and were tested under one-way condition. A uniformly distributed load was applied on the slab through a hydraulic jack and the deflection of the slab was noted at three locations i.e. at one fourth, at center and at three-fourth of the span. In the third slab, aluminium spacer tube was attached to the base through nuts and bolts to facilitate anchorage. The GFRP sheets used in the experimental work were bi-directional and thickness of the sheet used was 1mm. the ultimate tensile strength of the GFRP sheet in one direction was 31363.6 MPa. The load-deflection response, ultimate load- carrying capacity was noted during the experiment. Slabs containing GFRP sheets showed regain in stiffness whereas the slab having no GFRP laminate showed negligible improvement in stiffness. The ultimate load carrying capacity of the slab with bonded GFRP sheet was increased by 27.12% whereas for the slab which is bonded as well as anchored with GFRP sheet showed 79.97% increase in ultimate load carrying capacity as compared to the control slab. GFRP sheet showed no participation during initial linear stage as first crack load was almost same for all the slabs. De-lamination of GFRP sheet was noticed at few locations from the slab. The overall performance of bonded and anchored GFRP slab and bonded GFRP slab was better than the slab without any GFRP sheet. [3]

Lakshmikandhan K. N, Sivakumar P, Ravichandran R. (2013) this paper represents the repair and rehabilitation of concrete structures has become a necessary measure for deficient structures. The deficiency of structure is generally due to the unexpected loads, corrosion and upgradation of load standards. Concrete structures are generally subjected to very light to severe damage due to seismic and wind loads. The visual damages can be comfortably observed during visual inspection, but the damages occurred internally needs examination through experimental and/or analytical investigation. These methods also have their own limitations. The present study was carried out to arrive at the percentage of damage

in reinforced concrete beam from its stiffness degradation. A repair mechanism for concrete beam with a particular percentage of damage has been attempted. CFRP which is a well-accepted and efficient material for repair and rehabilitation is used in this study. The reinforced concrete beam has been tested and the performance under cyclic load has been observed. The stiffness degradation in each cycle has been observed for an equivalent damage assessment. The information on damage level from the results is used to predict the loading required to simulate the required percentage of damage. A guideline for simulation of required percentage damage has been arrived. In a set of experiments, beams were subjected to different levels of loading to create varying percentage damage and then the damaged beams were repaired with CFRP. The undamaged control beam has been strengthened with CFRP laminated the repaired/strengthened beams were tested under monotonic load for comparison. The study has confirmed the applicability of cyclic loading method to evolve the stiffness degradation and damage assessment. The bonding strength of CFRP governs the strength of the repaired beams in most cases. The bonding of CFRP is better in the cracked beams than in the un-cracked beam. The results have also shown that the repaired damaged beams outperformed than the undamaged control beam strengthened with CFRP. Figure 2.7 shows the curve with variation of stress strain for various FRP materials. [20]

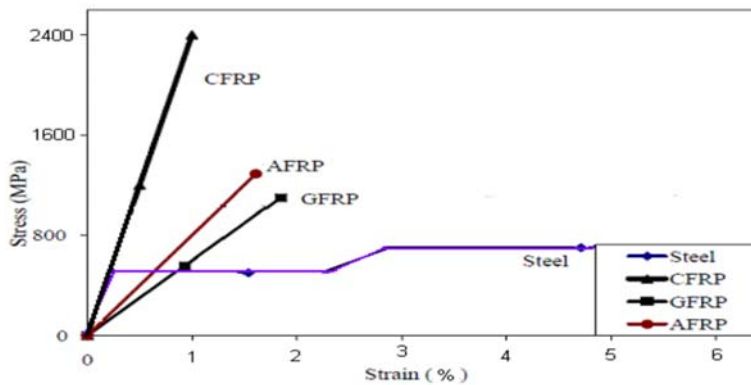


Figure 2.7: Typical stress strain relationship of FRP composite and mild steel

Mustafa Basheer Mahmood, V. C. Agarwal (2013) present study deals with the finite element modelling of control RC slabs and strengthened slabs with the help of ANSYS. ANSYS is software that is based on FE method in which modelling of RC structures is done. In this study, a control slab was modelled and the results were analyzed and then strengthened slabs were modelled and analysed. The results of the control and strengthened slabs were compared with the experimental results. It was observed that the results of the strengthened slabs are in close agreement with the experimental results. Figure 2.9 and 2.10 shows slab loading pattern and the cross-section of different FRP position

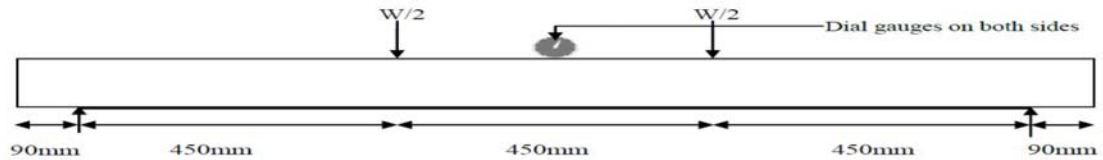


Figure 2.8: Slab loading pattern

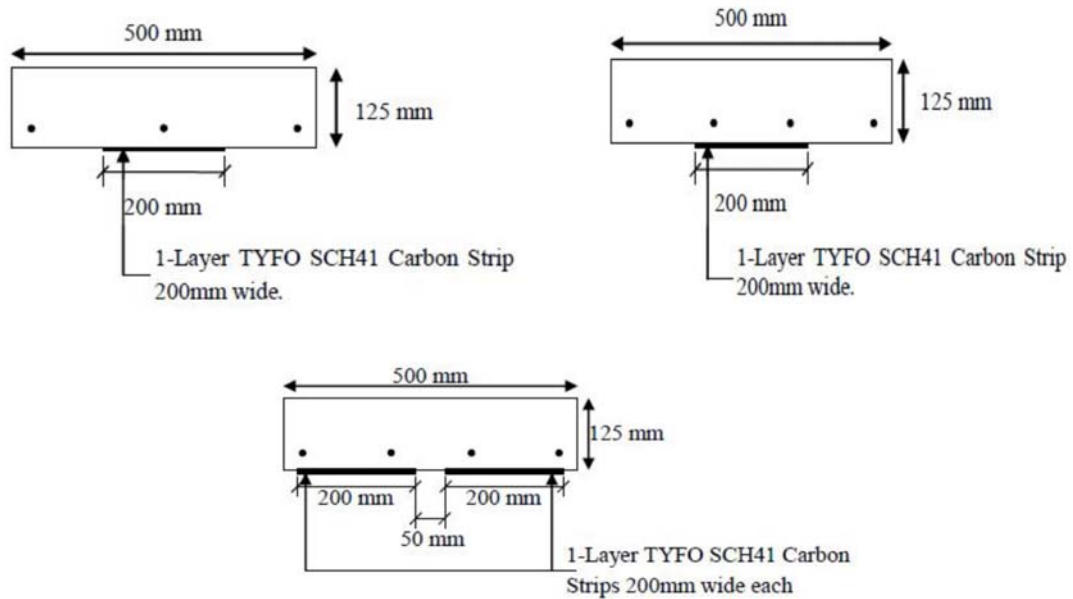


Figure 2.9: Slab cross-section with different CFRP position

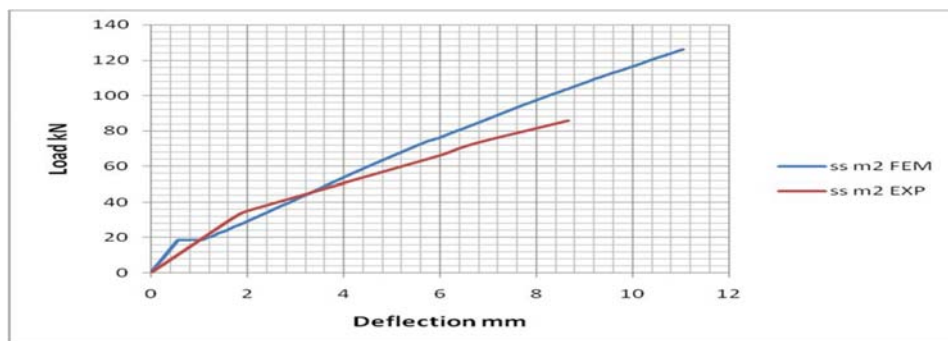


Figure 2.10: Load-deflection curve for strengthened slab mild reinforcement

Fig 2.11 shows the deflection at (82 kN) obtained from the F.E. is a flexural deflection of (6.2 mm), which is lower than the experimental deflection of (8.2 mm) about 32.258%. The other difference is the type of failure, where the experimental model failed by debonding the CFRP laminate the thing that not observed in F.E model. [21]

M.B.S Alferjani, A.A. Abdul Samad, Blkasem. S Elrawaff (2013) the use of Fiber Reinforced Polymer (FRP) is becoming a widely accepted solution for repairing and

strengthening ageing in the field of civil engineering around the world. Several researches have been carried out on reinforced concrete beams strengthened with fiber reinforced polymer composite. Some of the works were focused on shear strengthening compared with flexural strengthening that had the largest share. This paper reviews 10 articles on carbon fiber reinforced polymer strengthened reinforced concrete beams. Finally, this paper attempts to address an important practical issue that is encountered in shear strengthening of beams with carbon fibre reinforced polymer laminate. This paper also proposes a simple method of applying fibre reinforced polymer for strengthening the beam with carbon fiber reinforced polymer. Figure 2.12 shows setup of the FRP over the RC section for strengthening. [22]



Figure 2.11: Shear strengthening of reinforced concrete using CFRP laminate

Idrees M. Mahmood and Ali Ramadhan Yousif (2014) this paper presents an experimental investigation on the strengthening of two-way reinforced concrete slabs. Thirteen two-way reinforced concrete slabs with size of 1500x1000x50mm simply supported along four edges were tested. In addition to the edge support, two of the control specimens were tested and five of the slabs were preloaded with the existence of an interior support at mid line parallel to the short edge. They were loaded through two points placed at the centre along the short direction and one fourth from the exterior support along the long direction. The main variables studied were the steel reinforcement ratio (0.2% and 0.4%), Carbon Fiber Reinforced Polymers (CFRP) strip spacing (200 and 300mm c/c), strengthening condition (strengthened and preloaded) and support conditions (with and without interior support). The test results confirmed that applying CFRP strips as strengthening material can improve the load carrying capacity of the slabs up to 331% compared with the control specimens. The distinct result was that the application of CFRP strips can lead to the removal of the interior support (enlarging the panel area), the finding which allows changing the function of existing buildings. The yield line theory was used for theoretical evaluation and good agreement was found with experimental results. [24]

Fahmy A. Fathelbab, Mostafa S. Ramadan, Ayman Al-Tantawy (2014) the main purpose of this research is to study analytically the strengthening of a reinforced concrete bridge slabs due to excessive loads, using externally bonded FRP sheets technique. A commercial finite element program ANSYS was used to perform a structural linear and non-linear analysis for

strengthened slab models using several schemes of FRP sheets. A parametric study was performed to evaluate analytically the effect of changing both FRP stiffness and FRP schemes in strengthening RC slabs. Comparing the results with control slab (reinforced concrete slab without strengthening) it is obvious that attaching FRP sheets to the RC slab increases its capacity and enhances the ductility or toughness. In this paper represents the ANSYS computer program which is used in the analysis of different mechanical and structural applications based on the finite element modeling techniques. SOLID65 element is used to model the plain concrete material, since it has a capability of both cracking in tension and crushing in compression, SOLID65 element is defined by 8 nodes with three degrees of freedom at each node; translations in the nodal x, y, and z directions. The element material was assumed initially isotropic. The most important aspect of this element is the treatment of nonlinear material properties, where concrete is capable of directional cracking and crushing besides incorporating plastic and creep behavior. [25]

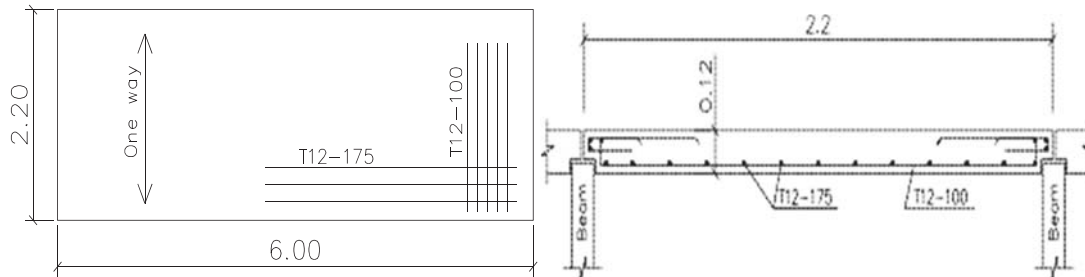


Figure 2.12: Plan and cross section details of the slab model, dimensions in meter

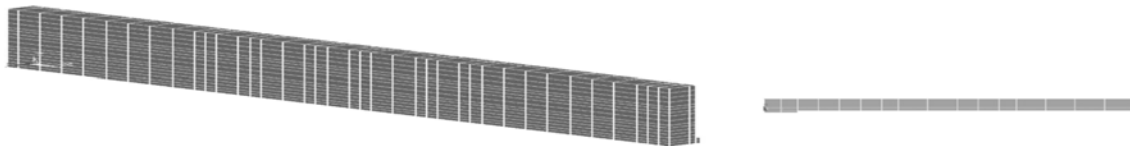


Figure 2.13: 3D and elevation of ANSYS model

Sheetal Gawas, Dr. S.V.Itti (2014) in the present work, finite element analysis of RCC slab models have been carried out. The study is based on the fact that stress and displacement variation depends on boundary conditions of slab. Present study is aimed to know the variation of displacement, stresses, in slab with different boundary conditions. Non-Linear static analysis is carried out using ANSYS 10 Software. Load on slab is calculated as per IS 875 part I for dead load and part II for live load. Parameter considered is to study the effect of opening in slab on stress and displacement. The study shows that displacement is highest in slab having simple support on all sides and stresses are least in same slab along the edges. Also slab with fixed support on all sides shows least displacement and highest stresses along the edges of the slab. [26]

CHAPTER 3

FINITE ELEMENT MODELLING OF RC SLAB

3.1 Introduction

From last two three decades, FEM of reinforced concrete structures and structural elements has become a major area of research. Choosing suitable elements, formulating proper material models and selecting proper solution method are required for a successful numerical simulation. The present work is aimed to analyze numerically the reinforced concrete slab strengthened with FRP laminates using FE method. This involves the proper choice of element, material properties, boundary conditions, solution techniques etc. In this chapter, different steps of FE modelling of the above mentioned slab is described with reference to the features available in the FE software ANSYS and models prepared are analyzed to obtain load deformation response analytically. To perform a parametric study, the numerical analysis of a RC slab with or without FRP laminates is done using different types of support condition, FRP position, FRP thickness and FRP orientation.

The structural analysis software suite, ANSYS, enables us to solve complex structural engineering problems and make better, faster design decisions. With finite element analysis (FEA) tools, it can customize and automate the simulations, and parameterize them to analyze multiple design scenarios. ANSYS Structural Mechanics software easily connects to other physics analysis tools, providing even greater realism in predicting the behavior and performance of complex products.

In nutshell, this chapter discusses the steps followed and input data required to create the model of RC slab with or without FRP in ANSYS. The validation of the FE model thus prepared is done by comparing the load deformation response with the same obtained by the layered element approach followed by previous researchers. For this purpose, the geometry, reinforcement details, support condition, loading, etc. of the RC slab and the pattern of load deformation curve without FRP are taken from the numerical work done by S. Roychowdhury and reported in his Ph.D. thesis [8]. Here ANSYS 15 has been used to create the finite element model of RC slab with and without FRP. All the necessary steps taken to create the finite model are explained in detail.

3.2 Numerical Embodiment

The numerical implementation of the finite element procedure used in the ANSYS software is based on the principles of virtual work or the postulation of minimum potential energy for assembly of the elements as formulated the following equilibrium equation:

$$[K]\{d\} + \{F\}_p + \{F\}_s + \{F\}_g + \{F\}_{\epsilon_0} - \{R\} = 0$$

The stiffness matrix [K],

$$[K] = -\Sigma \int [B]^T [D][B]dv$$

The nodal force due to the surface load,

$$\{F\}_p = -\Sigma \int [N]^T \{P\}dv$$

The nodal force due to the body load,

$$\{F\}_g = -\Sigma \int [N]^T \{g\}dv$$

The nodal force due to the initial strain,

$$\{F\}_{\epsilon_0} = \Sigma \int [N]^T [D] \{\epsilon_0\}dv$$

where [N] is the shape function matrix; {d} is the vector of nodal displacement; {R} is the vector of applied nodal force; {p} is the vector of surface load; and {g} is the vector of body load. The ANSYS software uses mainly the Newton-Raphson (N-R) method to obtain the convergent solution of the nonlinear equilibrium equation which is actually iterative to update the stiffness matrix of the system.

3.3 Model of RC Slab Structure

The RC Slab is being modeled with or without FRP laminates and validation is performed with the analytical solution of RC slab without FRP laminates as given in the Ph.D. thesis of S. Roychowdhury and shown in Figure 3.1. There are four FE models of the slab out of which one control slab (S1) is without FRP laminates and three retrofitted slab (S2, S3, S4) with FRP laminates. The dimensions of all the slab specimens are identical. The plan dimensions of all the RC slab is 1980 mm (in x-direction) and 1980 mm (in z-direction). Thickness of slab is 51 mm. The slab is reinforced with two layers of reinforcing bars (FE 500) of area 281 mm²/m provided at the bottom face only.

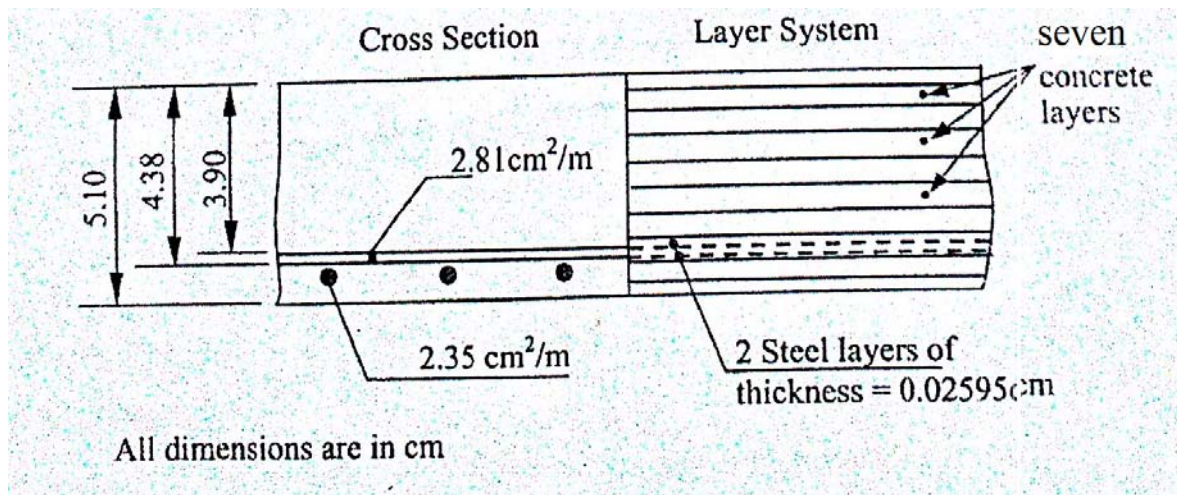
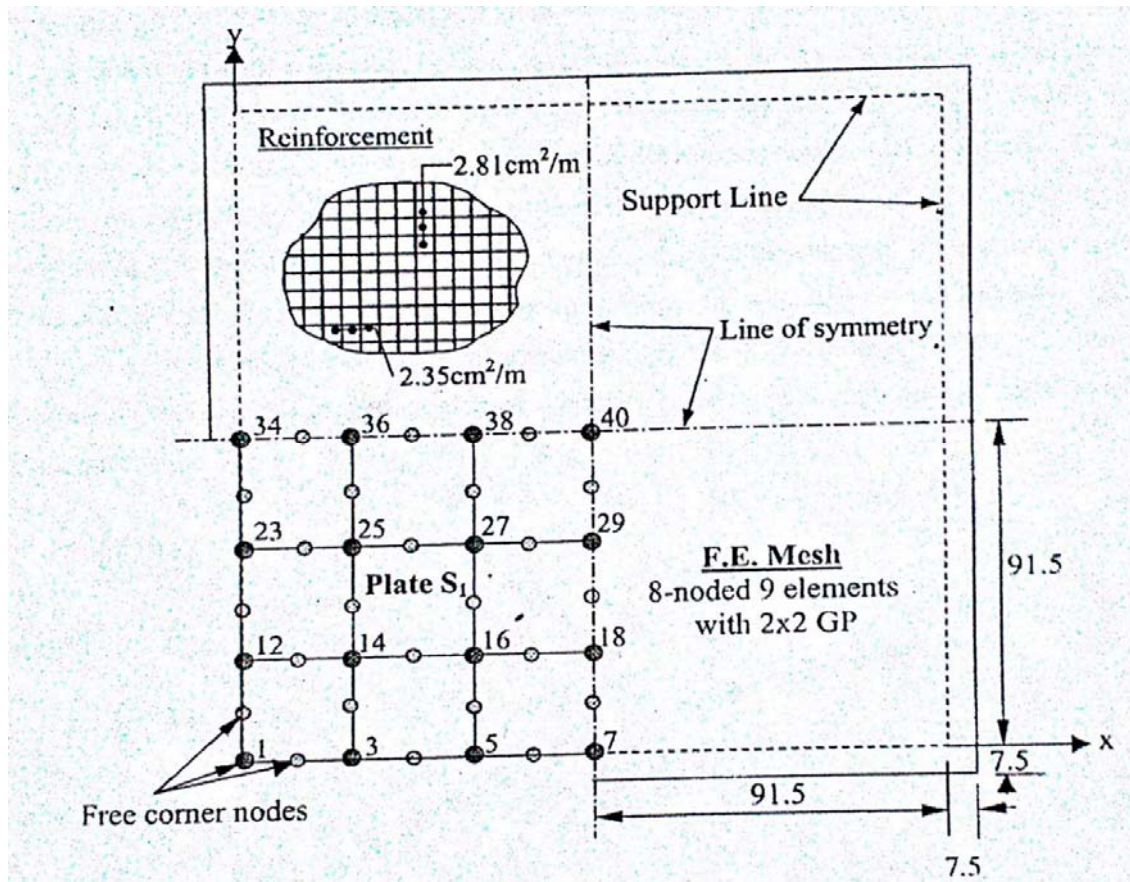


Figure 3.1: Plan and Cross section of RC slab and its FE representation [8]

3.4 Elements used in ANSYS to Model Un-retrofitted and Retrofitted RC Slab

3.4.1 Element Types

While modeling the RC slab in ANSYS, different elements are used to model concrete, steel reinforcement and FRP laminates as mentioned in table 3.1. SOLID65 element is chosen to model three dimensional concrete elements, LINK180 is adopted for flexural reinforcement bars. SOLID185 element has been taken to model the layer of FRP. Following are the brief descriptions of these elements along with the real constants required to be provided in ANSYS.

Table 3.1 – Element Types used in present F.E. model

Material Type	ANSYS Element
Concrete	Solid 65
Steel Reinforcement	Link 180
FRP Sheets	Solid 185

3.4.1.1 SOLID65

SOLID65 is used in the present work for the 3-D modeling of concrete with and without reinforcing bars (rebar). The element is capable of cracking (in three orthogonal directions) in tension and crushing in compression, plastic deformation, and creep. The most important aspect of this element is the treatment of nonlinear material properties. The rebar are capable of tension and compression, but not shear. They are also capable of plastic deformation and creep [27]. The element is defined by eight nodes having three degrees of freedom at each node: translations in the nodal x, y, and z directions. The concrete element SOLID65 is similar to a 3-D structural solid but become more superior with the addition of special cracking and crushing capabilities. [27] Figure 3.2 shows SOLID65 element.

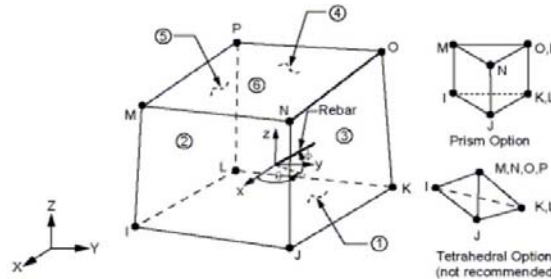


Figure.3.2 SOLID65 element [27]

3.4.1.2 LINK180

LINK180 is a 3-D spar that is useful in a variety of engineering applications. The element can be used to model trusses, sagging cables, links, springs, and so on. The element is a uniaxial tension-compression element with three degrees of freedom at each node: translations in the nodal x, y, and z directions. Tension-only (cable) and compression-only (gap) options are supported. As in a pin-jointed structure, no bending of the element is considered. Plasticity, creep, rotation, large deflection, and large strain capabilities are included.

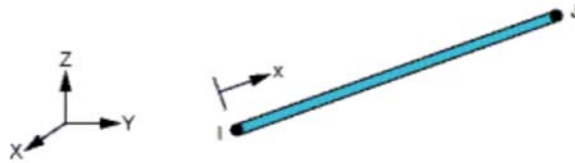


Figure 3.3: LINK180 Geometry [27]

LINK180 includes stress-stiffness terms in any analysis that includes large-deflection effects. Elasticity, isotropic hardening plasticity, kinematic hardening plasticity, Hill anisotropic plasticity, nonlinear hardening plasticity, and creep are supported. To simulate the tension-/compression-only options, a nonlinear iterative solution approach is necessary [27].

3.4.1.3 SOLID185

SOLID185 is used for 3-D modeling of solid structures. It is defined by eight nodes having three degrees of freedom at each node: translations in the nodal x, y, and z directions. The element has plasticity, stress stiffening, creep, large deflection, and large strain capabilities. SOLID185 is available in two forms.

- ❖ Homogeneous Structural Solid.
- ❖ Layered Structural Solid.

In the current study layered structural Solid185 is used to simulate the various layer properties of GFRP laminates. The layered section definition is given by section (SECxxx) commands in ANSYS.

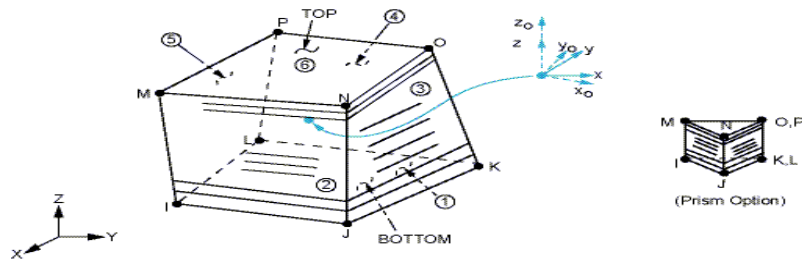


Figure 3.4: SOLID185 Layered Structural Solid Geometry. [27]

3.4.2 Real Constants

The real constants for this model are shown in Table 3.2 here for individual elements contain different real constants. There is no real constant set exists for the SOLID185 element.

Table 3.2 Real Constants for present Model

Real Constant Set	Element Type	Constants			
			Real Constant s for Rebar 1	Real Consta nts for Rebar 2	Real Constan ts for Rebar 3
1	Solid 65	Material Number	0	0	0
		Volume Ratio	0	0	0
		Orientation Angle	0	0	0
		Orientation Angle	0	0	0
2	Link 180	Cross-sectional area (m ²)	51.6 e ⁻⁶		
3	SOLID 185	No real constant is required			

Real Constant Set 1 is used for the Solid65 element. The values can be entered for Material Number, Volume Ratio, and Orientation Angles. The material number refers to the type of

material for the reinforcement. The volume ratio refers to the ratio of steel to concrete in the element. The orientation angles refer to the orientation of the reinforcement in the smeared model (Figure 3.7c). ANSYS 15.0 allows the user to enter one rebar material in the concrete. Each material corresponds to x, y, and z directions in the element (Figure 3.2). The reinforcement has uniaxial stiffness and the directional orientation is defined by the user. In the present study the slab is modeled using discrete reinforcement. Therefore, a value of zero was entered for all real constants which turned the smeared reinforcement capability of the Solid65 element.

Real Constant Sets 2 is defined for the Link180 element. Here only the value for cross-sectional area is entered.

No real constant is required for Real constant set 3 used for SOLID 185 element.

3.5 Modelling of Materials Behavior

In Reinforced concrete structures the behavior of concrete and reinforcing steel are different. Steel can be considered a homogeneous material and its material properties are generally well defined. Concrete is a heterogeneous material made up of cement, fine and coarse aggregates. Its mechanical properties scatter more widely and cannot be defined easily. For the purpose of analysis and design, however, in the macroscopic sense concrete is often considered a homogeneous material. The typical stages in the load-deformation behavior of a reinforced concrete are illustrated in Figure 3.5.

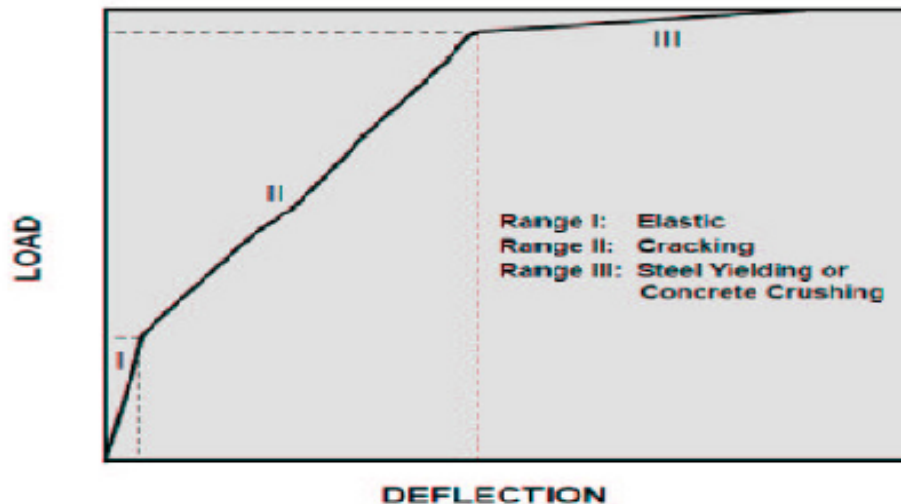


Figure 3.5: Typical load-displacement response of RC element

This nonlinear response can be divided into three ranges of behavior: the un-cracked elastic stage, the crack propagation and the plastic (yielding or crushing) stage. This nonlinear response is caused by three major effects

- ❖ Tension crack of concrete
- ❖ Yielding of the reinforcement
- ❖ Crushing in compression of concrete

The stress-strain relation of concrete is not only nonlinear, but is different in tension than in compression. Because of these complexities structures should be based on separate material models for reinforcing steel and concrete, which are then combined along with models of the interaction between the two constituents to describe the behavior of the composite reinforced concrete material. [5]

3.5.1 Finite Element modelling of concrete

The concrete stress-strain relation, in compression, exhibits nearly linear elastic response up to about 30% of the compressive strength. This is followed by gradual softening up to the concrete compressive strength, when the material stiffness drops to zero. Beyond the compressive strength the concrete stress-strain relation exhibits strain softening until failure takes place by crushing.

3.5.1.1 Concrete Models

Many mathematical models are available in ANSYS to simulate the mechanical behavior of concrete. These can be divided into four main groups:

- ❖ Orthotropic models,
- ❖ Nonlinear elastic models,
- ❖ Plastic models and
- ❖ Endochronic models

The nonlinear response of concrete is simulated by linear elastic model with variable moduli. The model is particularly well suited for finite element calculations. When unloading takes place, the behavior can be approximated by moduli which are different from those under loading conditions. As a result, the variable moduli model is unable to describe accurately the behavior of concrete under high stress condition, near the compressive strength and in the strain softening range.

3.5.1.2 Failure Criteria for Concrete

The model is capable of predicting failure for concrete materials. Both cracking and crushing failure modes are accounted for. The two input strength parameters i.e., ultimate uniaxial tensile and compressive strengths are needed to define a failure surface for the concrete. Consequently, a failure criterion of the concrete due to a multiracial stress state can be calculated (William and Warnke 1975).

A three-dimensional failure surface for concrete is shown in Figure 3.6. The most significant nonzero principal stresses are in the x and y directions, represented by σ_{xp} , σ_{yp} , respectively. Three failure surfaces are shown as projections on the σ_{xp} - σ_{yp} plane. The mode of failure is a function of the sign of σ_{zp} (principal stress in the z direction). For example, if σ_{xp} and σ_{yp} are both negative (compressive) and σ_{zp} is slightly positive (tensile), cracking would be predicted in a direction perpendicular to σ_{zp} . However, if σ_{zp} is zero or slightly negative, the material is assumed to crush.

In a concrete element, cracking occurs under tension when the principal tensile stress in any direction lies outside the failure surface. After cracking, the elastic modulus of the concrete element is set to zero in the direction parallel to the principal tensile stress direction. Crushing occurs when all principal stresses are compressive and lie outside the failure surface; subsequently, the elastic modulus is set to zero in all directions, and the element effectively disappears.

A pure “compression” failure of concrete is unlikely. In a compression test, the specimen is subjected to a uniaxial load. Secondary tensile strains induced by poisson’s effect occur perpendicular to the load. Because concrete is relatively weak in tension, these actually cause cracking and the eventual failure. Therefore, in this study, the crushing capability was turned off and cracking of the concrete had controlled the failure of the finite element models. [2]

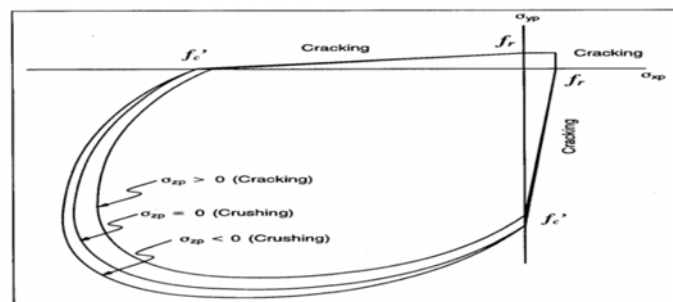


Figure 3.6: Dimension failure surface for concrete

3.5.2 Finite Element Modeling Reinforcing Steel

Analysis of RC structures using the finite element method requires a simple accurate way of representing the reinforcement. Three alternative models have been usually used to simulate the behavior reinforcement, which are:

- ❖ Discrete reinforcement model.
- ❖ Embedded reinforcement model.
- ❖ Smeared reinforcement model.

Discrete reinforcement model

The reinforcement in the discrete model (Figure 3.7a) uses bar or beam elements that are connected to concrete mesh nodes. Therefore, the concrete and the reinforcement mesh share the same nodes and concrete occupies the same regions occupied by the reinforcement. A drawback to this model is that the concrete mesh is restricted by the location of the reinforcement and the volume of the steel reinforcement is not deducted from the concrete volume.

Embedded reinforcement model

The embedded model (Figure 3.7b) assumes that the reinforcing bar as an axial member is built into the iso-parametric element whose displacements are consistent with those of the element. Bars are restricted to lie parallel to the local coordinate axes of the basic element and perfect bond must be assumed between concrete and the reinforcement.

Smeared reinforcement model

The smeared model (Figure 3.7c) assumes that reinforcement is uniformly spread throughout the concrete elements in a defined region of the FE mesh. This approach is used for large-scale models where the reinforcement does not significantly contribute to the overall response of the structure.

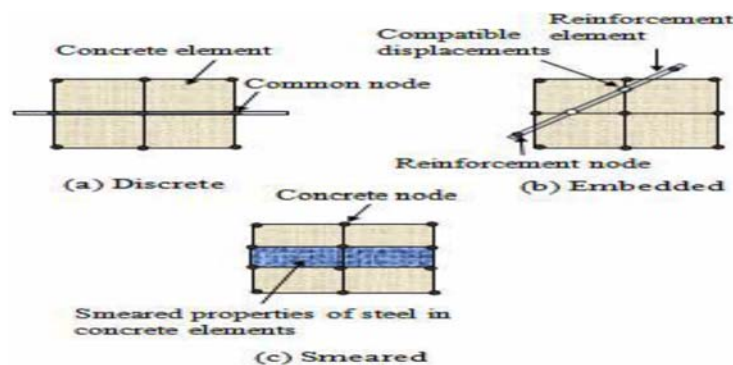


Figure 3.7: Models for Reinforcement in Reinforced Concrete (Tavarez 2001);
(a) Discrete; (b) embedded; and (c) smeared [1]

3.5.3 Input for Material Properties

Material plays an important role in ANSYS modeling. Correct values of material properties have to be given as input in ANSYS. Cube compressive strength and all other properties of concrete are taken from the previous experimental study by Taylor et.al.[30] and the numerical analysis has been conducted by Owen et.al. [29]

The modulus of elasticity of the concrete (E_c) and the Poisson's ratio (ν) are mandatory information for the material definition. In ANSYS, E_x is the modulus of elasticity of the concrete (E_c), and P_{RXY} is the Poisson's ratio (ν). The modulus is based on the equation (as per Cl. 6.2.3.1 of IS 456: 2000)[28]

- ❖ $f_{ck} = 35 \text{ Mpa}$
- ❖ $E_c = 5000\sqrt{f_{ck}} = 29,580.39892 \text{ MPa}$.
- ❖ Poisson's ratio = 0.18

Parameters needed to define the material properties for the slab models are given in Table 3.3.

Table 3.3 Material Properties for present Model

Material Model Number	Element Type	Material Properties		
		Multi Linear Isotropic		
		Reference point	Strain	Stress(MPa)
1	SOLID 65	1	0	0
		2	0.0002	0.665
		3	0.0004	1.26
		4	0.0006	1.785
		5	0.0008	2.24
		6	0.001	2.625
		7	0.0012	2.94
		8	0.0014	3.185
		9	0.0016	3.36
		10	0.0018	3.465
		11	0.002	3.5
		12	0.0035	3.5

1	SOLID 65	Non-metal Plasticity(Concrete)	
		Shear transfer coefficient for open crack	0.3
		Shear transfer coefficient for closed crack	1
		Uniaxial tensile cracking stress	3.79 e6
		Uniaxial crushing stress	-1
		Biaxial crushing stress	0
		Biaxial crushing stress	0
		Ambient Hydrostatic stress state	0
		Biaxial crushing stress under ambient hydrostatic stress state	0
		Uniaxial crushing stress under ambient hydrostatic stress state	0
		Stiffness multiplier for cracked tensile condition	0
		2	LINK 180
E _x	2.069 e11		
P _{RXY}	0.3		
Bilinear Isotropic			
Yield stress	3.759 e8		
	Tang Modulus	3 e10	
3	SOLID185	Linear Orthotropic	
		E _x (MPa)	20700
		E _y (MPa)	7000
		E _z (MPa)	7000
		V _{xz}	0.26
		V _{xy}	0.26
		V _{yz}	0.3
		G _{xz} (MPa)	1520
		G _{xy} (MPa)	1520
G _{yz} (MPa)	2650		

Material no.1

Material model number 1 refers to the Solid 65 element. The Solid65 element requires linear isotropic and multi-linear isotropic material properties to model concrete properly. The multilinear isotropic material uses the Von-Mises failure criterion along with the William and Warnke (1974) model [23] to define the failure of the concrete. In ANSYS, E_x is the modulus of elasticity of the concrete (E_c), and P_{RXY} is the poisson's ratio (ν). The modulus is based on the equation (as per cl. 6.2.3.1 of IS 456: 2000) [27].

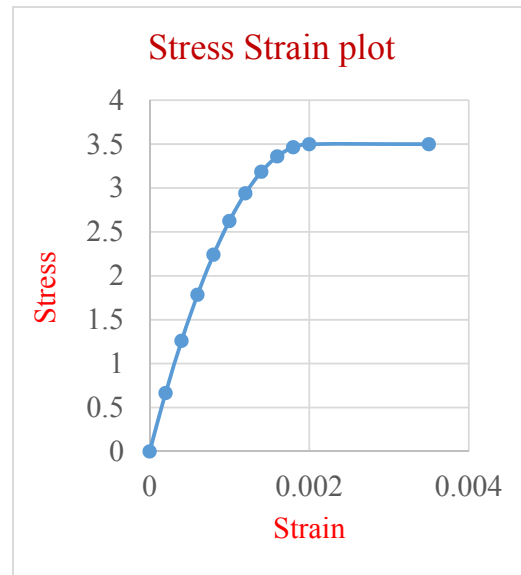
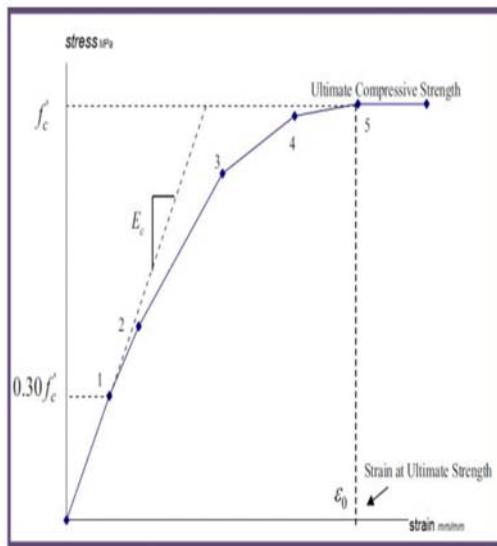


Figure 3.8: Uniaxial Stress-strain curve for concrete

In tension, the stress-strain curve for concrete is approximately linear elastic up to the maximum tensile strength. After this point, the concrete cracks and the strength decreases gradually to zero.

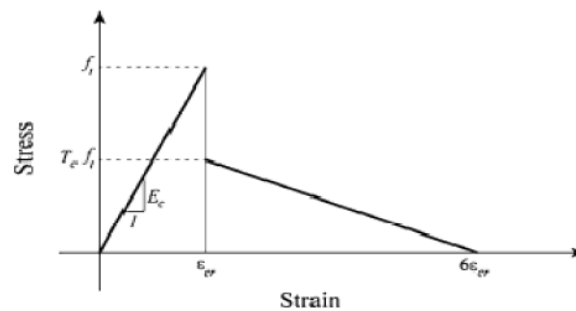


Figure 3.9: Post cracking model of concrete in tension [26]

The shear transfer coefficient for open and closed cracks represent the condition at the crack face while it is open (loaded) or closed (reversed load), respectively. The value of these coefficient ranges from 0.0 to 1.0, with 0.0 representing a smooth crack (complete loss of shear transfer) and 1.0 representing a rough crack (no loss of shear transfer) (ANSYS, Release 15.0 [27]). Convergence problem occurs when the shear transfer coefficient for the open crack drops below 0.2. No deviation of response occurs with the change of coefficient. The uniaxial cracking stress is based upon the modulus of rupture. This value is determined using the following equation (as per Cl.6.2.2 of IS 456; 2000[IS 456]) [28].

$$f_{cr} = 0.7\sqrt{f_{ck}}$$

Material no.2

Material Model Number 2 refers to the Link 180 element. The Link 180 element is being used for steel reinforcement and it is assumed to be bilinear isotropic. The bilinear isotropic material is also based on the Von Mises failure criteria. The bilinear model requires the yield stress (f_y), as well as the hardening modulus of the steel to be defined. The steel for the finite element models was assumed to be an elastic-perfectly plastic material and identical in tension and compression. Figure 3.10 shows the stress-strain relationship used in the study.

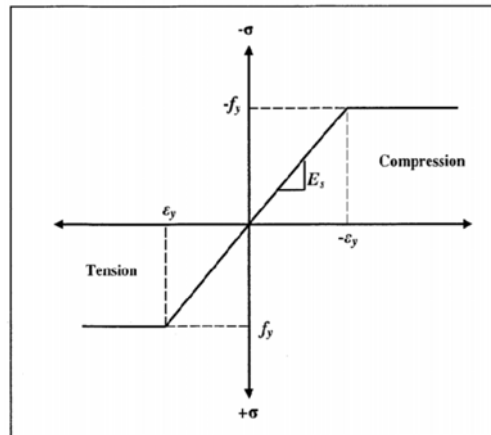


Fig.3.10 Stress-strain curve for steel reinforcement [4]

Material no.3

As for the modeling of GFRP composites in ANSYS software, a linear orthotropic material model is used. Material properties for GFRP as specified by previous literature [2] are taken in the present study and shown in Table 3.3

3.6 Details of the Present Finite Element Model

The two way RC slab is modeled as a volumes. Due to symmetry in geometry of the RC slab and loading, the Finite Element Analysis is done for one quarter of the slab. Since a quarter of the slab is modeled, the thickness of the slab model is 51.1 mm, with length 915mm and width 915 mm. The dimensions for the concrete volume are shown in Table 3.4. The zero values for the z-coordinates coincide with the center of the cross-section for the RC slab. The volume is shown in Figure 3.11, SOLID 65 element are chosen to discretize this concrete volume.

Table 3.4 Dimensions for concrete volume

ANSYS	Concrete (mm)	
X1,X2 X -cooriantes	0	915
Y1,Y2 Y-coordinates	0	51
Z1,Z2 Z -cooriantes	0	915

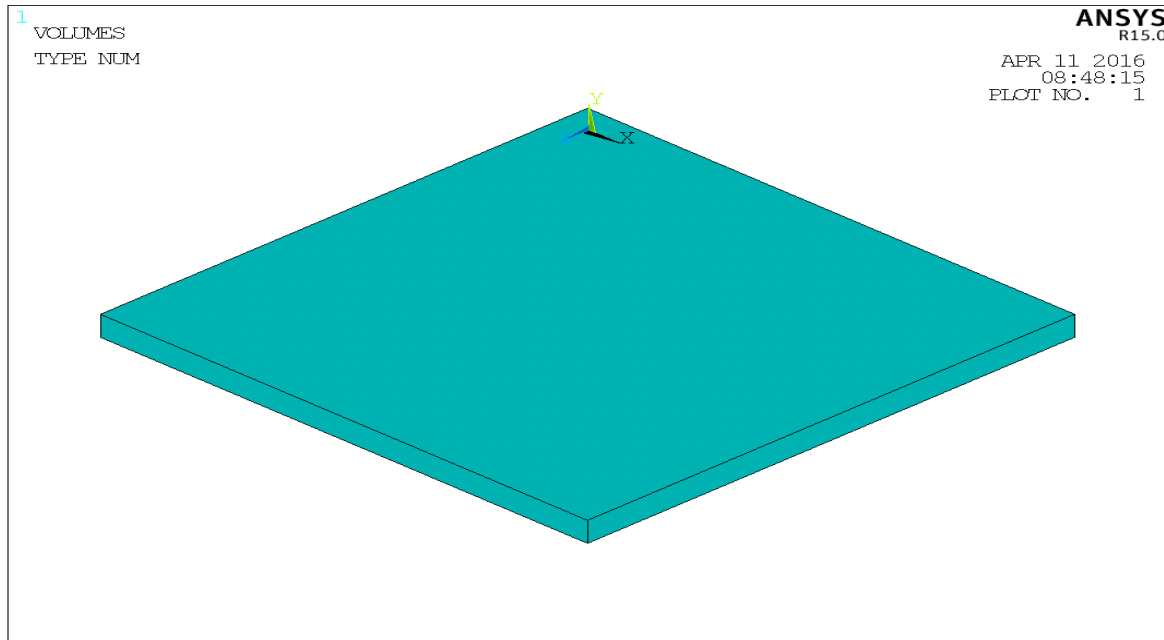


Figure 3.11: Volume created in ANSYS

Link180 elements are used to create the flexural reinforcement as shown in figure 3.15. The reinforcement elements are connected to the nodes of SOLID 65 elements at a specific depth keeping a clear cover at bottom.

Solid 185 elements are employed to model the GFRP composites that are attached at the bottom surface of the lowermost SOLID 65 elements like the LINK 180 elements. The areas are created for individual elements where we have intended to give the GFRP layers.

The perfect bonding was assumed between elements. The same approach was adopted for FRP composites as shown in Fig.3.12. The perfect bond assumption may be achieved using the high strength of the epoxy or by mechanical anchors used to attach the FRP sheets to the control slab.

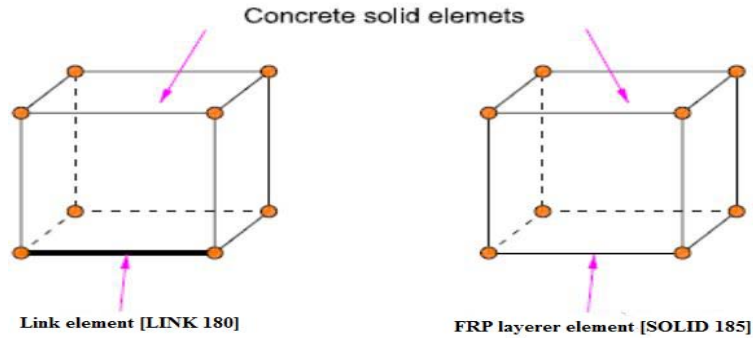


Figure 3.12: Element connectivity: (a) Concrete solid element and link element;
 (b) Concrete solid element and FRP layered elements

3.6.1 Meshing

For more exact results from the Solid65 element, the use of a rectangular mesh is recommended. For the purpose of present analysis, the concrete volume divided into seven layer with two reinforcement steel layers throughout the thickness of the slab shown in fig.3.12. There are 36 numbers of elements at the top surface of the slab when meshed the slab.

Table 3.5 Mesh Attributes for the Model

Model Parts	Material Number	Real Constant
Concrete slab	1	1
Reinforcement bar	2	2
GFRP layer	3	N/A

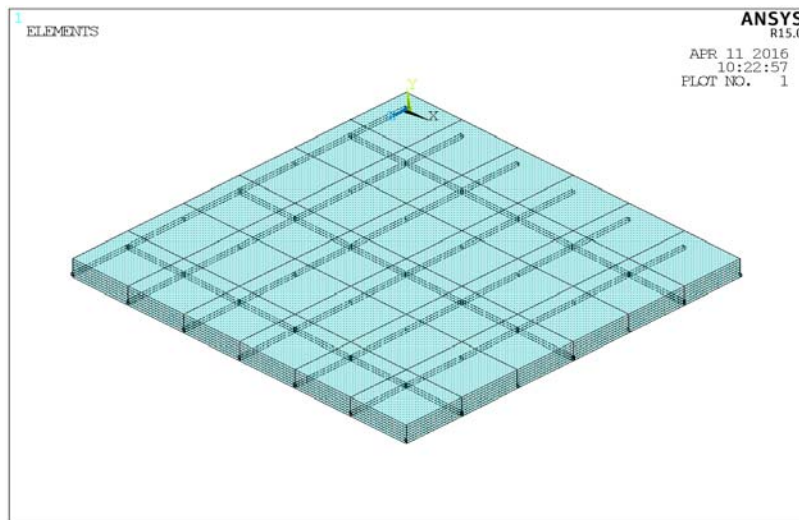


Figure 3.13: Mesh of the quarter volume of RC slab with rebar arrangement

3.6.2 Loading & Boundary Condition

Displacement boundary conditions are needed to constrain the model to get a unique solution. To ensure that the model acts the same way as the experimental and analytical slab boundary conditions need to be applied at points of symmetry, and where the support exist for control slab. The symmetry boundary conditions are set first. The model being used is symmetric about two planes. Nodes defining a vertical plane through the slab cross-section centroid define a plane of symmetry. To model the symmetry, nodes on this plane must be constrained in the perpendicular direction. These nodes (at $X=915$) therefore, have a degree of freedom constraint $U_x = 0$. Second, all nodes selected at $Z = 0$ define another plane of symmetry. These nodes were given the constraint $U_z = 0$. The support was modeled in such a way that a roller was created. A single line of nodes along the Z direction (at $X=0$ and $Y=0$) and X direction (at $Z=0$ and $Y=0$) were given constraint in the U_y , and U_z directions, applied as constant values of 0. By doing this, the slab will be allowed to rotate at the support.

A uniformly distributed load was applied over the span of the slab as increased gradually by 0.56 KN in each increment for mainly the control slab. This uniformly distributed load is applied as a point load on each and every top nodes of that slab. There were total 49 number of nodes at the top of the slab among these nodes 4 corner node, 24 edge (continuous edge and support edge) nodes loaded as $1/4^{\text{th}}$ and $1/8^{\text{th}}$ times of the load at each interior node shown in fig.3.14.

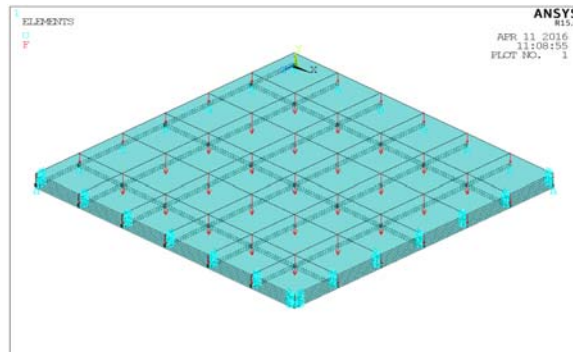


Figure 3.14: Application of loading and boundary condition on the RC slab model

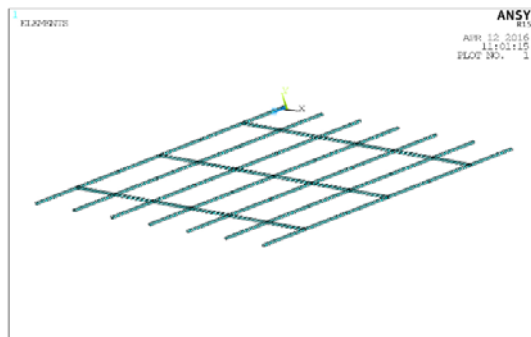


Figure 3.15: Modelling of reinforcement bars

3.6.3 Solution Control for Non-Linear Solution

In nonlinear analysis, the total load applied to a finite element model is divided into a series of load increments called load steps. After the completion of each incremental solution, the stiffness matrix of the model is adjusted to reflect nonlinear changes in structural stiffness before proceeding to the next load increment. The Newton–Raphson equilibrium iterations for updating the model stiffness are used in the nonlinear solutions. Prior to each solution, the Newton-Raphson approach assesses the out-of-balance load vector, which is the difference between the restoring forces (the loads corresponding to the element stresses) and the applied loads. Subsequently, the program carries out a linear solution using the out-of-balance loads and checks for convergence. If convergence criteria are not satisfied, the out-of-balance load vector is re-evaluated, the stiffness matrix is updated, and a new solution is carried out. This iterative procedure continues until the results converge. In this study, convergence criteria for the reinforced concrete solid elements are based on force and displacement, and the convergence tolerance limits are set as 0.1 for both force and displacement in order to obtain the convergence of the solutions [4].

For the nonlinear analysis, automatic time stepping in the ANSYS program predicts and controls the load step sizes. Based on the previous solution history and the physics of the models, if the convergence behavior is smooth, automatic time stepping will increase the load increment up to the given maximum load step size. If the convergence behavior is abrupt, automatic time stepping will bisect the load increment until it is equal to a selected minimum load step size.

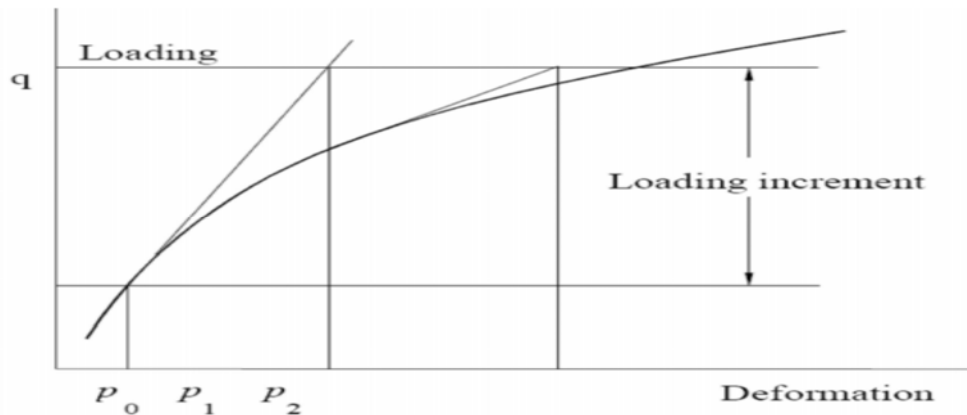


Figure 3.16: Nonlinear solutions as Newton-Raphson approach

The maximum and minimum load step sizes are required for the automatic time stepping. The total load is to be divided into number of suitable load steps (load increments) by conducting a few trial analyses until a smooth load versus deflection curve is obtained.

In ANSYS, the Solution Controls command dictates the use of a linear or non-linear solution for the finite element model. Typical commands utilized in a nonlinear static analysis are shown in Table 3.6.

Table 3.6 Commands used to Control Nonlinear Analysis

Analysis Options	Small Displacement
Calculate Prestress Effects	No
Time at End of Load step	1
Automatic Time Stepping	On
Number of Substeps	20
Max. no. of Substeps	1000
Min. no. of Substeps	5
Write items to Result File Frequency	All Solution Items
	Write Every Substep

In the particular case considered in this thesis the analysis is small displacement and static. The time at the end of the load step refers to the ending load per load step. Table 3.6 shows the first load step taken in the analysis. The sub steps are set to indicate load increments used for this analysis. The commands used to control the solver and outputs are shown in Table 3.7

Table 3.7 Commands Used to Control Output

Equation Solvers	Sparse Direct
Number of Restart Files	1
Frequency	Write Every Sub-

The commands used for the nonlinear algorithm and convergence criteria are shown in Table 3.8. All values for the nonlinear algorithm are set to defaults. The values for the convergence criteria are set to defaults except for the tolerances. Table 3.9 shows the commands used for the advanced nonlinear settings. The program behavior upon non convergence for this analysis is set such that the program will terminate but not exit. The rest of the commands are set to defaults as in ANSYS help [27].

Table 3.8 Nonlinear Algorithm and Convergence Criteria Parameters

Line search	Off	
DOF solution predictor	Prog chosen	
Maximum number of iteration	350	
Cutback control	Cutback according to predicted number of iteration	
Equiv. plastic strain	0.15	
Explicit creep ratio	0.1	
Implicit creep ratio	0	
Incremental displacement	10000000	
Points per cycle	13	
Set convergence criteria		
Label	F	U
Ref. value	Calculated	Calculated
Tolerance	0.1	0.1
Norm	L2	L2
Min. Ref.	Not applicable	Not applicable

Table 3.9 – Advanced Nonlinear Control Settings Used

Program behavior upon non convergence	Terminate but do not exit
Nodal DOF sol'n	0
Cumulative iter	0
Elapsed time	0
CPU time	0
Stabilization	Constant Stabilization
Control	Energy dissipation
Value	0.5

3.7 Steps for the development of the slab model with or without FRP

ANSYS program system consists of a solution core and several user interfaces. The solution core offers capabilities for variety of structural analysis tasks, such as: stress and failure analysis, transport of heat and humidity, time dependent problems (creep, dynamics), and their interactions. Solution core offers a wide range of 2D and 3D continuum models, libraries of finite elements, material models and solution methods. User interfaces are specialized on certain functions and thus one user interface need not necessarily provide access to all features of ANSYS solution core. This limitation is made in order to maintain transparent and user friendly applications of ANSYS.

The ANSYS program has three main processing windows

- ❖ **Pre-processor**: Input for element type used, real constant for some element, assigning material property, geometrical model and meshing the object to elements and nodes.
- ❖ **Solution**: Input for loading and boundary condition, solution control, run the program to analysis.
- ❖ **General Post-processor**: Access to a wide range of graphical and numerical results.

In **pre-processor** window, following steps are performed:-

- ❖ **Step1**: Different elements, compatible with different materials are chosen as described in section 3.4
- ❖ **Step2**: Real constants are given for solid 65 and link180 element as described in section 3.4.2
- ❖ **Step3**: Various material models are created depending on different material properties as described in section 3.5.3
- ❖ **Step4**: Solid geometry of FE model is generated by creating different size of block as a volume. It has been presented in Fig. 3.11.
- ❖ **Step5**: Solid volumes are then discretized into a finite number of nodes and element followed by assigning element type, real constant, material property to the element and meshed volume is created, shown in fig. 3.12.

- ❖ **Step6:** Node merging followed by key point merging is done to add different meshed volume and create a single entity object. Following the above steps PCC structure is modeled.
- ❖ **Step7:** As the discrete model of reinforcement is used in the current study the reinforcement is modeled by creating element through nodes followed by assigning appropriate material properties. Following this step RCC structure i.e. control slab is modeled. It has been presented in Fig. 3.13. Reinforcement modeling has been presented in Fig. 3.14.
- ❖ **Step8:** By following the above steps retrofitted specimen is also created under different retrofitting scheme which are presented in the next section.

In **solution** window following step is performed:-

- ❖ **Step9:** Boundary condition and loading is applied and run the program for analyzing those specimens. A loaded specimen model with boundary condition has also been presented in figure 3.16.

In **Post-processor** window following step is performed:-

- ❖ **Step10:** A wide range of graphical and numerical results i.e. output of analysis is generated and presented in chapter-4.

3.8 Model of Retrofitted Material under Different Retrofitted Setup

The present study encompasses the suitability of different retrofitting mode for RC two way slab strengthened with FRP. For this purpose, different retrofitting setup have been adopted and followed in the modeling of retrofitted RC two way slab in ANSYS.

- ❖ **Setup 1** (By Varying the FRP Location at the Bottom of the RC Slab)

1. Two way RC slab with support edge FRP
2. Two way RC slab with continuous edge FRP
3. Two way RC slab with diagonal FRP

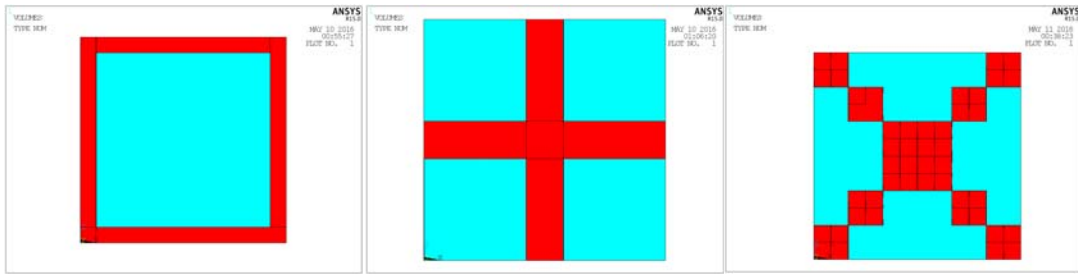


Figure 3.17: Locations of FRP at the bottom of the slab

❖ **Setup 2** (By Increasing the FRP area at different locations of the RC Slab)

By increasing the FRP area from 30% to 100% (Fully retrofitted RC slab) gradually for all three FRP locations of the slab

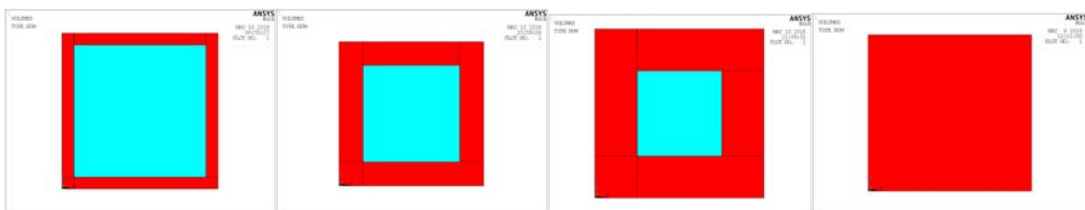


Figure 3.18: Increasing the FRP area along support edge

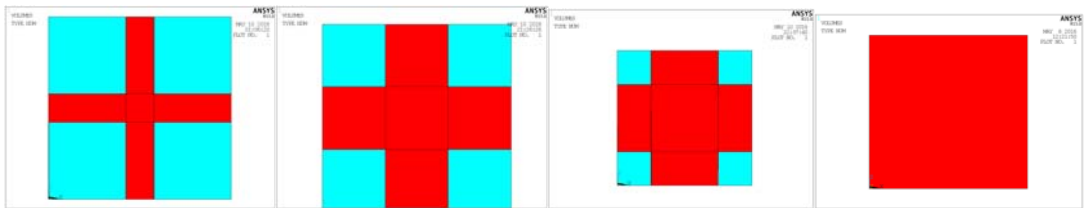


Figure 3.19: Increasing the FRP area along continuous edge

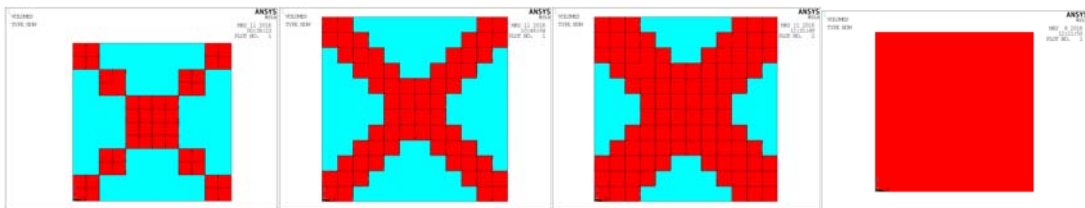


Figure 3.20: Increasing the FRP area along diagonal

❖ **Setup 3** (By Varying the numbers of FRP layers of RC slab)

By varying the number of FRP layers like 2, 3 and 5 layers for all three FRP locations of the slab

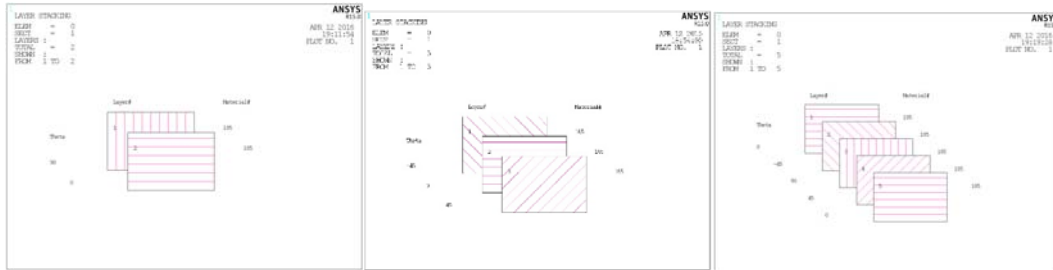


Figure 3.21: Increasing no of layers of the FRP

❖ **Setup 4** (By Varying FRP layer thickness of RC slab)

By varying 3mm and 5mm FRP layers for all three FRP locations of the slab

❖ **Setup 5** (By Varying the orientation of FRP layers of the RC Slab)

By changing the orientation like 45, 60 and 90 degree for all three FRP locations.

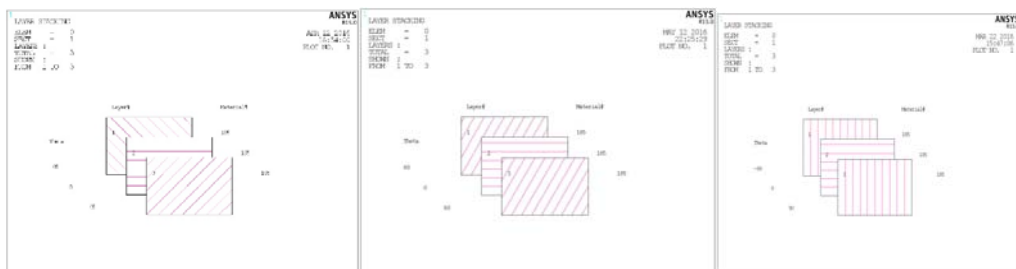


Figure 3.22: Changing the orientation of the FRP layers

Based on the information mentioned above, the finite element model for all the control and retrofitted slabs are developed in ANSYS (version 15.0) for the present numerical study.

CHAPTER 4

RESULTS & DISCUSSIONS

4.1 Introduction

The finite element models of reinforced concrete slab strengthened with FRP laminates prepared using the software ANSYS as described in the previous chapter are analyzed against gradually increasing uniformly distributed transverse load to assess the suitability and effectiveness of the process of strengthening of slab using FRP. The results of this analysis of a large number of RC slab are presented and discussed in this chapter. To begin with the numerical experiments, the finite element model of a reinforced concrete slab analyzed numerically by previous researchers [8] has been taken as a control slab and the results are compared with the previous results to validate the present model. To assess the applicability of the present approach, different case studies have been performed by varying different parameters like support condition, location of FRP laminates, the width of FRP band, the thickness of FRP, number of layers in FRP laminates, the orientation of fibers etc. All these results are reported in the following sections.

4.2 Validation of proposed model

For the purpose of validation of the present numerical approach, a simply supported reinforced concrete slab analyzed numerically earlier by S. Roychowdhury and reported in his Ph.D. thesis [8] has been taken presently for finite element analysis using ANSYS. This simply supported square reinforced concrete slab was tested previously by Taylor et.al.[30] and was analyzed numerically by Owen et.al. [29] and S. Roychowdhury [8] under uniformly distributed mechanical load is analyzed here for the verification of the results obtained from the present formulation with ANSYS. The details of this slab thus taken from the same reference are used to prepare the model in ANSYS. The plan dimension of the full slab is 1980 mm (in x-direction) and 1980 cm (in z-direction). Thickness of slab is 51 mm. The uniformly spaced reinforcing bars are provided at the bottom face of the slab only. All nodes at simply supported boundary are assumed to be free in the horizontal direction. The details of the problem i.e. geometrical data, finite element discretization, boundary condition and material properties of concrete and steel shown in Figure 4.1. Material properties for concrete and steel are considered from the same reference and given here in Table 4.1. For the purpose of present analysis, 8-noded SOLID 65 elements are used. Seven concrete layers across the thickness, as considered previously, are replaced by seven SOLID 65 elements. The steel reinforcements are modeled using LINK 180 elements connecting the nodes of SOLID 65 elements. The LINK 180 elements in both the steel layers has unidirectional properties parallel to each of the two the longitudinal directional of the elements Due to symmetry of geometry, boundary condition and load, only one-fourth portion of the slab is analyzed by ANSYS. The finite element

discretization of the present model is shown in Figure 4.2. Uniformly distributed load is increased gradually by 0.56 KN in each increment.

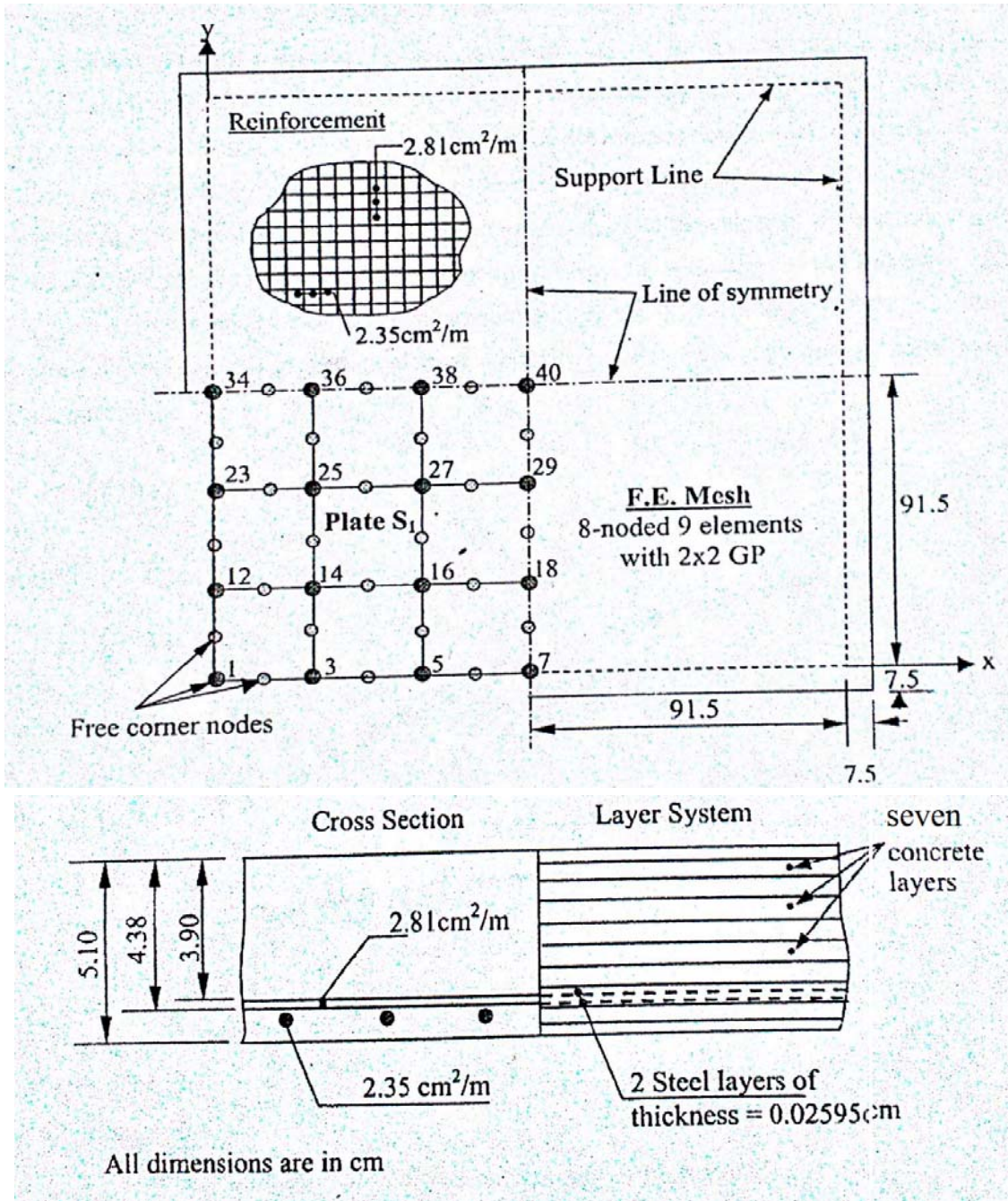


Figure 4.1: Details of RC slab and its finite element representation [8]

Table 4.1: Material Properties for Concrete and Steel [8]

Concrete		Steel	
Young's Modulus	32420 N/mm ²	Young's Modulus	206910 N/mm ²
Poisson's Ratio	0.18	Yield Stress	375.9 N/mm ²
Ultimate Comp. Strength	35 N/mm ²	Thermal Coeff.	0.00001
Ultimate Tensile Strength	3.79N/mm ²		
Tension Stiff. Coeff.α	0.6		
Tension Stiff. Coeff.ε _m	0.002		
Thermal Coeff.	0.00001		
Ultimate Comp. Strain ε	0.0035		

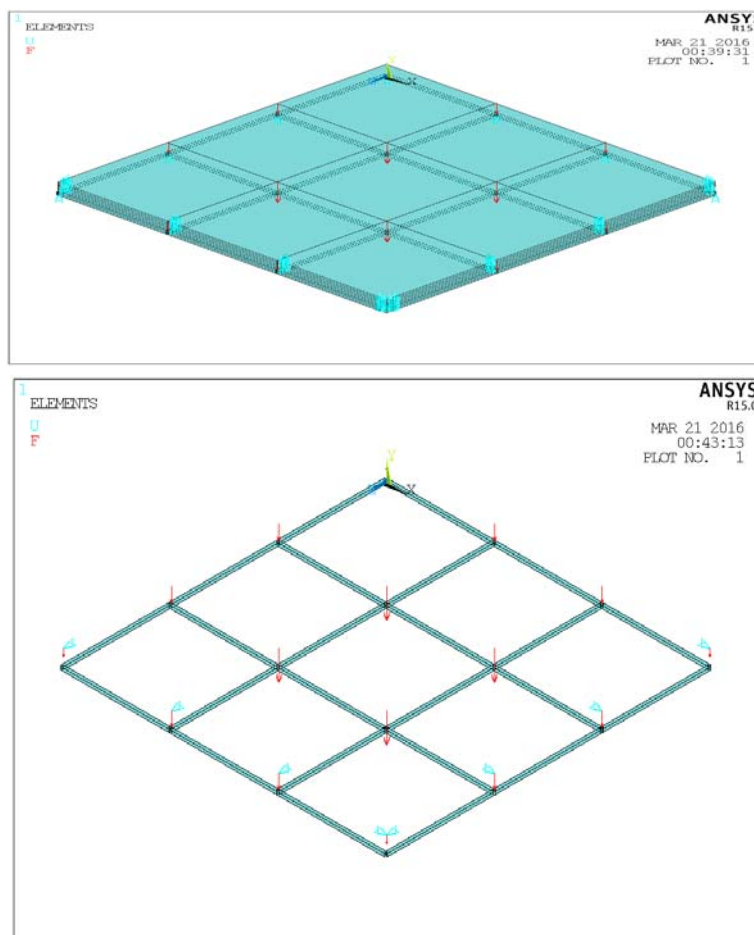


Figure 4.2: a) Discretization of quarter RC slab in X-Z plane with (3 x 3) mesh of 9 elements
 b) Modelling of reinforcement bars

For the purpose of the validation, the numerical results i.e. the load deflection curve are compared with the same reported in the above mentioned thesis [8]. More specifically, the load deflection response of this slab obtained by Taylor et.al. [30] From his experimental study and

the same obtained by Owen et.al. [29]. from his numerical study have compared with the numerical results obtained by S. Roychowdhury in his thesis [8]. The finite element solutions coming from the present numerical model has been superimposed as shown in Figure 4.3 to compare the present solution with the earlier three solutions.

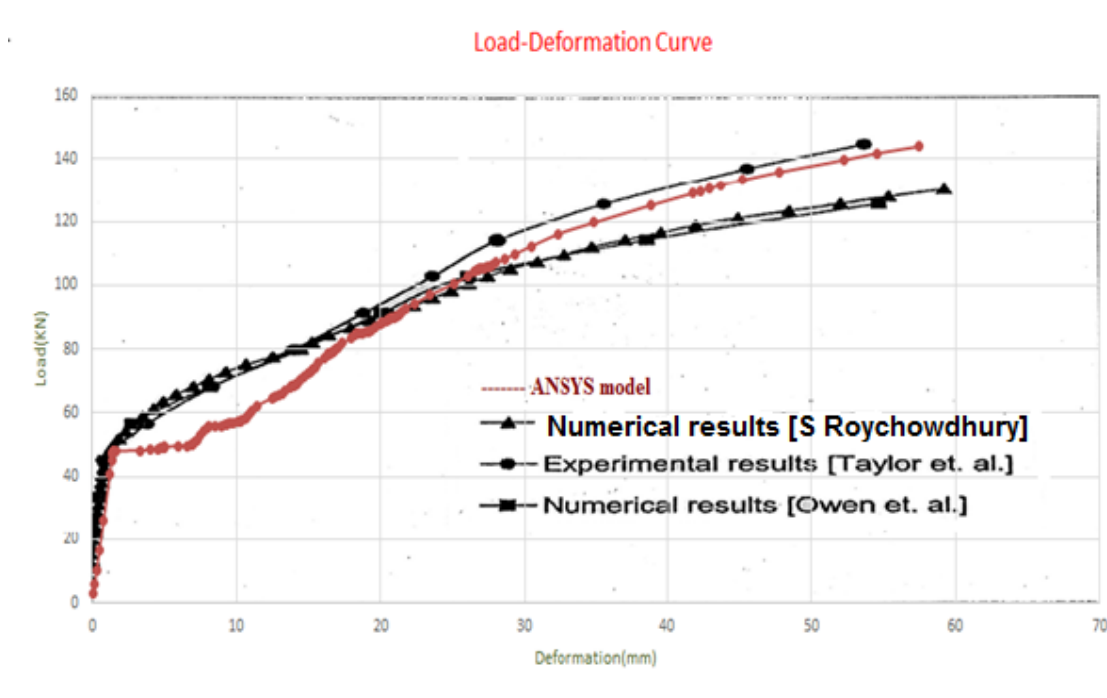


Figure 4.3: Comparison of load deflection curve of the present ANSYS model with the same obtained by other previous researchers

It is clear from the comparison shown in Figure 4.3 that the present numerical solution is identical with the other three solutions in the elastic range. But, the behavior of the slab just after the development of initial cracks in the present model differs with the previous models. This may due to the fact that the post-cracking behavior of concrete considered in the present model is not matching with the model considered in the previous numerical analysis. But the load-deflection pattern is almost matching with the experimental one obtained by Taylor et.al. [30]. This indicates that the present approach for finite element analysis of reinforced concrete slab using ANSYS can be considered for further parametric study.

4.3 Parametric study

The finite element approach for analysis of the reinforced concrete slab taken for validation in the previous section is used to study the behavior of reinforced concrete slab strengthened with FRP laminates. The steps for modelling the same in ANSYS are described in detail in chapter 3. The applicability and suitability of the present approach can be established by performing different parametric studies on this. For the purpose of parametric study with the present numerical approach, a simply supported reinforced concrete slab analyzed previously by other researchers [8] as mentioned in section 4.2 is considered and strengthened with FRP. For preparing the model, the aspects considered in the previous example are kept same.

To perform the parametric study, it has been tried to consider the variation regarding the change of i) mesh size or discretization (6x6, 9x9, 12x12 in one quarter of the slab), ii) support condition of the RC slab (simply supported slab and fixed supported slab), iii) location of FRP laminates (along the support edge, along the continuous edge and along the diagonal), iv) width of the FRP laminates for different FRP positions, v) numbers of FRP layers (2, 3 and 5 layers), vi) thickness of the FRP laminates, vii) fiber orientations (-45°/0°/+45°, -60°/0°/+60°, -90°/0°/+90°).

Table 4.2a: Notation used for different variable parameters

Notation	Representation of variable parameter
CS	Control slab
SS	Simply supported slab
FS	Fixed supported slab
S	FRP at support edge
C	FRP at continuous edge
D	FRP along diagonal
W0	16.66% FRP area for Diagonal location
W1	30-33% FRP area for all location
W2	50-55% FRP area for all location
W3	66.67-75% FRP area for all location
W4	100% FRP area
L2	2 FRP layers
L3	3 FRP layers
L5	5 FRP layers
T3	3 mm thick FRP
T5	5 mm thick FRP
R45	Orientation of FRP layers(- 45°/0°/+45°)
R60	Orientation of FRP layers(- 60°/0°/+60°)
R90	Orientation of FRP layers(- 90°/0°/+90°)

Table 4.2b: Details of parameters used in different slabs

Slab Mark	Slab Details	Slab Mark	Slab Details
SS1	CS(SS)	FS1	CS(FS)
SS2	SS-S-W1-L3-T3-R45	FS2	FS-S-W1-L3-T3-R45
SS3	SS-C-W1-L3-T3-R45	FS3	FS-C-W1-L3-T3-R45
SS4	SS-D-W1-L3-T3-R45	FS4	FS-D-W1-L3-T3-R45
SS2a	SS-S-W2-L3-T3-R45	FS2a	FS-S-W2-L3-T3-R45
SS2b	SS-S-W3-L3-T3-R45	FS2b	FS-S-W3-L3-T3-R45
SS11	SS-W4-L3-T3-R45	FS11	FS-W4-L3-T3-R45
SS3a	SS-C-W2-L3-T3-R45	FS3a	FS-C-W2-L3-T3-R45
SS3b	SS-C-W3-L3-T3-R45	FS3b	FS-C-W3-L3-T3-R45
SS4a	SS-D-W0-L3-T3-R45	FS4a	FS-D-W0-L3-T3-R45
SS4b	SS-D-W2-L3-T3-R45	FS4b	FS-D-W2-L3-T3-R45
SS4c	SS-D-W3-L3-T3-R45	FS4c	FS-D-W3-L3-T3-R45
SS5	SS-S-W1-L2-T3-R45	FS5	FS-S-W1-L2-T3-R45
SS6	SS-S-W1-L5-T3-R45	FS6	FS-S-W1-L5-T3-R45
SS7	SS-C-W1-L2-T3-R45	FS7	FS-C-W1-L2-T3-R45
SS8	SS-C-W1-L5-T3-R45	FS8	FS-C-W1-L5-T3-R45
SS9	SS-D-W2-L2-T3-R45	FS9	FS-D-W2-L2-T3-R45
SS10	SS-D-W2-L5-T3-R45	FS10	FS-D-W2-L5-T3-R45
SS12	SS-S-W1-L3-T5-R45	FS12	FS-S-W1-L3-T5-R45
SS13	SS-C-W1-L3-T5-R45	FS13	FS-C-W1-L3-T5-R45
SS14	SS-D-W2-L3-T5-R45	FS14	FS-D-W2-L3-T5-R45
SS15	SS-S-W1-L3-T3-R60	FS15	FS-S-W1-L3-T3-R60
SS16	SS-S-W1-L3-T3-R90	FS16	FS-S-W1-L3-T3-R90
SS17	SS-C-W1-L3-T3-R60	FS17	FS-C-W1-L3-T3-R60
SS18	SS-C-W1-L3-T3-R90	FS18	FS-C-W1-L3-T3-R90
SS19	SS-D-W2-L3-T3-R60	FS19	FS-D-W2-L3-T3-R60
SS20	SS-D-W2-L3-T3-R90	FS20	FS-D-W2-L3-T3-R90

Based on the above a large number of models of reinforced concrete slab strengthened with FRP have been prepared using ANSYS and analyzed. According to the variation in the parameters, these slab models are numbered as SS1 to SS20 and FS1 to FS20. The details of these are given in Table 4.2a and Table 4.2b. The load-deflection curve of each of these models have been plotted to study the change in behavior due to the variation of these parameters. Along with that the contour of deflection, stress in different directions and pattern of cracks are also obtained from ANSYS and reported in the following sections.

4.3.1 Support Conditions

In this parametric study, the support condition is considered as the first parameter. The total set of slabs are divided into two groups – one is simply supported slab and the other is fixed slab. Accordingly the naming starts either with SS or FS. As the load-displacement response of simply supported slab and fixed slab differs a lot, they are not compared in a single plot. Alternatively all simply supported models compared with each other and all fixed slabs are compared with each other. Thus the parametric study for simply supported slab and fixed slab are discussed in the following sections separately.

Part A: Simply Supported Slab

4.3.2 Discretization or Mesh Size

Before starting the parametric study, a mesh convergence study has been done. For this purpose three different mesh discretization have been considered over the basic model as mentioned in section 4.2. These are 6x6 i.e. 36 elements (shown in Figure4.4a), 9x9 i.e. 81 elements (shown in Figure4.4b) and 12x12 i.e. 144 elements (shown in Figure4.4c) in one quarter of the slab. All other data are kept same.

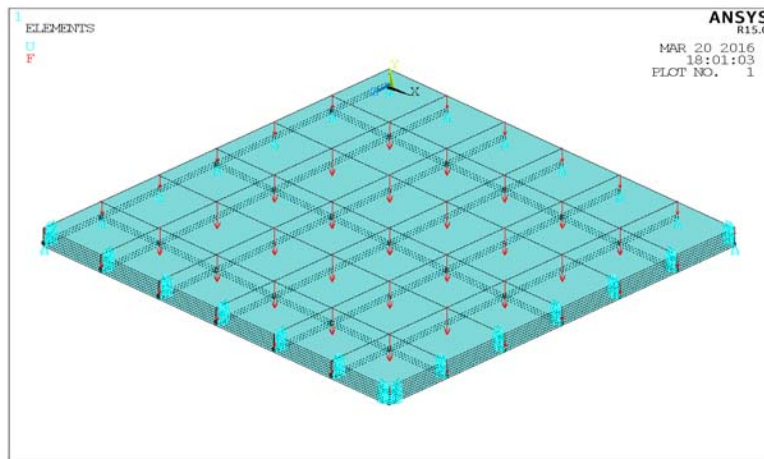


Figure 4.4a: Discretization of quarter RC slab in X-Z plane with (6 x 6) mesh of 36 elements

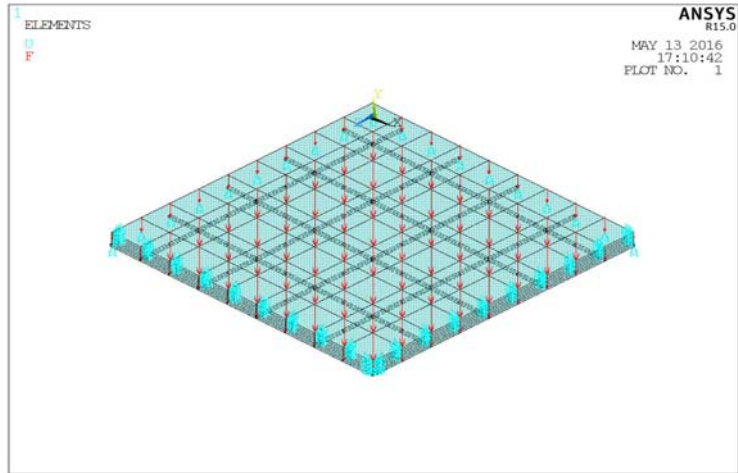


Figure 4.4b: Discretization of quarter RC slab in X-Z plane with (9 x 9) mesh of 81 elements

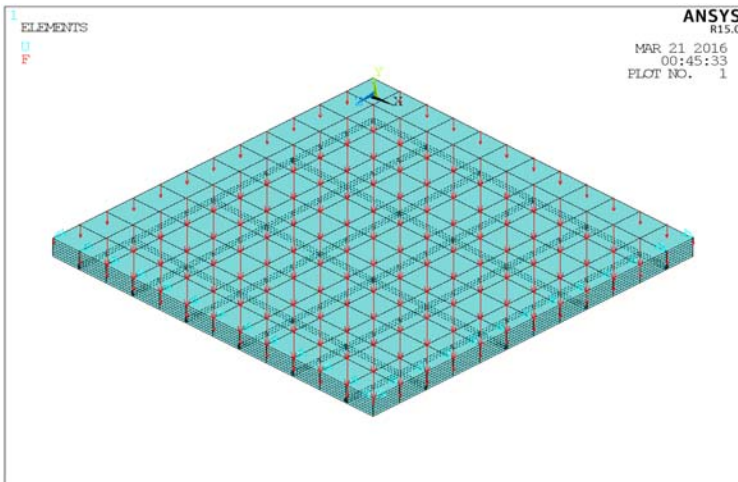


Figure 4.4c: Discretization of quarter RC slab in X-Z plane with (12 x 12) mesh of 144 elements

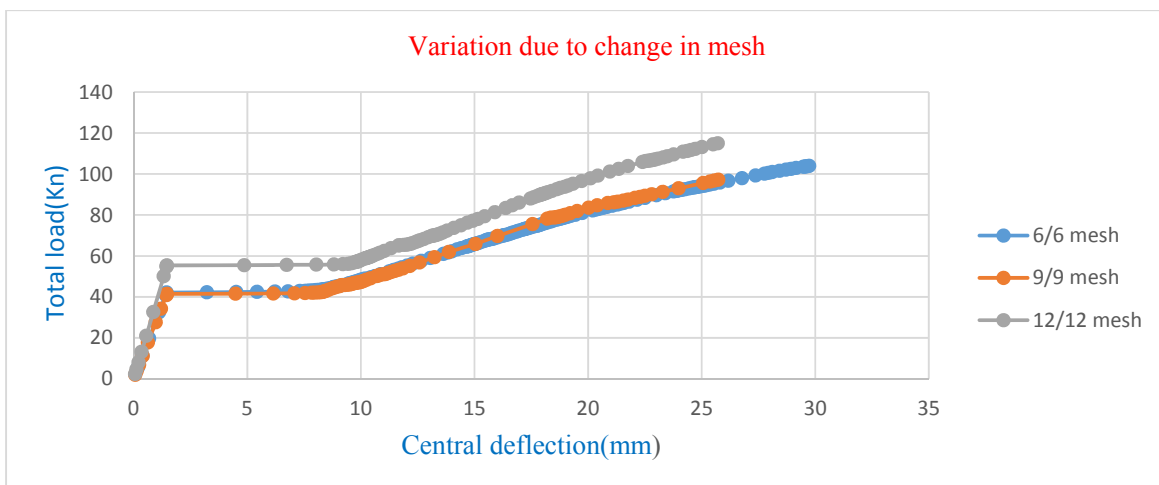


Figure 4.4d: Variation of load-deflection plot due to change in mesh size

The load deflection plot of these three models are superimposed as shown in Figure 4.4d. This indicates that the solution of 6x6 mesh and 9x9 mesh are almost identical compared to the same of 12x12 mesh. Also Table 4.3 gives the deflection of the slab at 96kN load for these three different mesh types. It can be noted that the change in deflection due to the variation in mesh is converging. Thus further parametric studies are done with this 6x6 mesh over the basic slab model as described in section 4.2. This simply supported reinforced concrete un-retrofitted slab having 6x6 mesh is designated as the simply supported control slab and denoted throughout the following sections by SS1 or CS (SS).

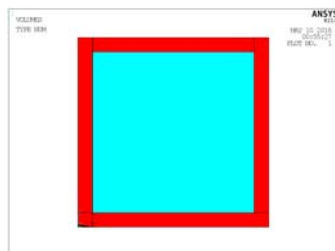
Table 4.3: Comparison of deflection at load 96KN due to change in mesh

Type of mesh in slab	No of elements	Deflection (mm.)	Change (%)
6 x 6	36	29.7359	0.0
9 x 9	81	25.7312	13.46
12 x 12	144	24.8812	16.326

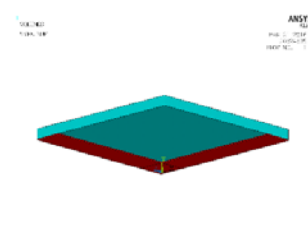
4.3.3 Location of FRP in simply supported slab

To strengthen the basic reinforced concrete slab (also termed here as control slab CS) FRP laminates are considered as attached with the bottom surface of the slab. The behavior of the slab under external mechanical load may depend on the location of FRP strips. To study this effect, three different locations of the FRP strips are considered – a) along the simply supported edge, b) along the continuous edge (for one quarter model) and c) along the diagonal. The slab SS1 has been strengthened with FRP (using SOLID 185 in the model) sheet at the bottom of the slab at support edge (named as SS2), continuous edge (named as SS3) and diagonal position (named as SS4) of the RC slab in simply supported condition as shown in Figure 4.5a, 4.5b and 4.5c respectively. The thickness of FRP used is 3 mm and the orientation of 3 FRP layers are (-45°, 0°, 45°).

a) FRP along the simply supported edge



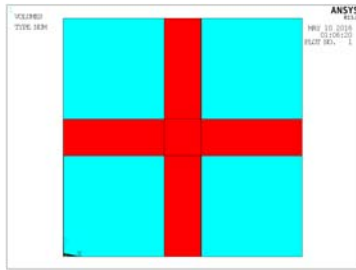
Full model



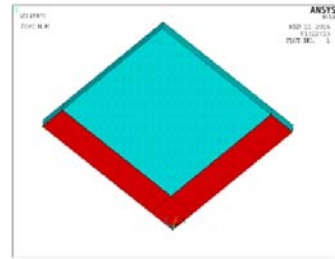
One quarter model

Figure 4.5a: FRP along support edge in Slab SS2

b) FRP along the continuous edge (for one quarter model)



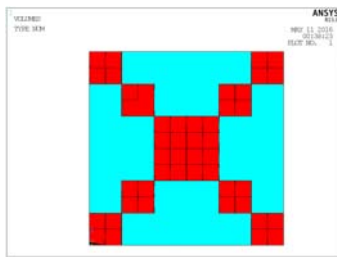
Full model



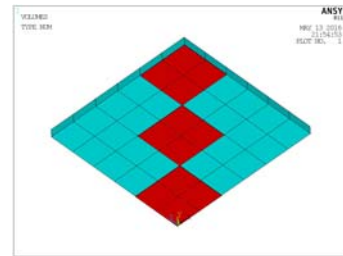
One quarter model

Figure 4.5b: FRP along continuous edge in Slab SS3

c) FRP along the diagonal



Full model



One quarter model

Figure 4.5c: FRP along the diagonal in Slab SS4

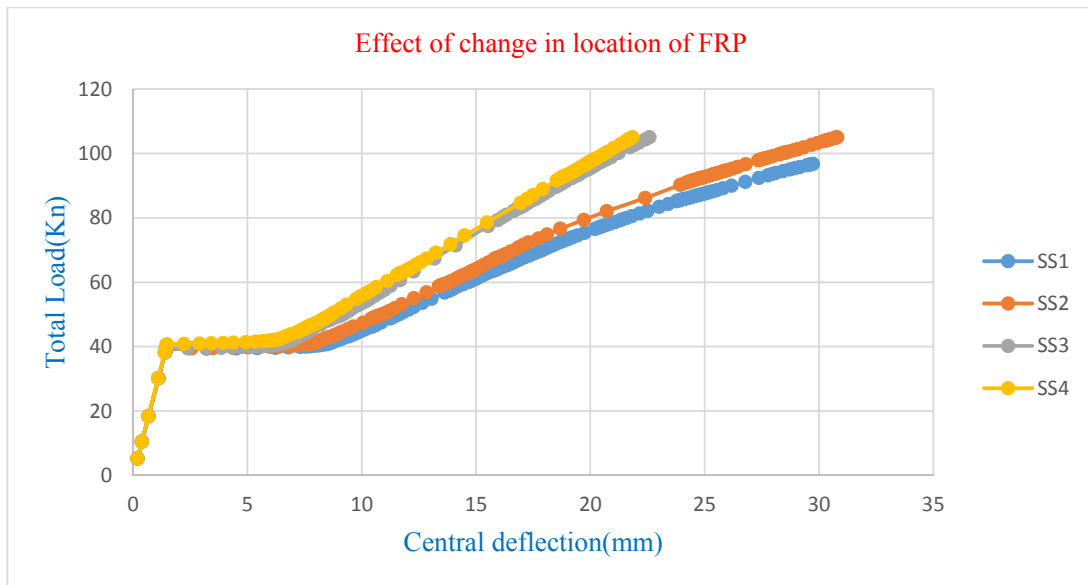


Figure 4.6: Variation of load deflection curve of the slab S2, S3, S4 (retrofitted) with S1 (control slab)

The result coming from the analysis of control slab SS1 and the same for retrofitted slab SS2, SS3 and SS4 are compared graphically in the plot of load deflection curve as given in Fig.4.6. These three retrofitted slabs carry more load than SS1 slab and also the stiffness is more than that of SS1 slab. Among these three retrofitted slabs SS3 and SS4 are stiffer than slab SS2 with SS4 being the most stiff. From this it can be suggested that for simply supported slab, the location of FRP along diagonal is the best alternative.

Contour plot of Nodal Solution in slabs SS1, SS2, SS3 and SS4

The contour plots of stresses in various directions and deflection in Y direction have been shown for the simply supported control slab (SS1) and the retrofitted slabs (SS2, SS3 & SS4) in the following figures. The plots are found to be quite realistic one.

a) Contour plot of nodal solution of slab SS1

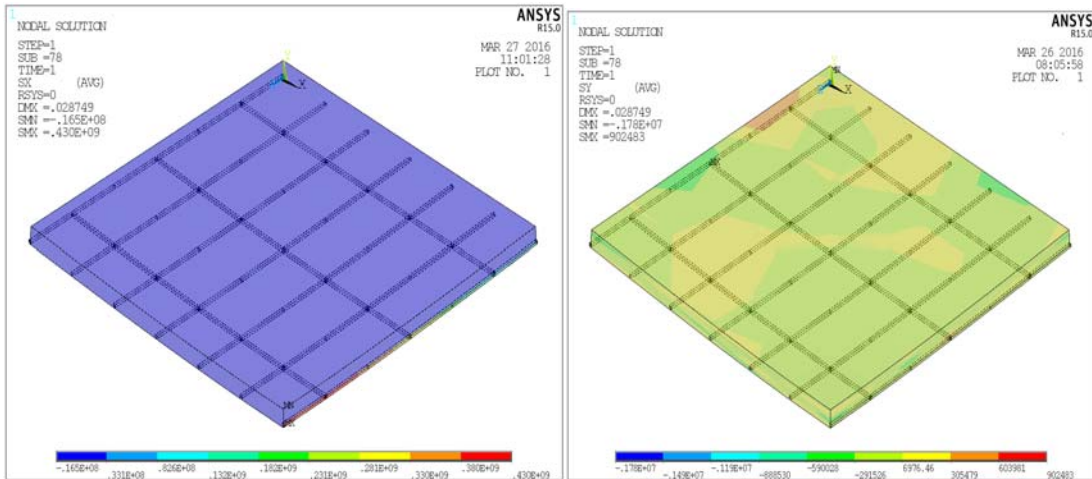


Figure 4.7a: Contour of x-component stress in slab SS1

Figure 4.7b: Contour of y-component stress in slab SS1

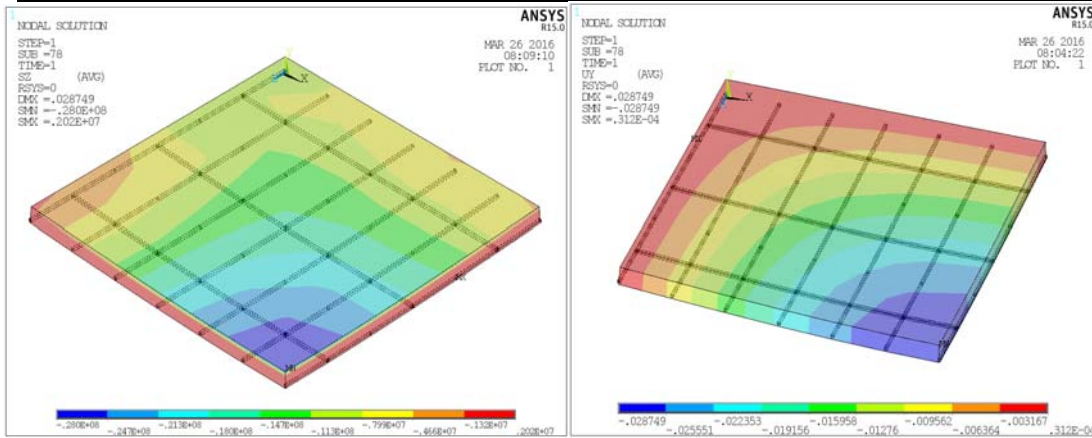


Figure 4.7c: Contour of -Z component stress in slab SS1

Figure 4.7d: Contour of y-component deflection in slab SS1

b) Contour plot of nodal solution of slab SS2

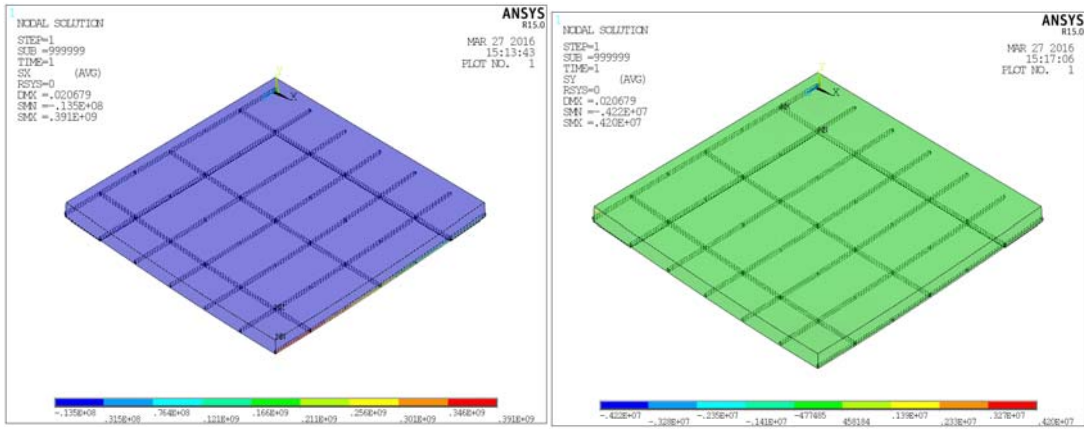


Figure 4.8a: Contour of x-component stress in slab SS2

Figure 4.8b: Contour of y-component stress in slab SS2

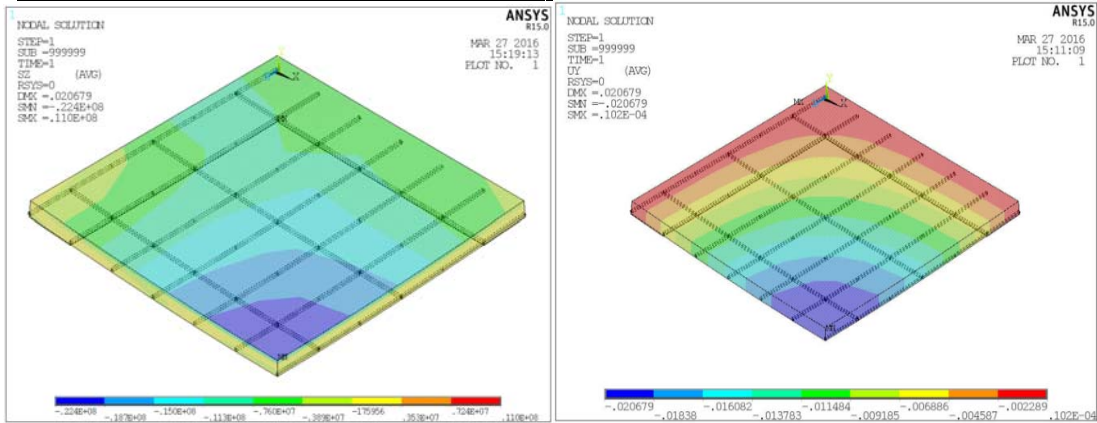


Figure 4.8c: Contour of z-component stress in slab SS2

Figure 4.8d: Contour of y-component deflection in slab SS2

c) Contour plot of nodal solution of slab SS3

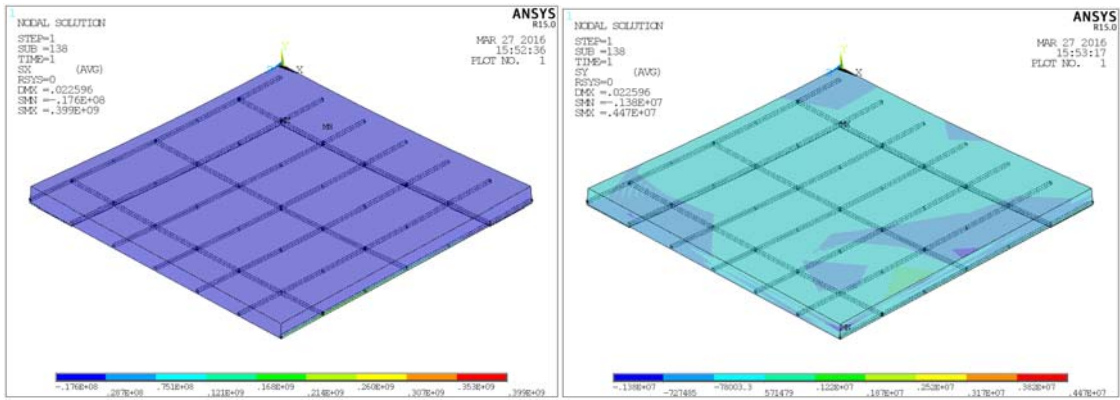


Figure 4.9a: Contour of x-component stress in slab SS3

Figure 4.9b: Contour of y-component stress in slab SS3

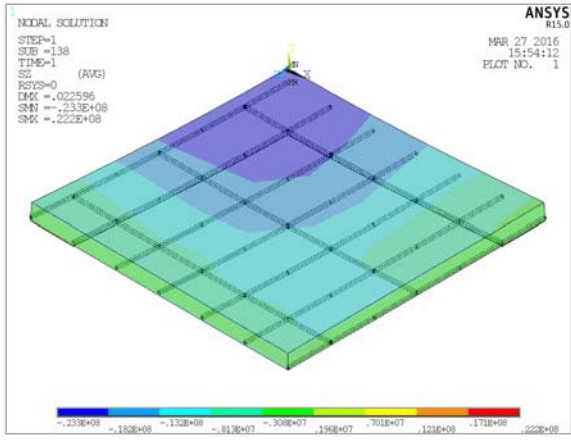


Figure 4.9c: Contour of z-component stress in slab SS3

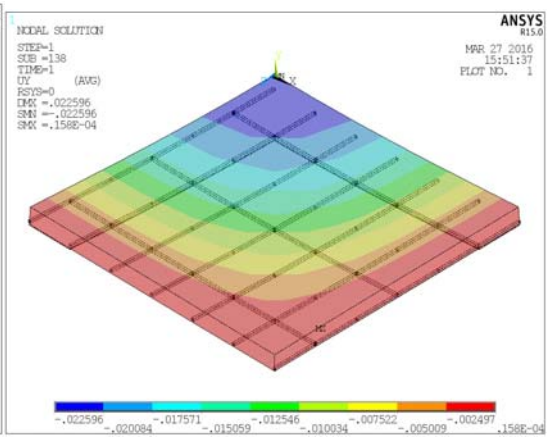


Figure 4.9d: Contour of y-component deformation in slab SS3

d) Contour plot of nodal solution of slab SS4

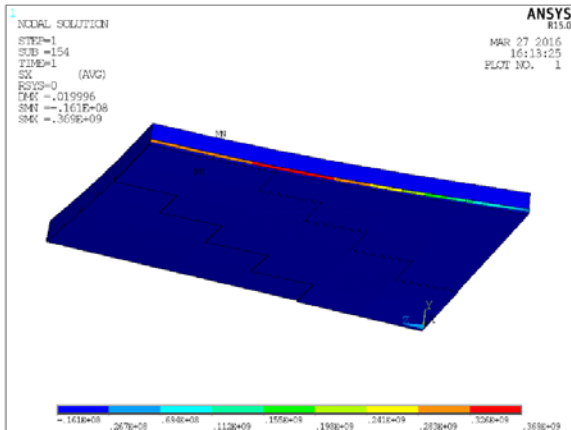


Figure 4.10a: contour of x-component stress in slab SS4

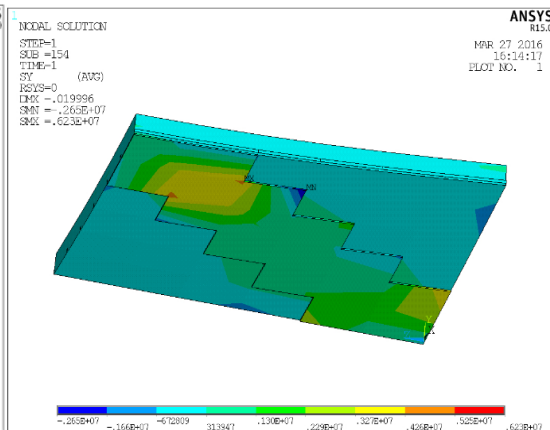


Figure 4.10b: contour of y-component stress in slab SS4

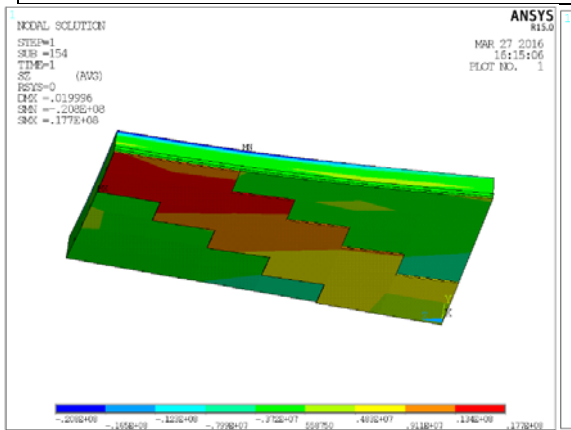


Figure 4.10c: Contour of z-component stress in slab SS4

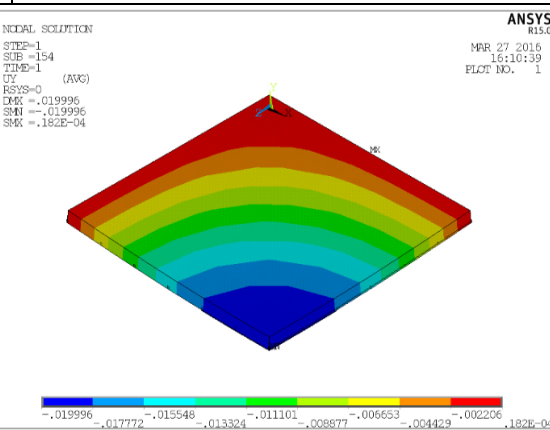


Figure 4.10d: Contour of y-component deflection in slab SS4

Crack pattern in slabs SS1, SS2, SS3 & SS4

The ANSYS program records the crack pattern at each applied load step. The cracking pattern in the slab can be obtained using the Crack/Crushing plot option in ANSYS. Vector Mode plots must be turned on to view the cracking in the model. A cracking sign represented by a circle appears when a principal tensile stress exceeds the ultimate tensile strength of the concrete. The cracking sign appears perpendicular to the direction of the principal stress. ANSYS program displays circles or octahedrons at locations of cracking or crushing in concrete elements. Cracking is shown with a circle outline in the plane of the crack, and crushing is shown with an octahedron outline. The first crack at an integration point is shown with a red circle outline, the second crack with a green circle outline and the third crack with a blue circle outline.

Figures 4.11a to 4.14d shows evolutions of crack patterns developing for each slab at the last loading step. At the early stages of loading, the behavior of slab has been observed to be elastic until the appearance of the first crack. Invariably, the crack has been initiated at the support, continuous edge and also at the center of the slab.

Comparing the crack patterns in different slabs, it is observed that area of cracked zone is considerably less in the slab SS4 having the FRP along the diagonal. Though the difference is not so noticeable in the 1st crack, but in the 2nd crack and mainly in the 3rd crack, the difference is prominent.

a) 1st Crack Pattern for slab SS1, SS2, SS3 & SS4

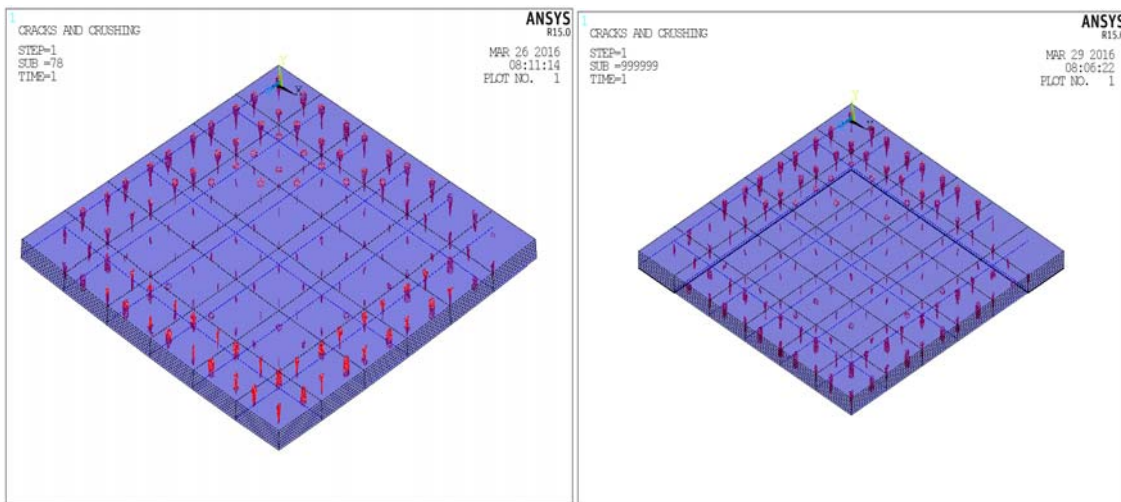


Figure 4.11a: Pattern of 1st crack in slab SS1

Figure 4.11b: Pattern of 1st crack in slab SS2

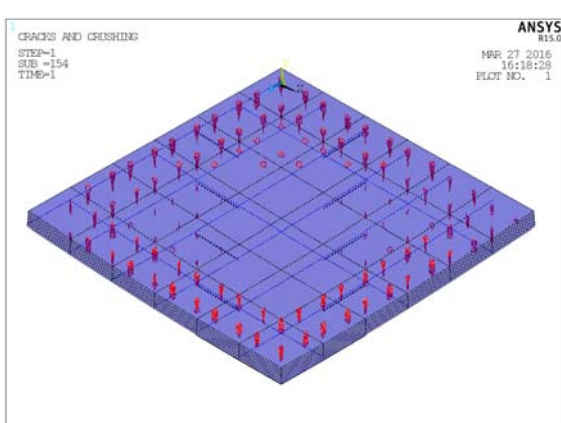


Figure 4.11c: Pattern of 1st crack in slab SS3

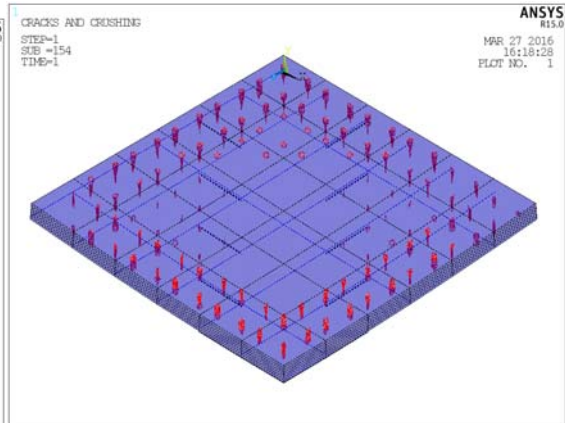


Figure 4.11d: Pattern of 1st crack in slab SS4

b) 2nd Crack Pattern for slab SS1, SS2, SS3 & SS4

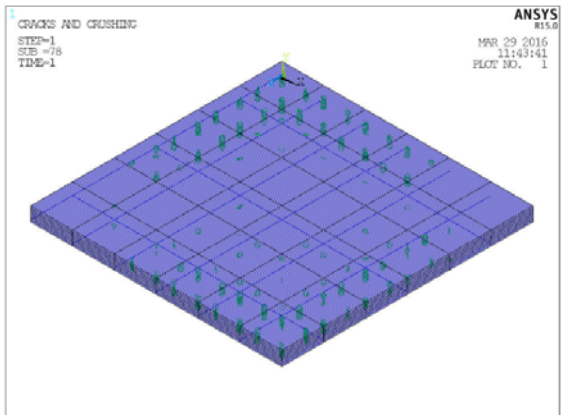


Figure 4.12a: Pattern of 2nd crack in slab SS1

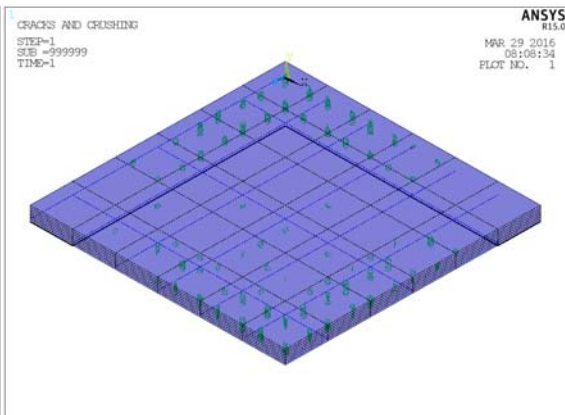


Figure 4.12b: Pattern of 2nd crack in slab SS2

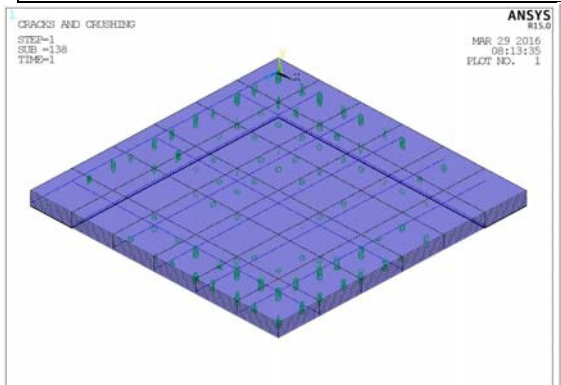


Figure 4.12c: Pattern of 2nd crack in slab SS3

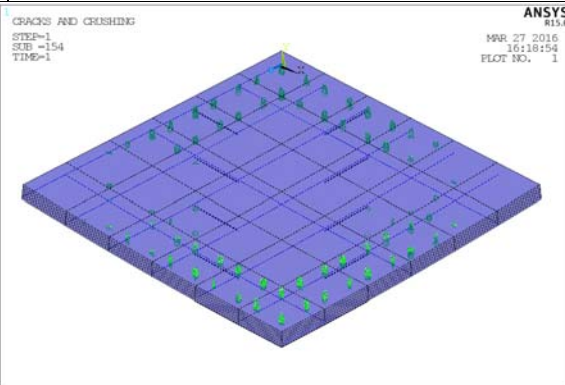


Figure 4.12d: Pattern of 2nd crack in slab SS4

c) 3rd Crack Pattern for slab SS1, SS2, SS3 & SS4

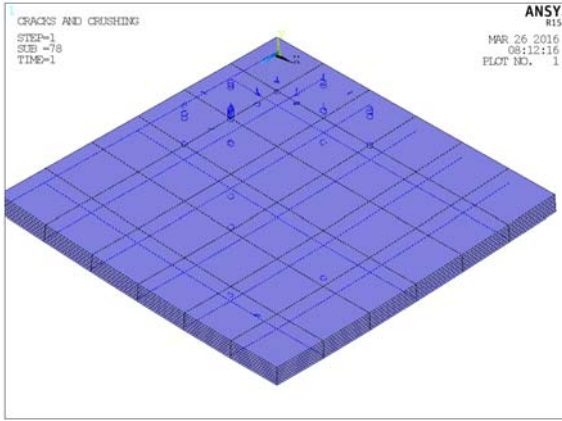


Figure 4.13a: Pattern of 3rd crack in slab SS1

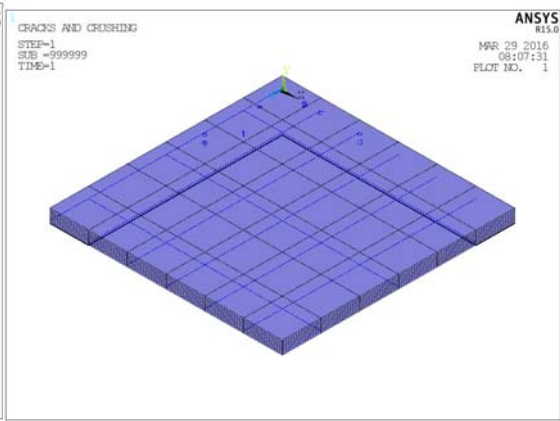


Figure 4.13b: Pattern of 3rd crack in slab SS2

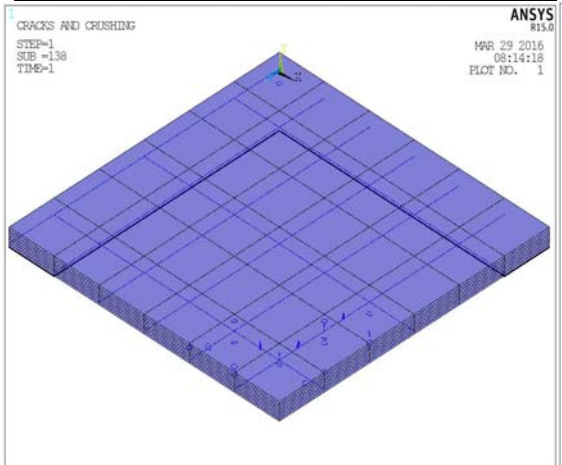


Figure 4.13c: Pattern of 3rd crack in slab SS3

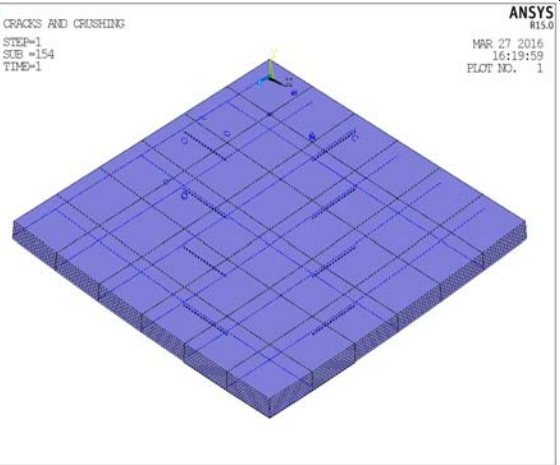


Figure 4.13d: Pattern of 3rd crack in slab SS4

d) All cracks for the slab SS1, SS2, SS3, and SS4

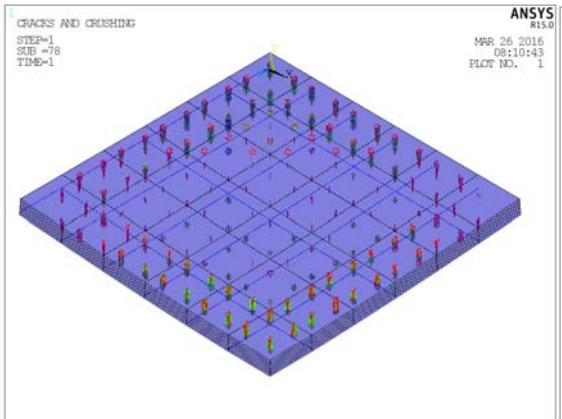


Figure 4.14a: Pattern of all cracks in slab SS1

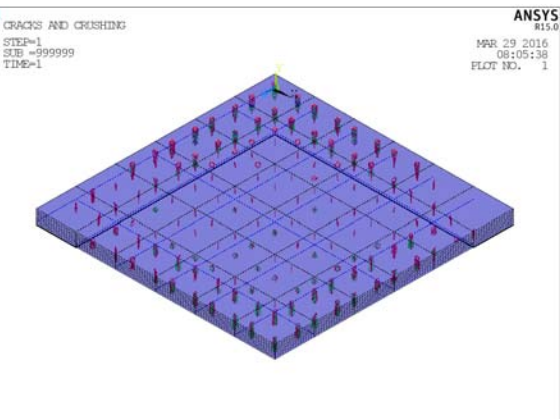


Figure 4.14b: Pattern of all cracks in slab SS2

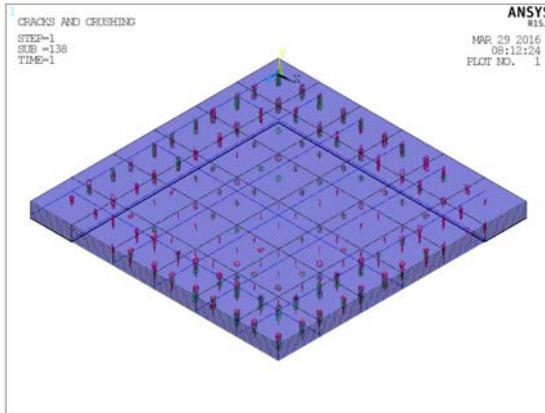


Figure 4.14c: Pattern of all cracks in slab SS3

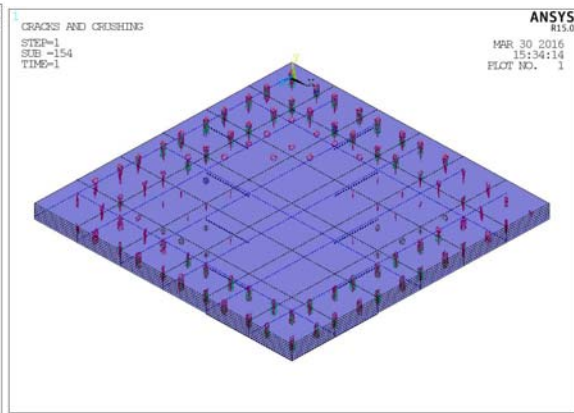


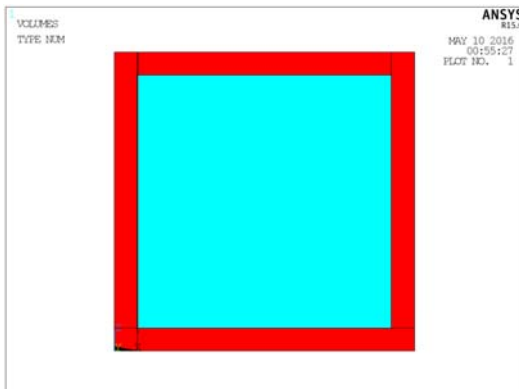
Figure 4.14d: Pattern of all cracks in slab SS4

4.3.4 Width of FRP in the simply supported slab

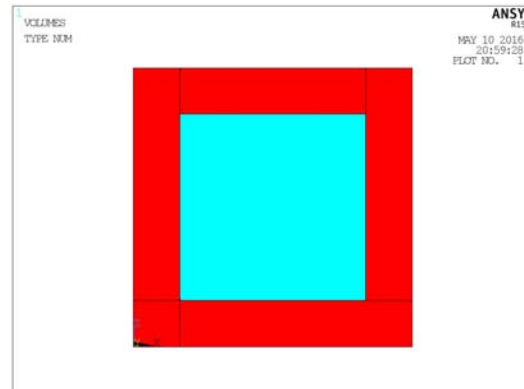
The width of FRP laminate in each of the retrofitted slabs SS2, SS3 and SS4 is considered as a variable parameter in this section as this has a considerable effect on the behaviour of the slab.

4.3.4.1 FRP along the support edge of the simply supported slab

In slab SS2, the FRP has been provided along the support edge. But initially in the model, FRP elements are attached with the outermost elements of the model as shown in Figure 4.15a. Then it has been extended in the next element line as shown in Figure 4.15b. Then it is increased again in the same manner as shown in Figure 4.15c. Finally all the elements are covered with FRP elements as shown in Figure 4.15d. Thus the percentage of slab area covered with FRP are 30%, 55%, 75% and 100% respectively. All these models are analysed and the load-deflection plots coming from the analysis are compared as shown in Figure 4.16. The comparison not only shows that the slabs gets more stiffer with the increment in the area of FRP laminates but also indicates that the failure load increases with higher FRP area.



A : 30% area of Slab SS2 covered by FRP



B : 55% area of Slab SS2a covered by FRP

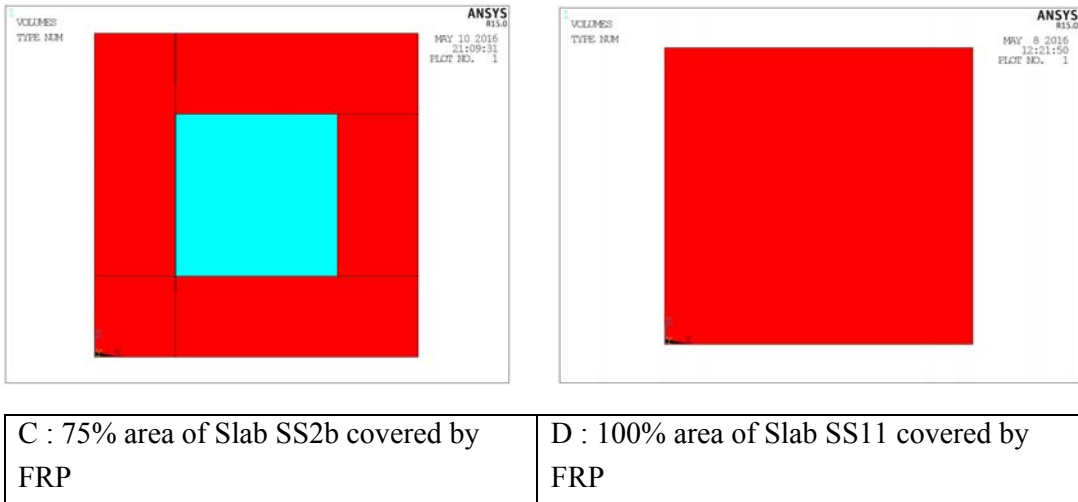


Figure 4.15: Location of FRP along support edge in the full model of simply supported retrofitted slab

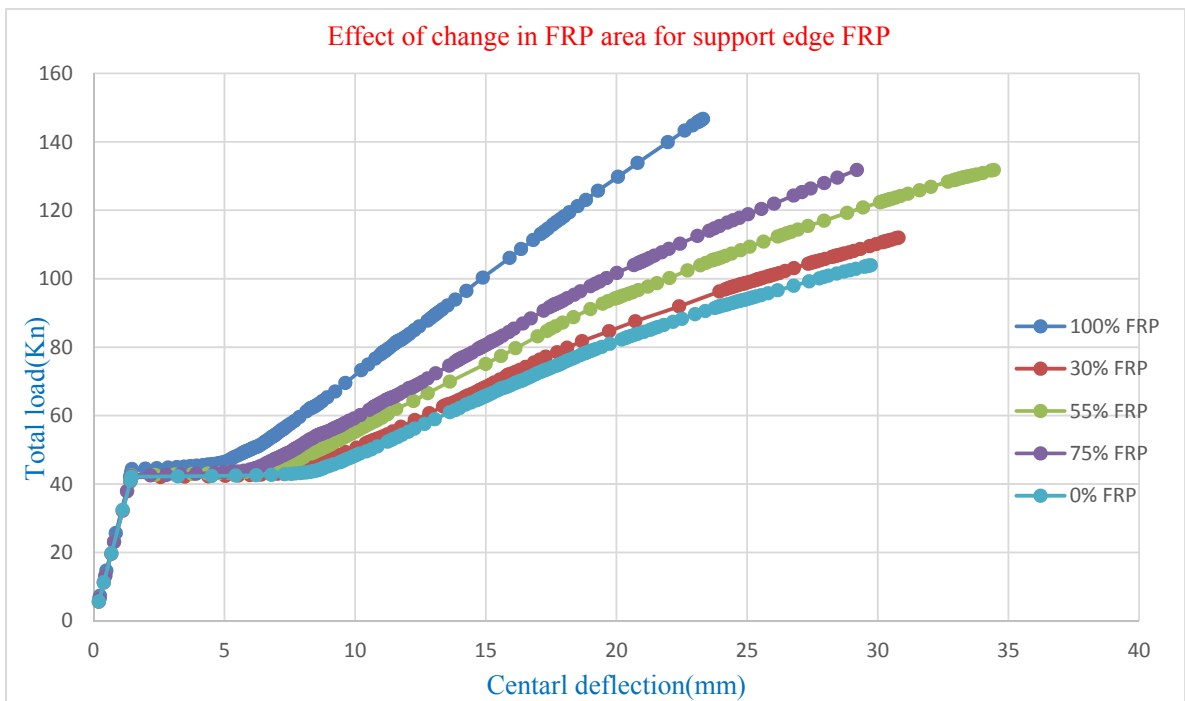


Figure 4.16: Variation of load deformation behavior of retrofitted simply supported RC slab due to change in the area covered with FRP along support edge

4.3.4.2 FRP along the continuous edge of the simply supported slab

In slab SS3, the FRP has been provided along the continuous edge of the one-quarter of the slab i.e. along the middle lines (line of symmetry) of the full slab. Initially in the model, FRP elements are attached with the extreme elements of the one-quarter model i.e. FRP of two-element width along X and Z directions in full model as shown in Figure 4.17a. Then it has been extended in the next element line i.e. forming FRP of four-element width in full slab as shown in Figure 4.17b. Then it is increased again in the same manner as shown in Figure 4.17c. Finally all the elements are covered with FRP elements as shown in Figure 4.17d. Thus the percentage of slab area covered with FRP are 30%, 55%, 75% and 100% respectively. All these models are analysed and the load-deflection plots coming from the analysis are compared as shown in Figure 4.18. The comparison not only shows that the slabs gets more stiffer with the increment in the area of FRP laminates but also indicates that the failure load increases with higher FRP area with the exception in the slab SS3b having 75% area covered with FRP. There may remain an error in the result of this analysis (SS3b).

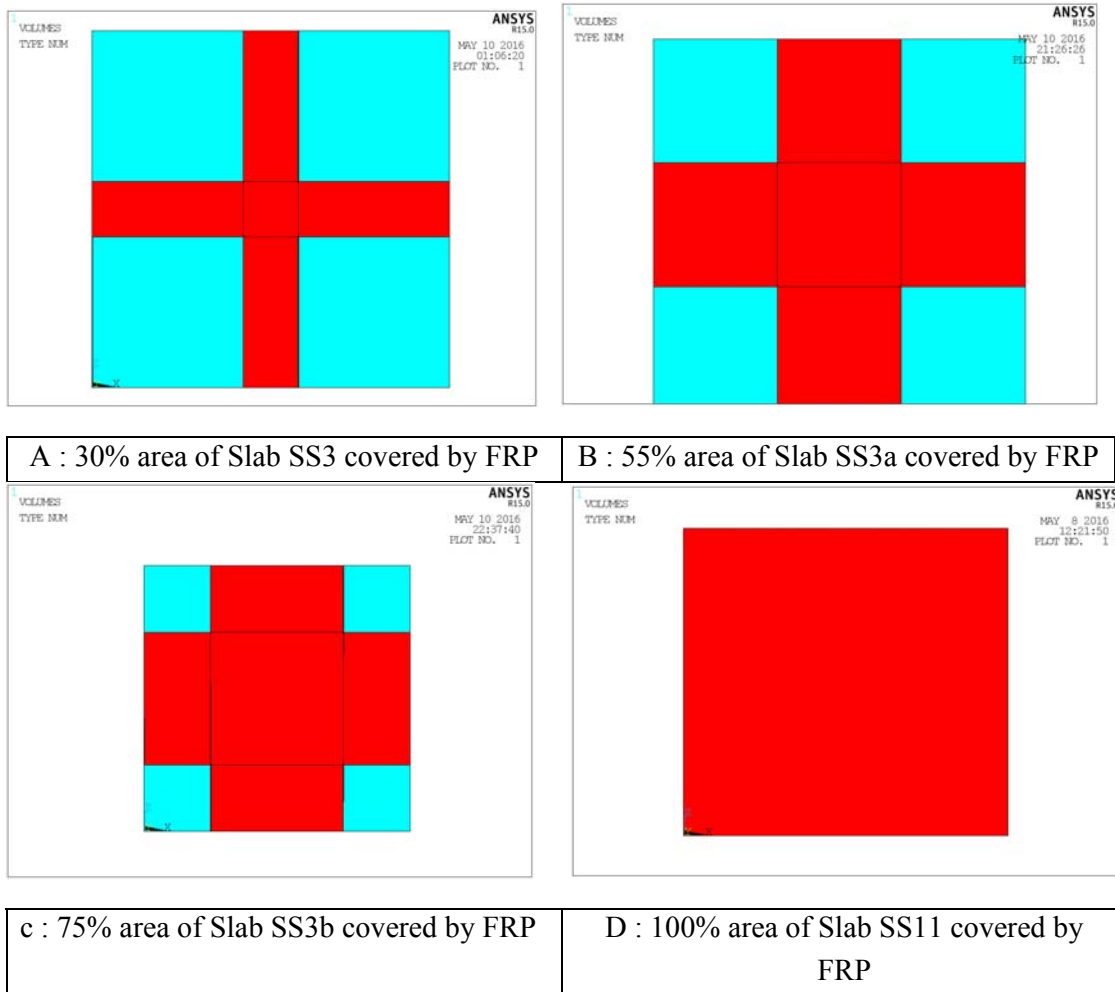


Figure 4.17: Location of FRP along continuous edge in the full model of simply supported retrofitted slab

Variation of load deformation curve for simply supported RC slab FRP at continuous edge

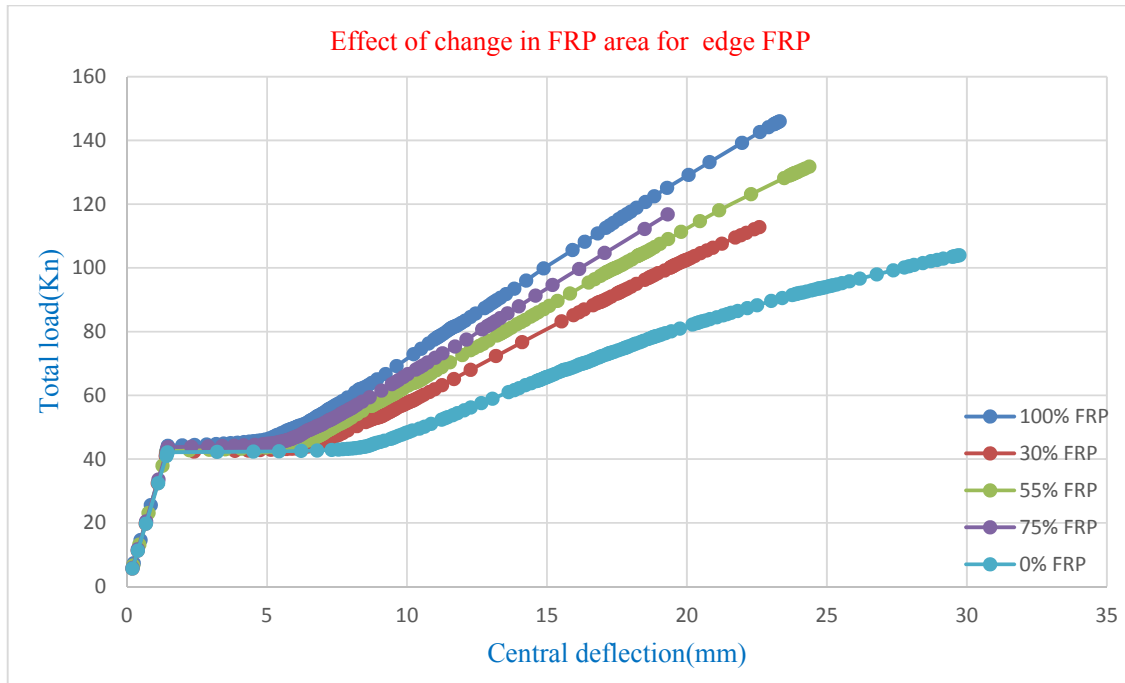


Figure 4.18: Variation of load deformation behavior of retrofitted simply supported RC slab due to change in the area covered with FRP along continuous edge

4.3.4.3 FRP along the diagonal of the simply supported slab

In slab SS4, the FRP has been provided along the diagonal direction of the one-quarter of the slab i.e. along both the diagonals of the full slab. Initially in the model, FRP elements are attached with twelve elements along the diagonal of the one-quarter model i.e. forty eight elements in full model giving 33% FRP area as shown in Figure 4.19b. Then it has been reduced to six elements along the diagonal of the one-quarter model i.e. twenty four elements in full model giving 16.67% FRP area as shown in Figure 4.19a. Then it is increased to cover sixteen elements along the diagonal of the one-quarter model i.e. sixty four elements in full model giving 50% FRP area as shown in Figure 4.19c. Then it is increased in the same manner to cover twenty four elements along the diagonal of the one-quarter model i.e. ninety six elements in full model giving 66.67% FRP area as shown in Figure 4.19d. Finally all the elements are covered with FRP elements as shown in the previous Figure 4.17d. All these models are analysed and the load-deflection plots coming from the analysis are compared as shown in Figure 4.20. The comparison shows that the slabs get more stiffer with the increment in the area of FRP laminates indicating smaller deflection at the ultimate load. It is also observed that there is a variation in the failure load which increases just after increasing the width of FRP area but there is minor changes (reduction in some cases also) when the FRP area is increased further.

In addition to the above, the change of load carrying capacity of simply supported RC slab retrofitted with FRP at different locations and having different width i.e.area of FRP are shown in the following Table 4.4 and change of deformation at ultimate load of those slab retrofitted with FRP are shown in the Table 4.5. It can easily be observed that to achieve maximum benefit 100% of the slab area should be covered with FRP. But in case of location of FRP along support edge or continuous edge, coverage of 50%-55% area will give satisfactory improvement. But for the location of FRP along diagonal, the requirement of coverage with FRP is found to be 75%. The deformation at ultimate load has also a tendency to reduce with the increase in the area of slab covered with FRP which is quite obvious.

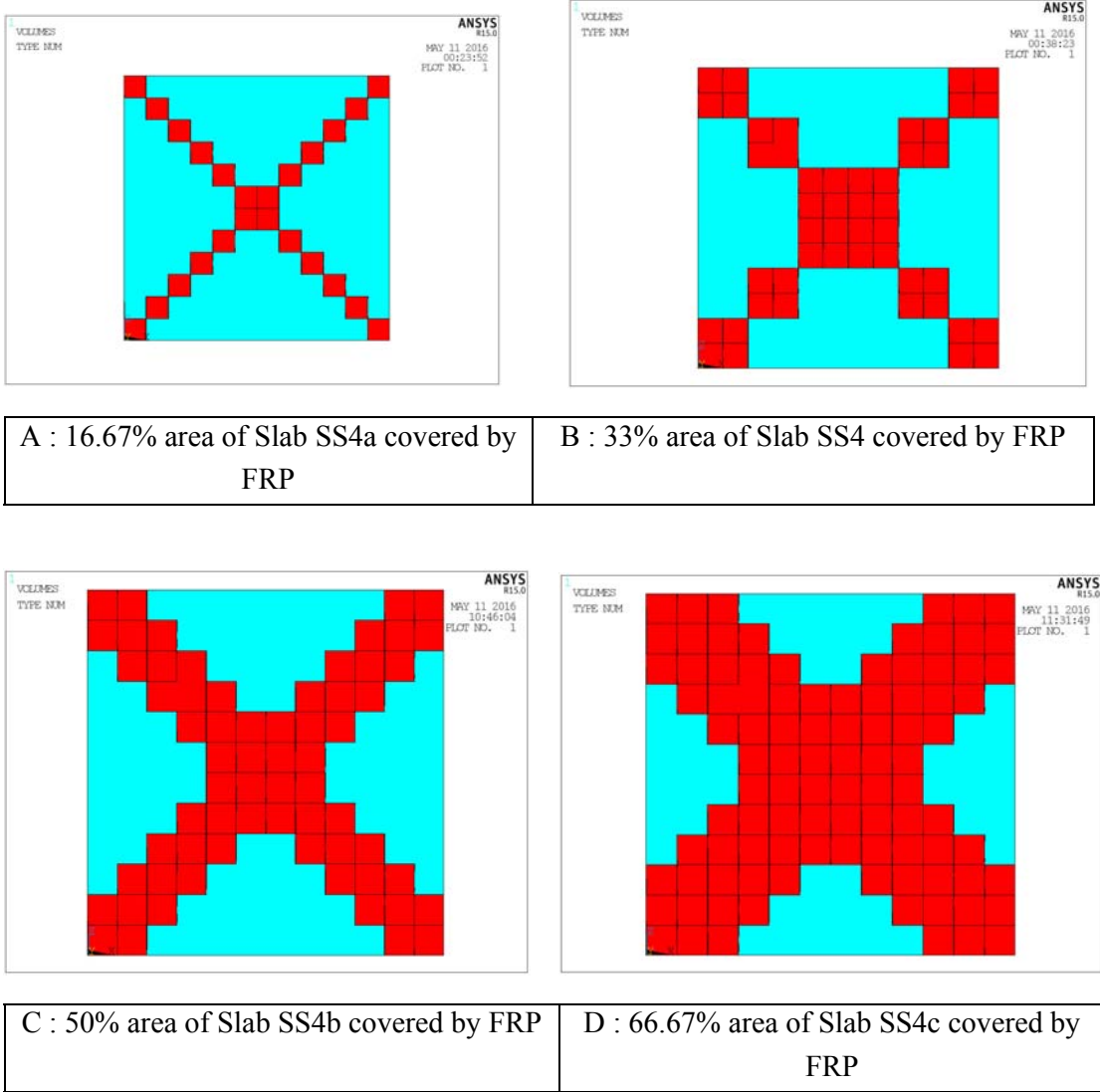


Figure 4.19: Location of FRP along diagonal in the full model of simply supported retrofitted slab

Variation of load deformation curve for simply supported RC slab FRP at diagonal

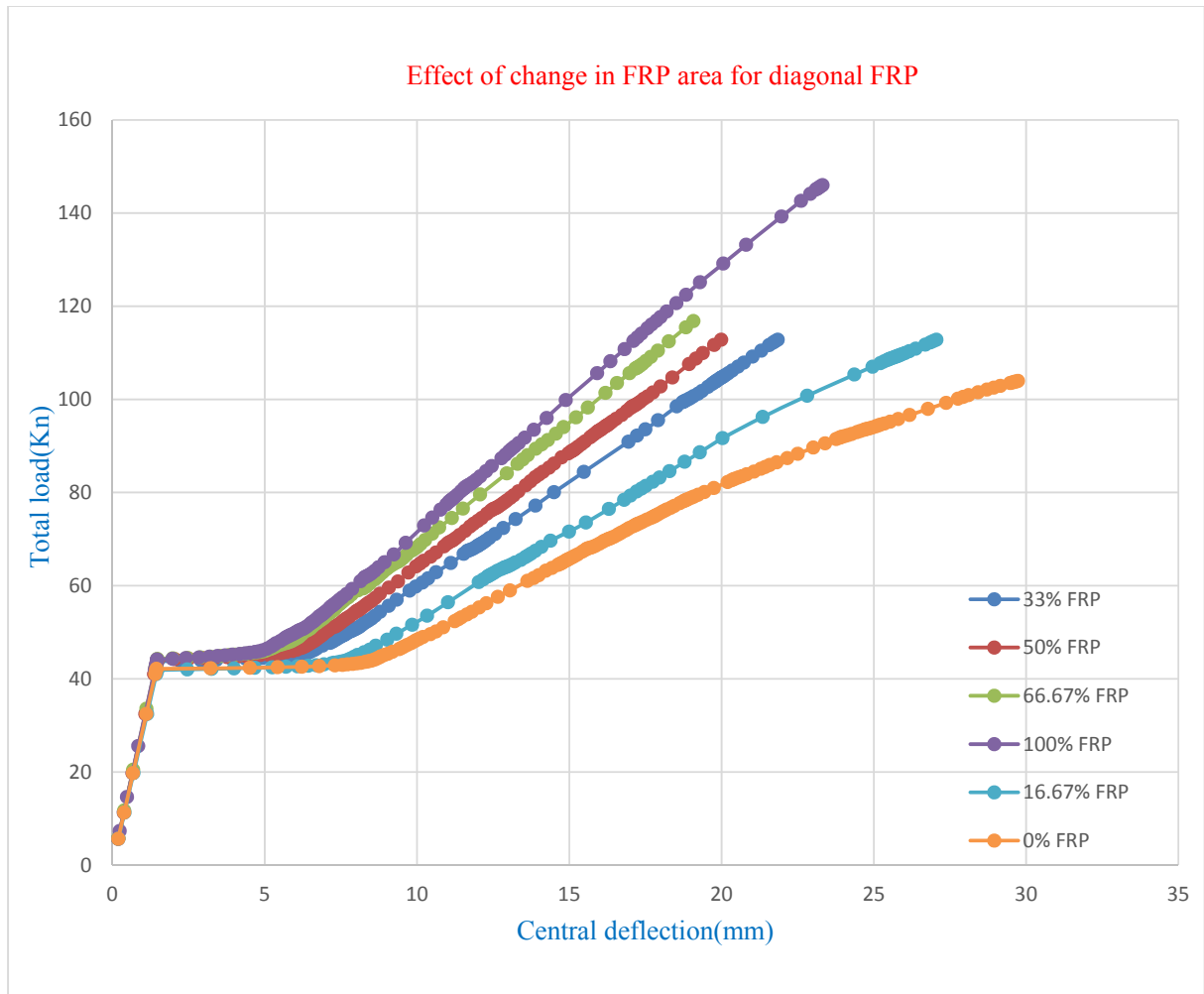


Figure 4.20: Variation of load deformation behavior of retrofitted simply supported RC slab due to change in the area covered with FRP along both the diagonals

Table 4.4: Change of load carrying capacity of simply supported RC slab retrofitted with FRP

Percentage of FRP area	Increment of load carrying capacity in percentage		
	RC slab retrofitted with Support edge FRP	RC slab retrofitted with diagonal FRP	RC slab retrofitted with Continuous edge FRP
16.67		8.73	
30 to 33.33	8.73	8.73	8.73
50 to 55	27.1	8.73	27.1
66.67 to 75	27.1	12.62	12.62
100	41.75	41.75	41.75

Table 4.5: Change of deformation at ultimate load of simply supported RC slab retrofitted with FRP

Percentage of FRP area	Deformation at ultimate load(mm)		
	RC slab retrofitted with Support edge FRP	RC slab retrofitted with diagonal FRP	RC slab retrofitted with Continuous edge FRP
16.67		27.06	
30 to 33.33	30.79	21.84	22.58
50 to 55	34.44	20	26.08
66.67 to 75	29.2	19.07	19.31
100	23.32	23.32	23.32

4.3.5 Layers of FRP in simply supported slab

FRP laminate is a laminated composite. In the finite element software ANSYS, a layered solid element SOLID185 has been used to develop the model of FRP laminates. Thus number of layers considered in the SOLID185 element is also a factor that may influence the behavior of retrofitted slab. In this section, the number of layers considered in the FRP model has been considered as a parameter. In slab SS2, SS3 and SS4, the FRP has been provided along support edge, continuous edge and diagonal respectively of the reinforced concrete slab having 3 FRP layers in it. To choose the variation, the number of layers has been changed to 2 layers and 5 layers keeping the thickness of FRP same. As a result, the slab models SS5 (2 layers) and SS6 (5 layers) are prepared by modifying the model SS2 (FRP along support edge), the slab models SS7 (2 layers) and SS8 (5 layers) are prepared by modifying the model SS3 (FRP along continuous edge) and the slab models SS9 (2 layers) and SS10 (5 layers) are prepared by modifying the model SS4 (FRP along diagonal). All these models are analysed and the load-deflection plots coming from the analysis are compared as shown in Figure 4.21a, 4.21b, 4.21c.

Variation due to the change in layers of FRP in slab SS2, SS5 and SS6:

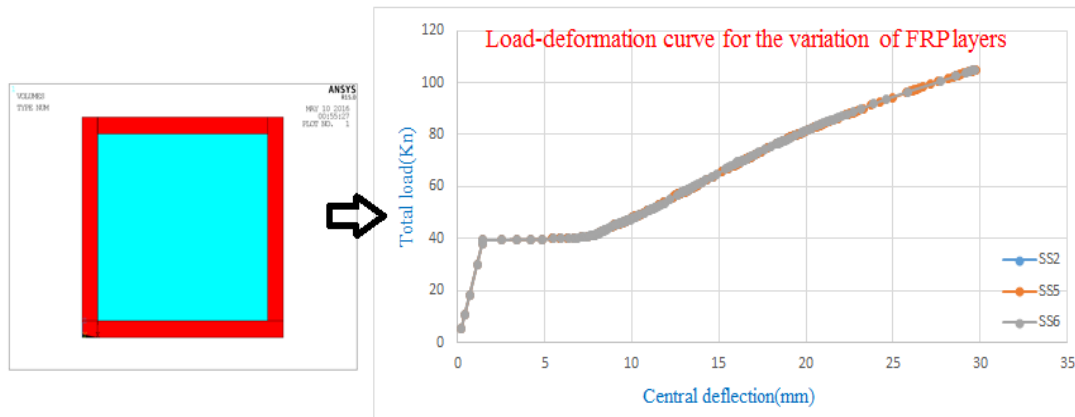


Figure 4.21a: Variation of load deformation behavior of retrofitted simply supported RC slab due to change in number of layers in FRP along support edge

From the comparison of Figure 4.21a and 4.21b, the load deformation curve shows that there is no considerable variation in these two curves, but some nominal variation has shown in the curve as shown Figure 4.21c i.e. the curve for the variation of FRP layers at diagonal position. It shows that the slabs gets more stiffer with the increment in the layers of FRP laminates near failure.

Variation due to the change in layers of FRP in slab SS3, SS7 and SS8:

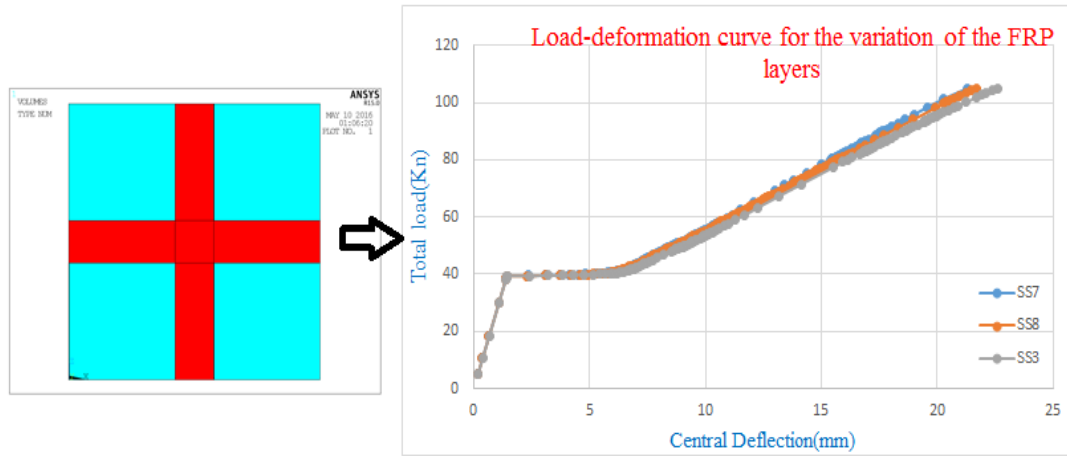


Figure 4.21b: Variation of load deformation behavior of retrofitted simply supported RC slab due to change in number of layers in FRP along continuous edge

Variation due to the change in layers of FRP in slab SS4, SS9 and SS10:

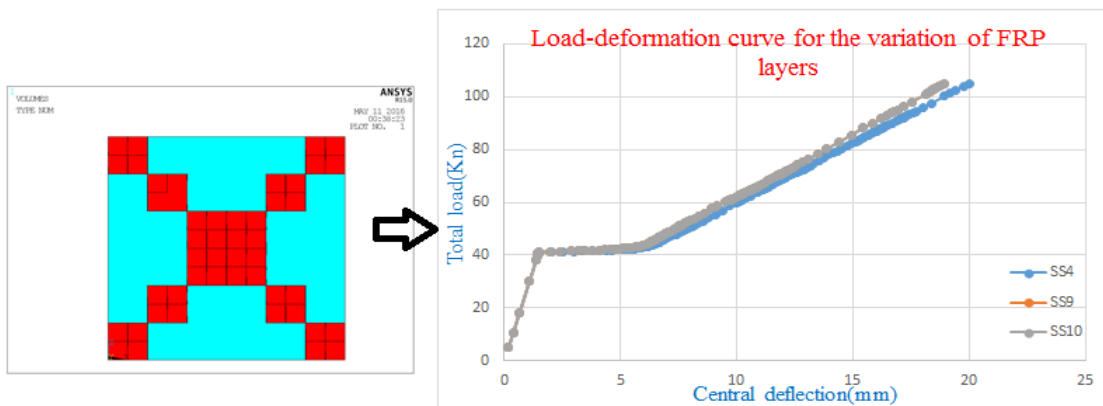


Figure 4.21c: Variation of load deformation behavior of retrofitted simply supported RC slab due to change in number of layers in FRP along diagonal position

4.3.6 Thickness of FRP in simply supported slab

While strengthening the reinforced concrete slab using FRP laminates, the thickness of FRP laminate may also be a factor influencing the behavior of the slab. Thus, in this section an attempt has been made to study the behavior of the retrofitted slab due to the change in the thickness of the FRP laminates. Initially the slab models SS2, SS3 and SS4 have been prepared considering the thickness of FRP as 3mm. Here, this thickness has been increased to 5mm. Thus SS2 (3mm thick FRP along support edge) has been changed to SS12 (5mm thick FRP

along support edge), SS3 (3mm thick FRP along continuous edge) has been changed to SS13 (5mm thick FRP along continuous edge) and SS4 (3mm thick FRP along diagonal) has been changed to SS14 (5mm thick FRP along diagonal). All these models are analysed and the load-deflection plots coming from the analysis are compared as shown in Figure 4.22b, 4.23b, 4.23b for the three different location of FRP respectively.

Effect of change of thickness of FRP along support edge i.e. variation of SS2 and SS12:

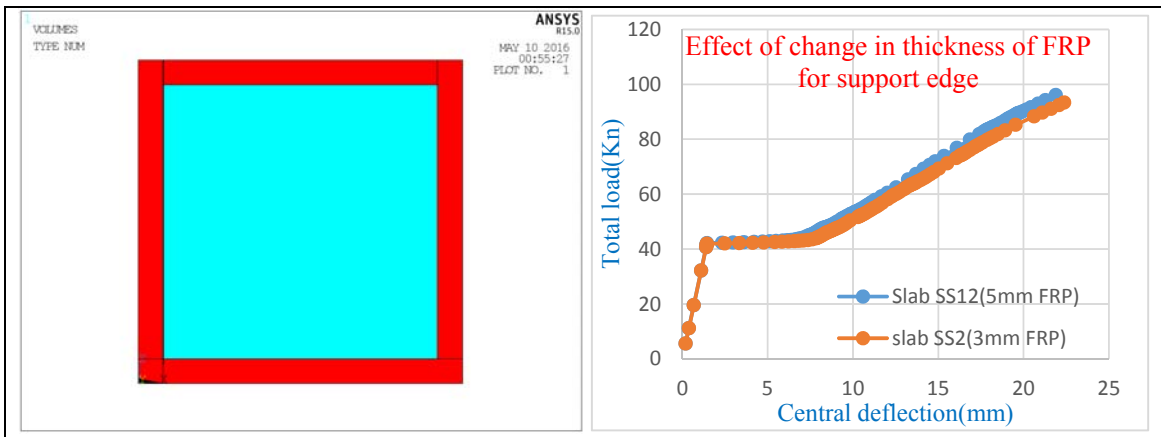


Figure 4.22a: Finite element model of slab SS12

Figure 4.22b: Variation of load deformation behavior of retrofitted simply supported RC slab due to change in thickness of FRP along support edge

Effect of change of thickness of FRP along continuous edge i.e. variation of SS3 and SS13:

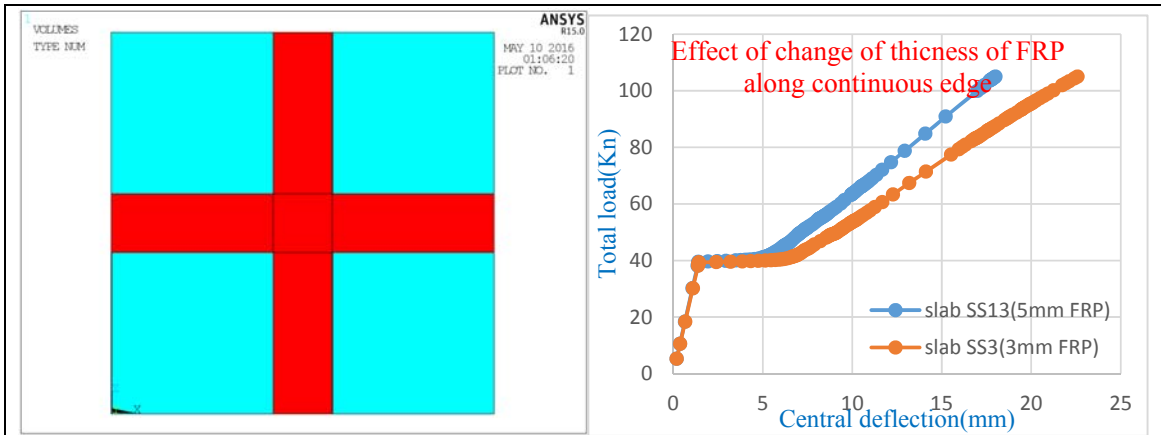


Figure 4.23a: Finite element model of slab SS13

Figure 4.23b: Variation of load deformation behavior of retrofitted simply supported RC slab due to change in thickness of FRP along continuous edge

Effect of change of thickness of FRP along diagonal i.e. variation of SS4 and SS14:

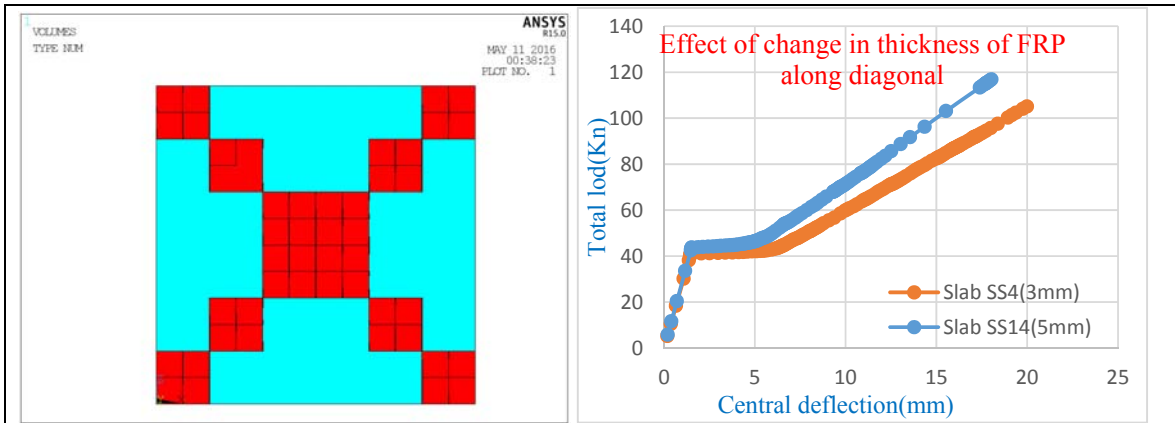


Figure 4.24a: Finite element model of slab SS14

Figure 4.24b: Variation of load deformation behavior of retrofitted simply supported RC slab due to change in thickness of FRP along diagonal

From the comparisons shown in Figure 4.22b, 4.23b and 4.24b, it is observed that due to the increase in the thickness of FRP, the load-deflection curve gets stiffer and gives higher ultimate load compared to that with lower thickness of FRP in all three locations of FRP i.e. along support edge, along continuous edge and along diagonal. But the change of stiffness is considerably high in case of the location of FRP along continuous edge and diagonal. It is comparatively less in the case of FRP along support edge.

4.3.7 Orientation of FRP in simply supported slab

In the layers of FRP laminates, the orientation of the fibers is considered in this section as a parameter that may affect the load-displacement response of the slab retrofitted with FRP laminates. Three different sets of orientation of FRP have been considered here: $-45^{\circ}/0^{\circ}/45^{\circ}$, $-60^{\circ}/0^{\circ}/60^{\circ}$ and $-90^{\circ}/0^{\circ}/90^{\circ}$. Initially the slab models SS2 (FRP along support edge), SS3 (FRP along continuous edge) and SS4 (FRP along diagonal) have been prepared by choosing the orientation as $-45^{\circ}/0^{\circ}/45^{\circ}$. Subsequently, these have been modified by changing the orientation of the fibers of FRP. Thus SS15 ($-60^{\circ}/0^{\circ}/60^{\circ}$) and SS16 ($-90^{\circ}/0^{\circ}/90^{\circ}$) have been prepared from SS2 ($-45^{\circ}/0^{\circ}/45^{\circ}$), SS17 ($-60^{\circ}/0^{\circ}/60^{\circ}$) and SS18 ($-90^{\circ}/0^{\circ}/90^{\circ}$) have been prepared from SS3 ($-45^{\circ}/0^{\circ}/45^{\circ}$) and SS19 ($-60^{\circ}/0^{\circ}/60^{\circ}$) and SS20 ($-90^{\circ}/0^{\circ}/90^{\circ}$) have been prepared from SS4 ($-45^{\circ}/0^{\circ}/45^{\circ}$) keeping the other parameters same. All these models are analyzed and the load-deflection curves are plotted in Figure 4.25, 4.26 and 4.27 for comparison.

Effect of change of orientation of FRP provided along the support edge in SS2 (-45°/0°/45°), SS15 (-60°/0°/60°) and SS16 (-90°/0°/90°):

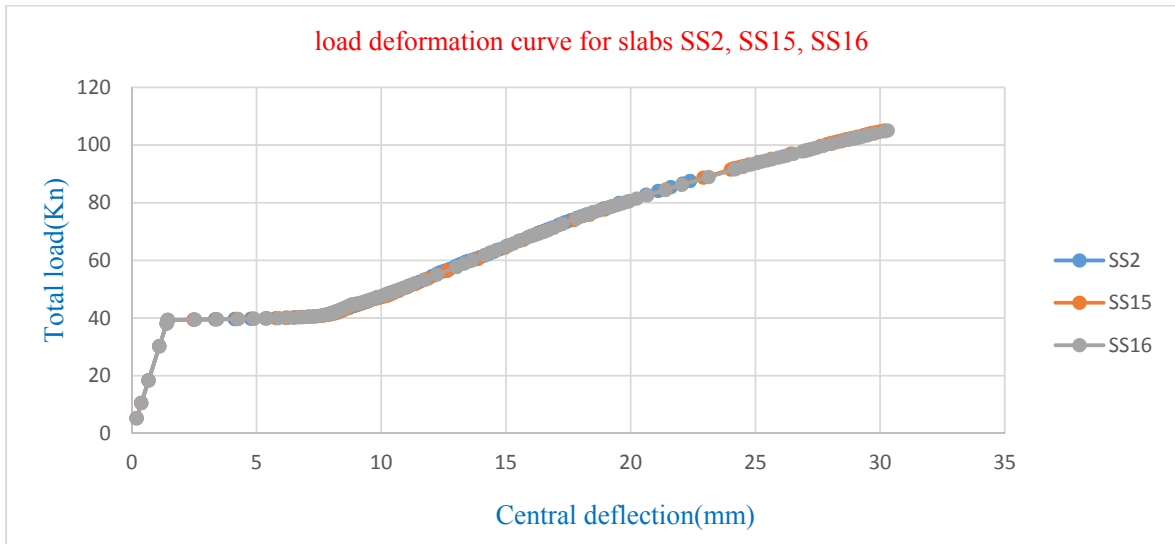


Figure 4.25: Variation of load deformation behavior of retrofitted simply supported RC slab due to change in the orientation of FRP along support edge

Effect of change of orientation of FRP provided along the continuous edge in SS3 (-45°/0°/45°), SS17 (-60°/0°/60°) and SS18 (-90°/0°/90°):

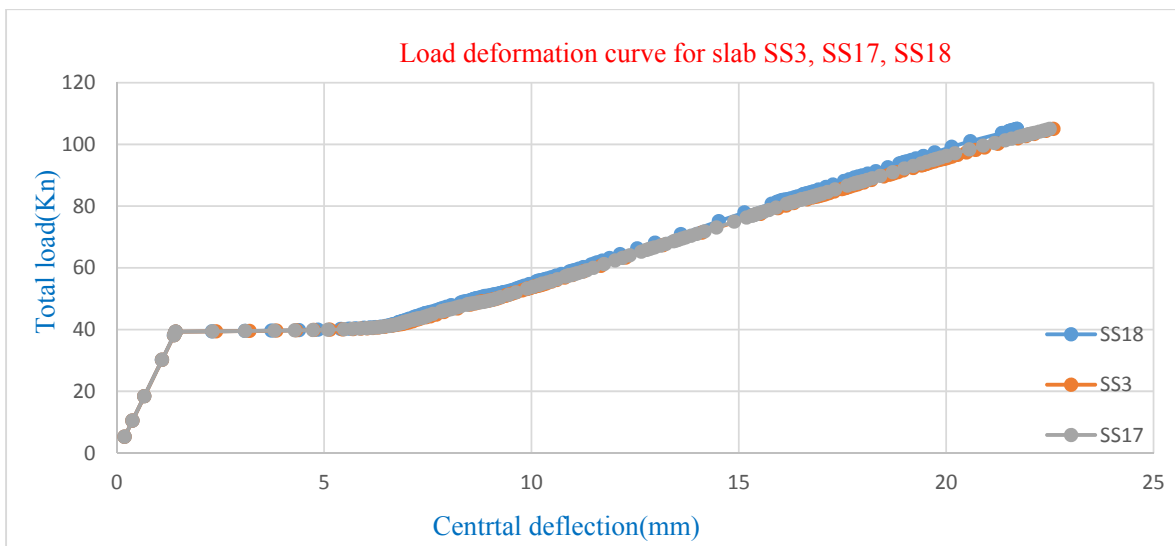


Figure 4.26: Variation of load deformation behavior of retrofitted simply supported RC slab due to change in the orientation of FRP along continuous edge

Effect of change of orientation of FRP provided along the diagonal in SS4 (-45°/0°/45°), SS19 (-60°/0°/60°) and SS20 (-90°/0°/90°):

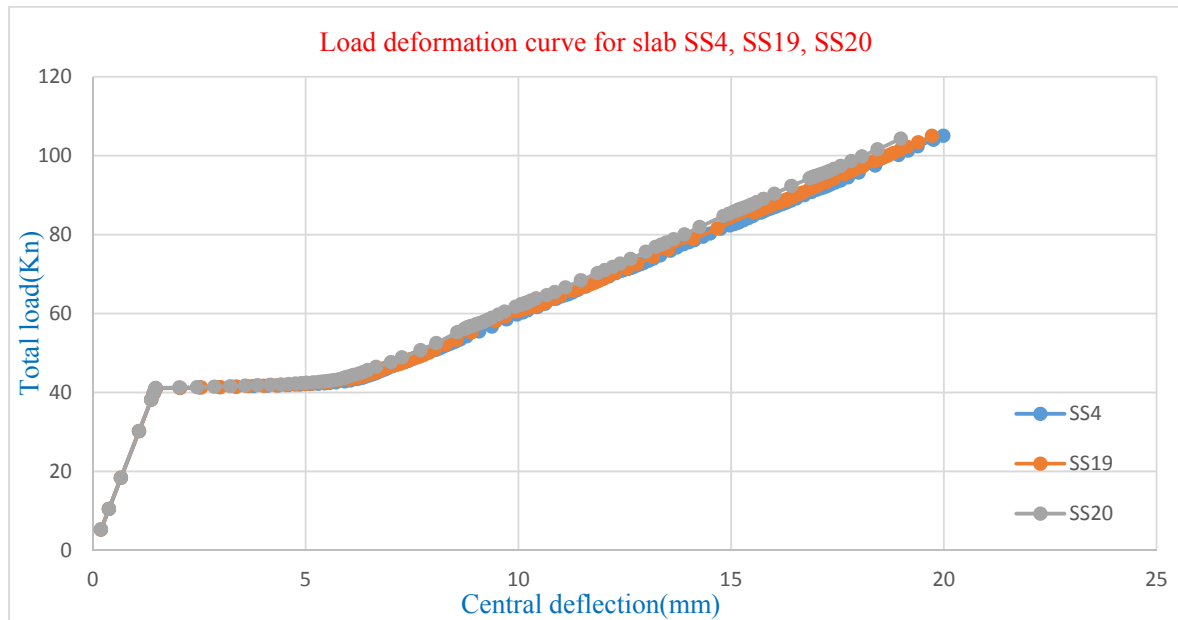


Figure 4.27: Variation of load deformation behavior of retrofitted simply supported RC slab due to change in the orientation of FRP along diagonal

From the Figure 4.25, 4.26 and 4.27, it is seen that there no considerable difference found in the load deflection curves due to the change in the orientation of FRP for the first two cases i.e. the location of FRP along support edge and continuous edge. But there is slight differences in the curves shown in Figure 4.27 for the location of FRP along diagonal.

Part B: Fixed Slab

Control Slab

To perform the parametric study on fixed slab, the model of a fixed supported control slab (un-retrofitted slab) FS1 shown in figure 4.28a is prepared taking the same geometrical data, material data, element type, solution parameters as that of the simply supported control slab (SS1) as shown in figure 4.3 . But there are two changes: one is the support condition i.e. all degrees of freedom are defined as zero at the nodes along boundary and the other is the magnitude of total uniformly distributed load which is considered as 0.163 N/mm² over the entire slab. This finite element model has been used for modification in the following sections considering variations in different parameters and the results like the load deformation behavior, nodal solutions (x, y and z-component stress and y component deformation) and also the crack pattern coming from the analysis are reported.

4.3.8 Discretization of the fixed control slab

A variation in the mesh size in the discretization of the fixed slab has been done to perform the mesh convergence study. In the model of one-quarter of the slab, 6x6, 9x9 and 12x12 elements are considered as shown in Figure 4.28a, 4.28b and 4.28c respectively. The reinforcement modelling of each of these slabs are shown in Figure 4.29a, 4.29b and 4.29c respectively. All other parameters are kept identical. All these models are analyzed using ANSYS.

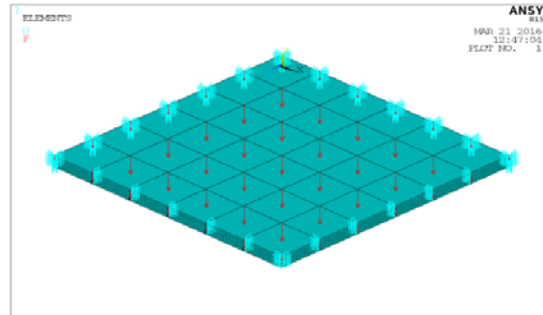


Figure 4.28a: Discretization of quarter RC slab in X-Z plane with (6 x 6) mesh of 36 elements

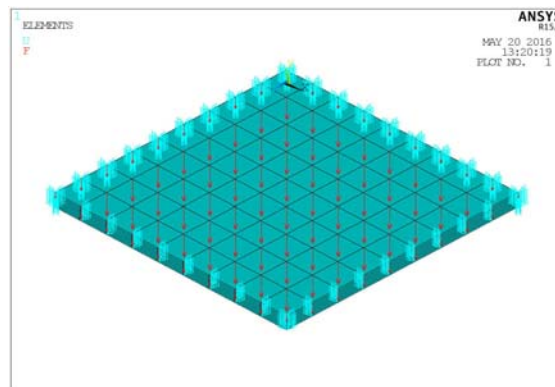


Figure 4.28b: Discretization of quarter RC slab in X-Z plane with (9 x 9) mesh of 81 elements

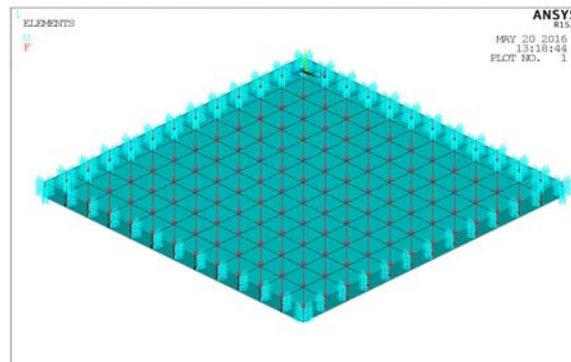


Figure 4.28c: Discretization of quarter RC slab in X-Z plane with (12 x 12) mesh of 144 elements

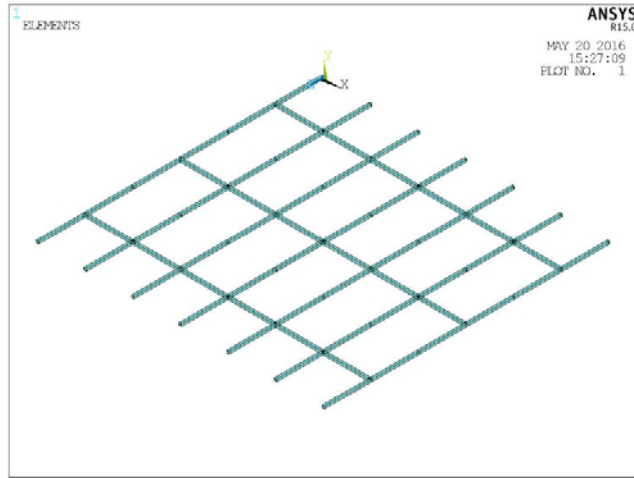


Figure 4.29a: Modelling of reinforcing bars with (6 x 6) mesh of 36 elements

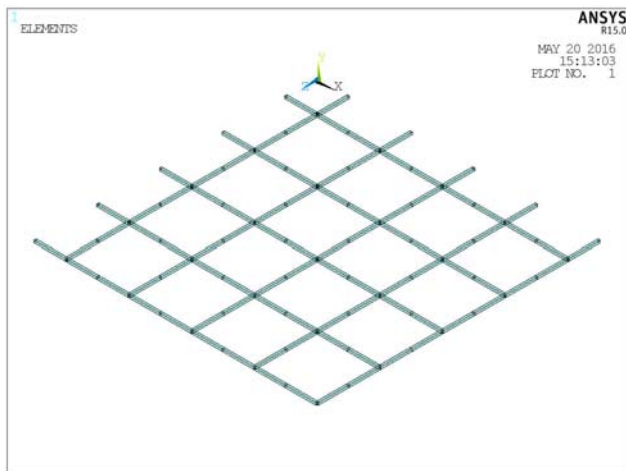


Figure 4.29b: Modelling of reinforcing bars with (9 x 9) mesh of 81 elements

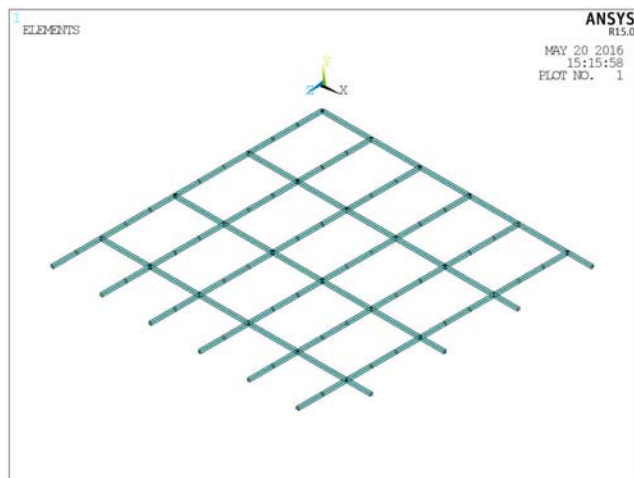


Figure 4.29c: Modelling of reinforcing bars with (12 x 12) mesh of 144 elements

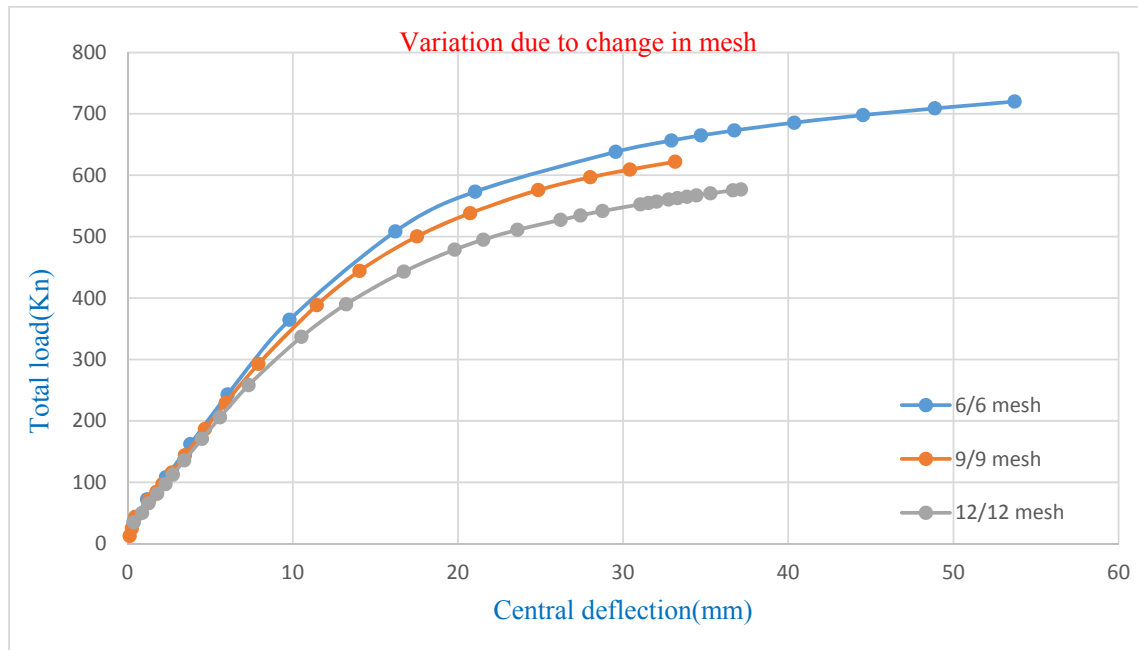


Figure 4.30: Variation of load-deflection plot due to change in mesh size in fixed slab

The variation in the load-deflection curves among three models are shown in Figure 4.30. It is observed that the load-deflection curve for 6x6 discretization showing higher stiffness and also higher ultimate load compared to the other two. Also Table 4.6 gives the deflection of the slab at 575 kN load for these three different mesh types. It can be noted that the change in deflection due to the variation in mesh is converging. Consequently, this particular mesh discretization i.e. 6x6 for the slab FS1 has been followed in the following sections for parametric study of retrofitted slabs.

Table 4.6: Comparison of deflection at load 575 KN due to change in mesh

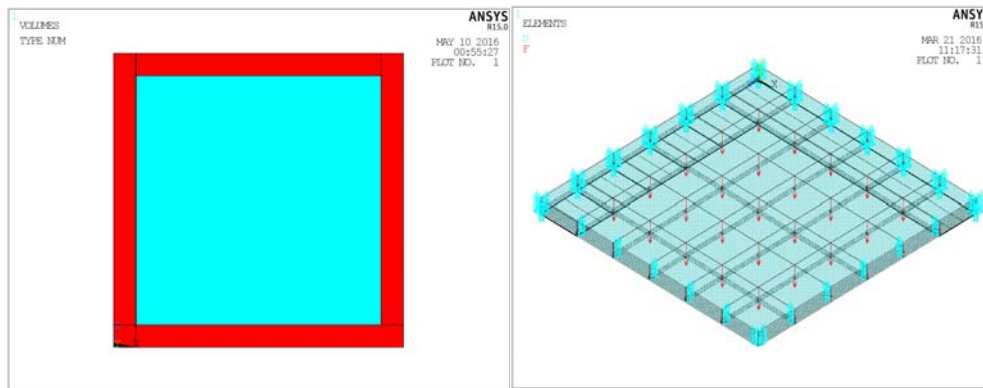
Type of mesh in slab	No of elements	Deflection (mm.)	Change (%)
6 x 6	36	21.0464	0.0
9 x 9	81	24.8667	18.15
12 x 12	144	36.6534	74.15

4.3.9 Location of FRP in fixed slab

Just like the simply supported slab, the basic reinforced concrete fixed slab (also termed here as control fixed slab CS, FS1) are strengthened with FRP laminates considering as attached with the bottom surface of the slab. The behavior of the retrofitted slab under external mechanical load may depend on the location of FRP strips. To study this effect on fixed slab,

three different locations of the FRP strips are considered a) along the fixed edge, b) along the continuous edge (for one quarter model) and c) along the diagonal. The slab FS1 has been strengthened with FRP (using SOLID 185 in the model) sheet at the bottom of the slab along support edge (named as FS2), continuous edge (named as FS3) and diagonal position (named as FS4) of the RC slab in fixed supported condition as shown in Figure 4.31a, 4.31b and 4.31c respectively. The thickness of FRP used is 3 mm and the orientation of 3 FRP layers are (-45°, 0°, 45°).

a) FRP along the fixed edge

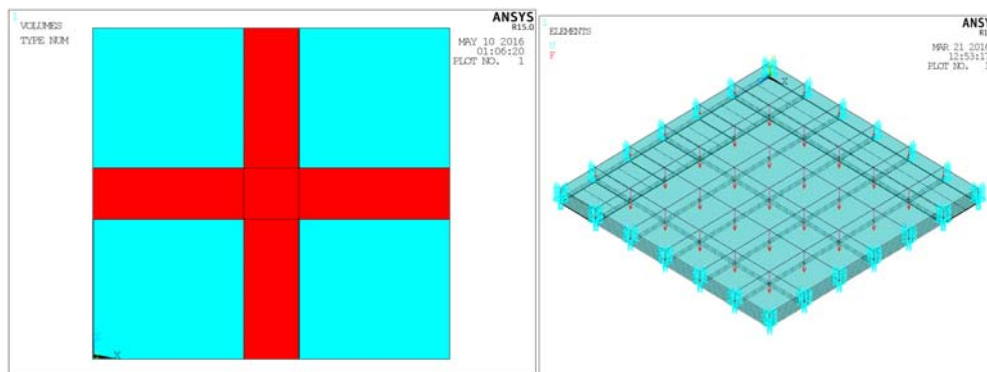


Full model

One quarter model

Figure 4.31a: FRP along support edge in slab FS2

b) FRP along the continuous edge (for one quarter model)



Full model

One quarter model

Figure 4.31b: FRP along continuous edge in the slab FS3

c) FRP along the diagonal

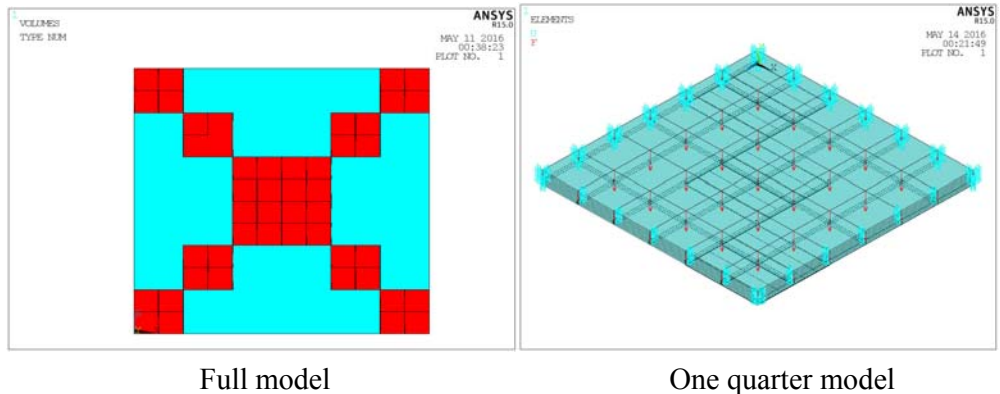


Figure 4.31c: FRP along diagonal in the slab FS4

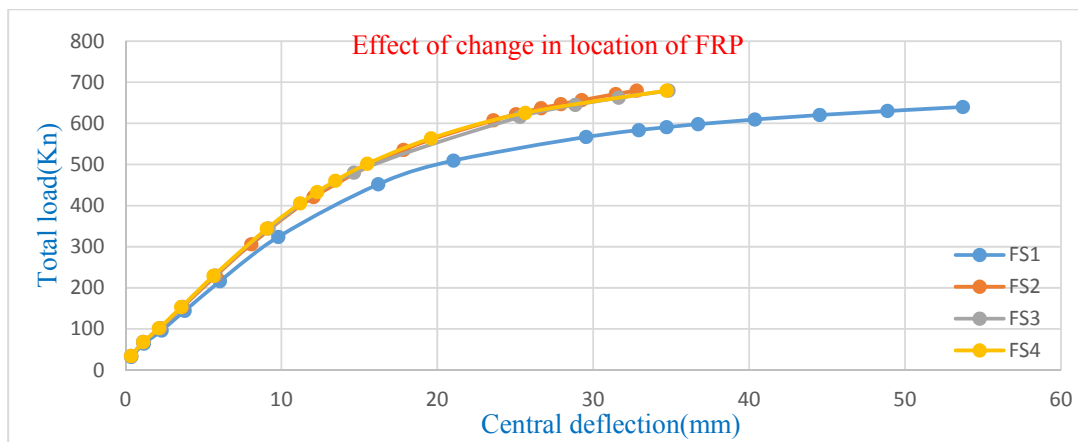


Figure 4.32: Variation of load deflection curve of the slab FS2, FS3, FS4 (retrofitted) with FS1 (control slab)

The result coming from the analysis of control slab FS1 and the same for retrofitted slab FS2, FS3 and FS4 are compared graphically in the plot of load deflection curve as given in Fig.4.32. These three retrofitted slabs carry more load than FS1 slab and also the stiffness is more than that of FS1 slab. All these three retrofitted slabs FS2, FS3 and FS4 have more or less same stiffness. From this, it can be suggested that for fixed supported slab, the location may not contribute very large change. Any of these three locations can be considered for the purpose of strengthening of the fixed slab with FRP laminates.

Contour plot of Nodal Solution in slabs FS1, FS2, FS3 and FS4

The contour plots of stresses in various directions and deflection in Y direction have been shown for the fixed control slab (FS1) and the retrofitted slabs (FS2, FS3 & FS4) in the following figures. The plots are found to be quite realistic one.

a) Contour plot of nodal solution of slab FS1

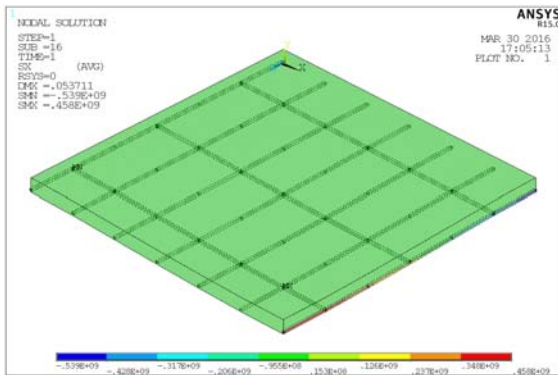


Figure 4.33a: Contour of x-component stress in slab FS1

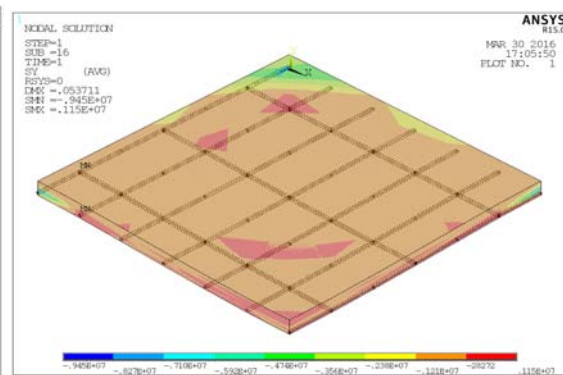


Figure 4.33b: Contour of y-component stress in slab FS1

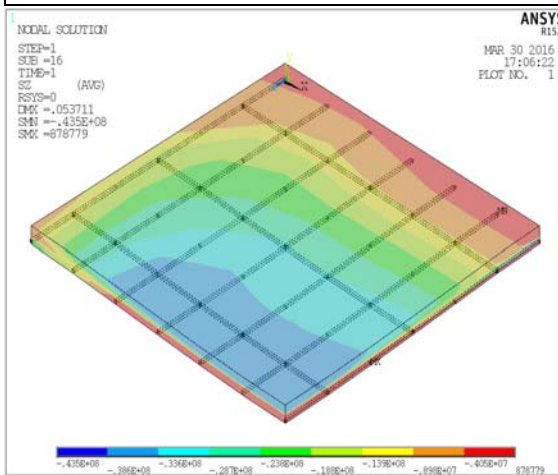


Figure 4.33c: Contour of z-component stress in slab FS1

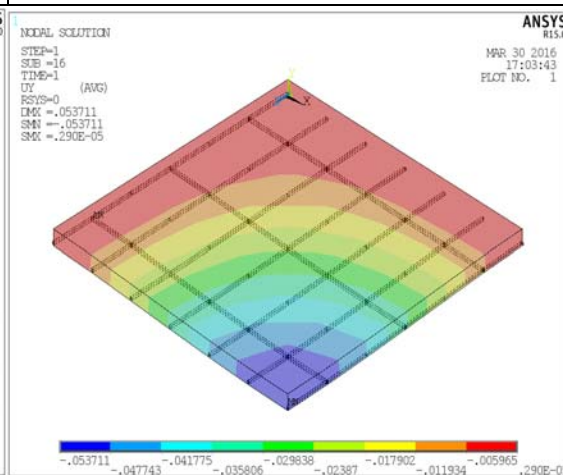


Figure 4.33d: Contour of y-component deformation in slab FS1

b) Contour plot of nodal solution of slab FS2

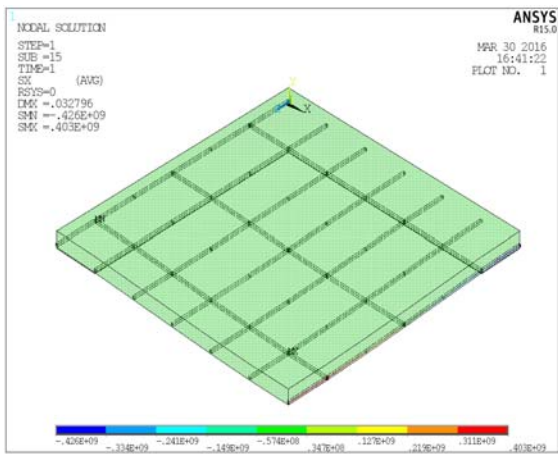


Figure 4.34a: Contour of x-component stress in slab FS2

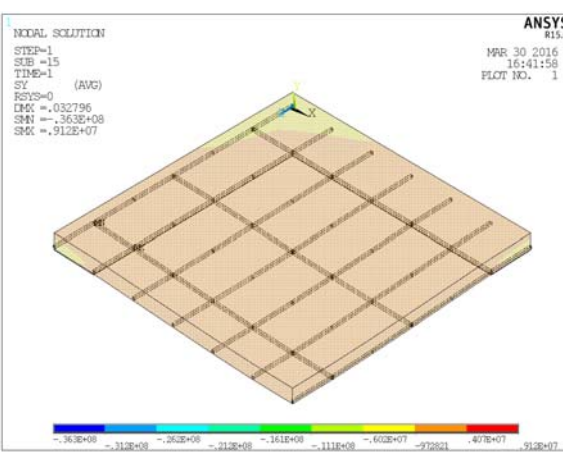


Figure 4.34b: Contour of y-component stress in slab FS2

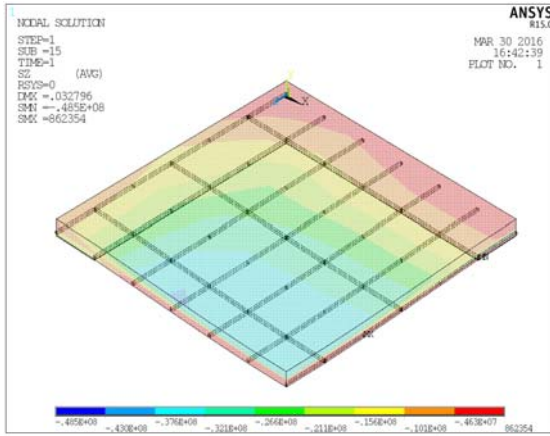


Figure 4.34c: Contour of z-component stress in slab FS2

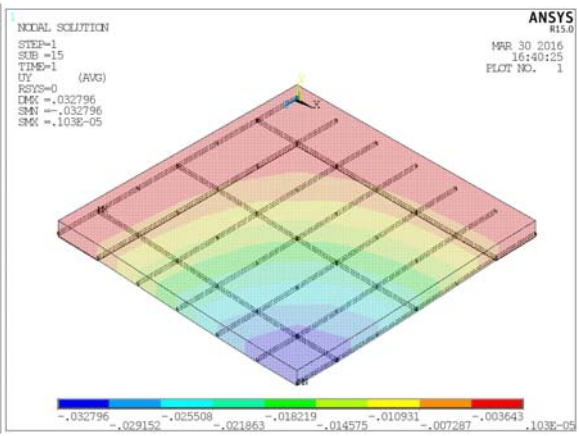


Figure 4.34d: Contour of y-component deformation in slab FS2

c) Contour plot of nodal solution of slab FS3

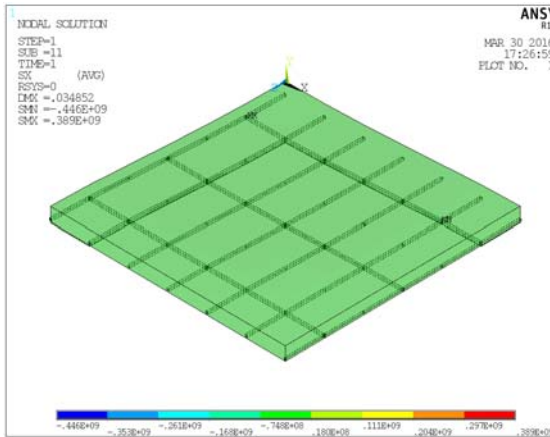


Figure 4.35a: Contour of x-component stress in slab FS3

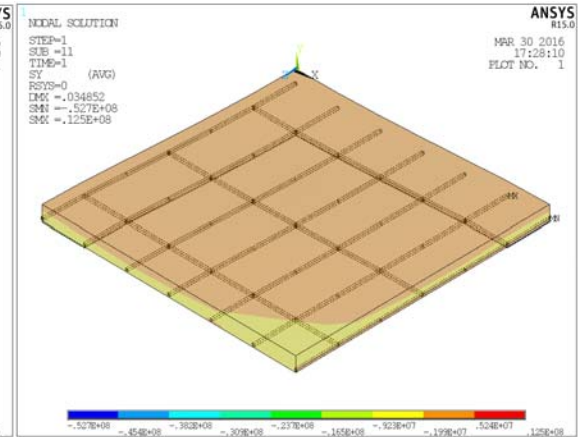


Figure 4.35b: Contour of y-component stress in slab FS3

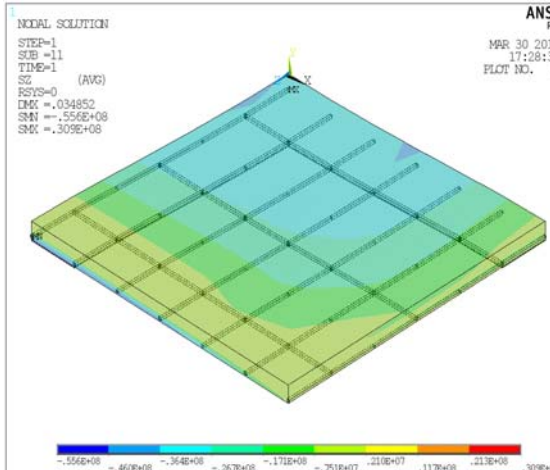


Figure 4.35c: Contour of z-component stress in slab FS3

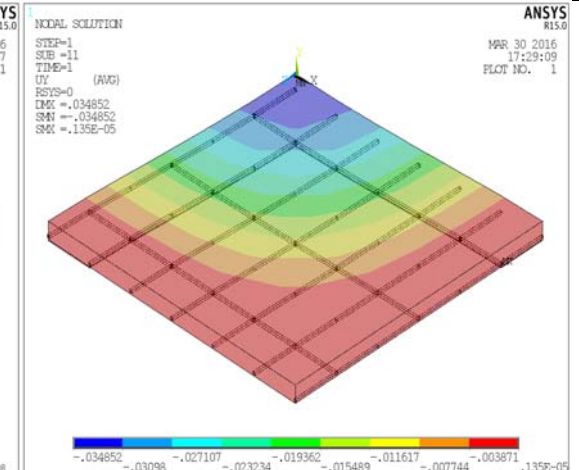


Figure 4.35d: Contour of y-component deflection in slab FS3

d) Contour plot of nodal solution of slab FS4

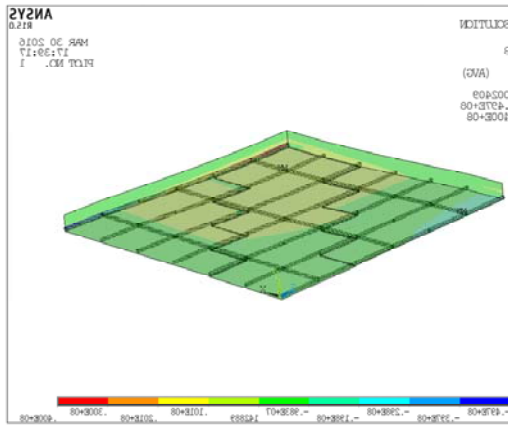


Figure 4.36a: Contour of x-component stress in slab FS4

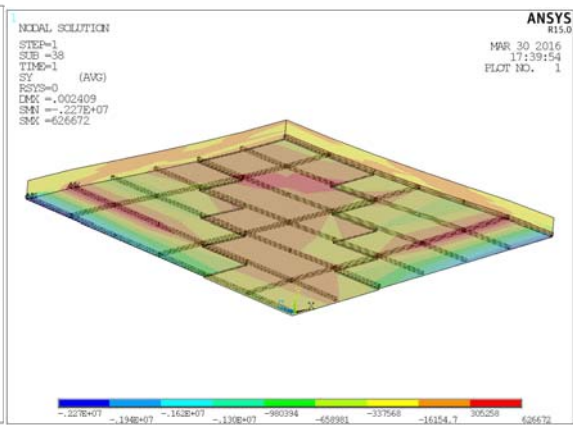


Figure 4.36b: Contour of y-component stress in slab FS4

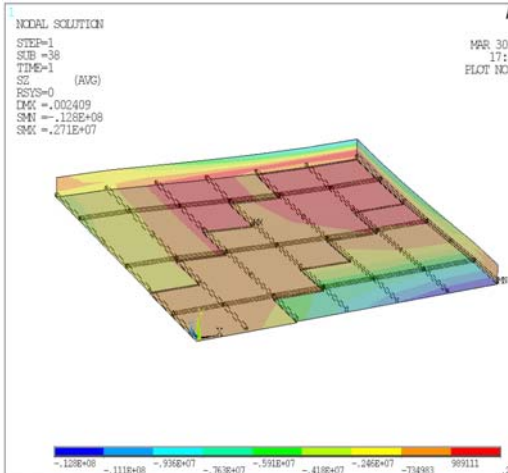


Figure 4.36c: Contour of z-component stress in slab FS4

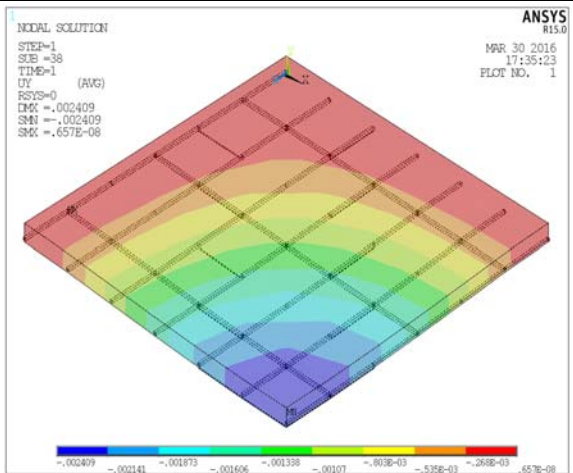


Figure 4.36d: Contour of y-component deflection in slab FS4

Crack pattern in slabs FS1, FS2, FS3 and FS4

Similar to the cases of simply supported slabs, the crack patterns are obtained from the software ANSYS. Figures 4.37a to 4.40d shows evolutions of crack patterns developing for each slab (FS1, FS2, FS3 and FS4) at the last loading step. At the early stages of loading, the behavior of slab has been observed to be elastic until the appearance of the first crack. Invariably, the crack has been initiated at the support, continuous edge and also at the center of the slab.

a) 1st Crack Pattern for slab FS1, FS2, FS3 & FS4

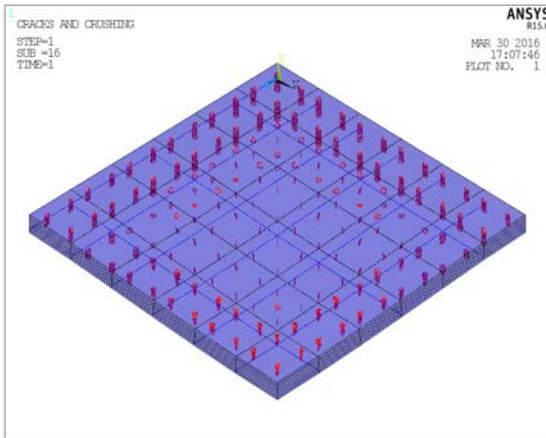


Figure 4.37a: Pattern of 1st crack in slab FS1

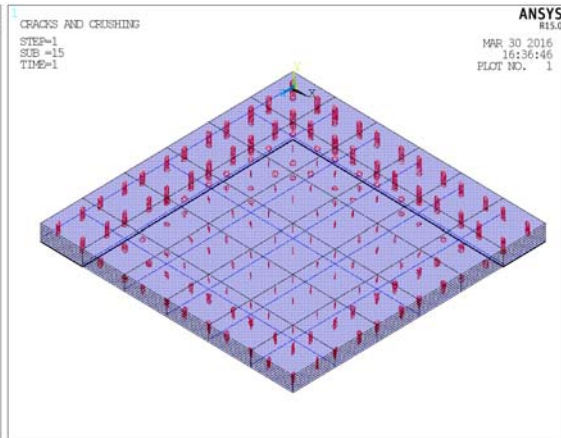


Figure 4.37b: Pattern of 1st crack in slab FS2

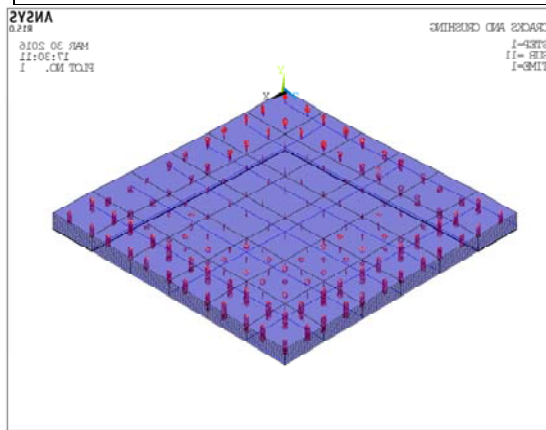


Figure 4.37c: Pattern of 1st crack in slab FS3

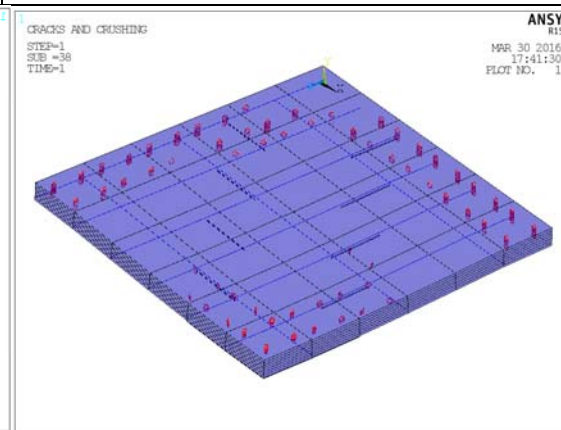


Figure 4.37d: Pattern of 1st crack in slab FS4

b) 2nd Crack Pattern for slab FS1, FS2, FS3 & FS4

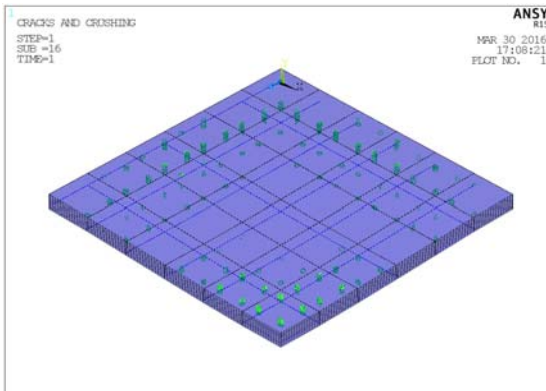


Figure 4.38a: Pattern of 2nd crack in slab FS1

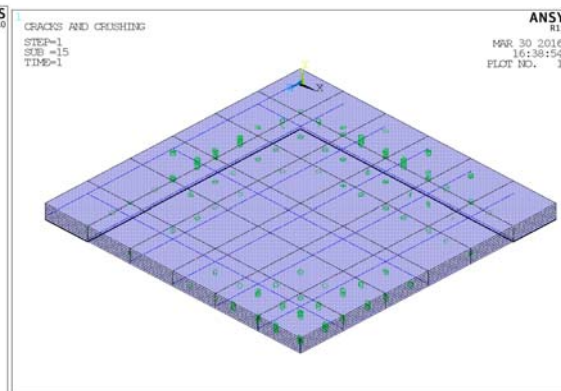


Figure 4.38b: Pattern of 2nd crack in slab FS2

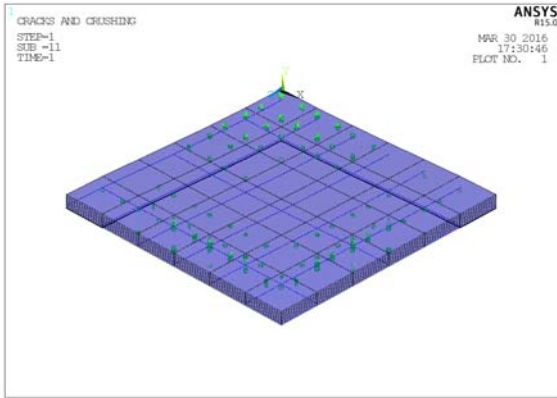


Figure 4.38c: Pattern of 2nd crack in slab FS3

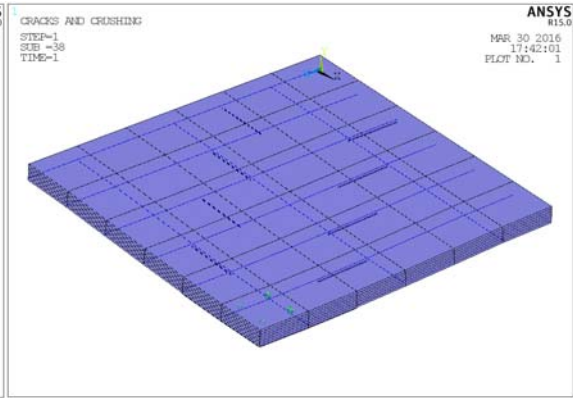


Figure 4.38d: Pattern of 2nd crack in slab FS4

C) 3rd Crack Pattern for slab FS1, FS2, FS3 & FS4

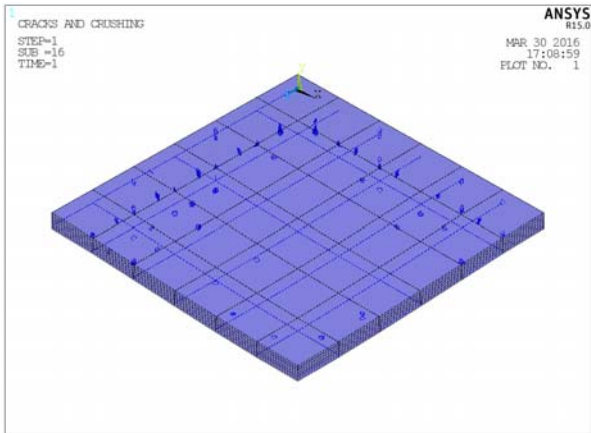


Figure 4.39a: Pattern of 3rd crack in slab FS1

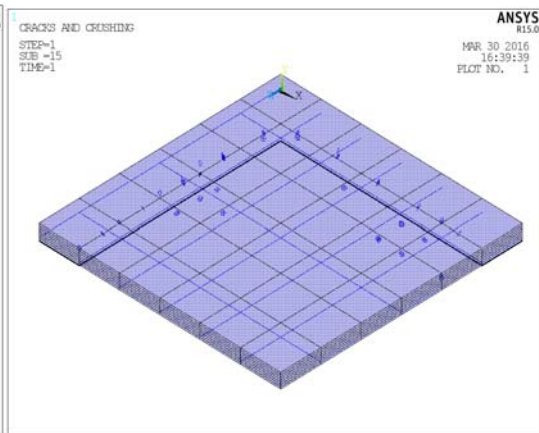


Figure 4.39b: Pattern of 3rd crack in slab FS2

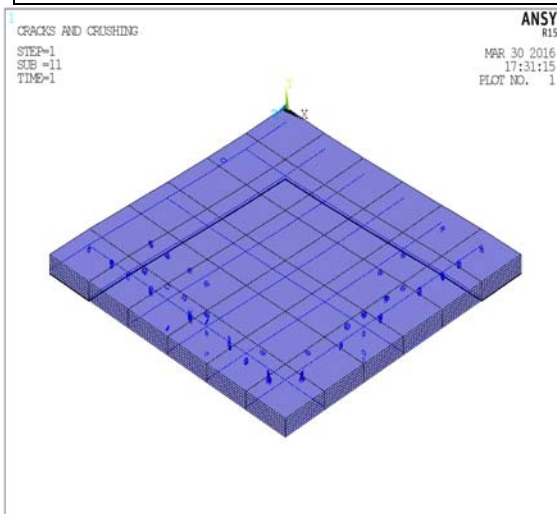


Figure 4.39c: Pattern of 3rd crack in slab FS3

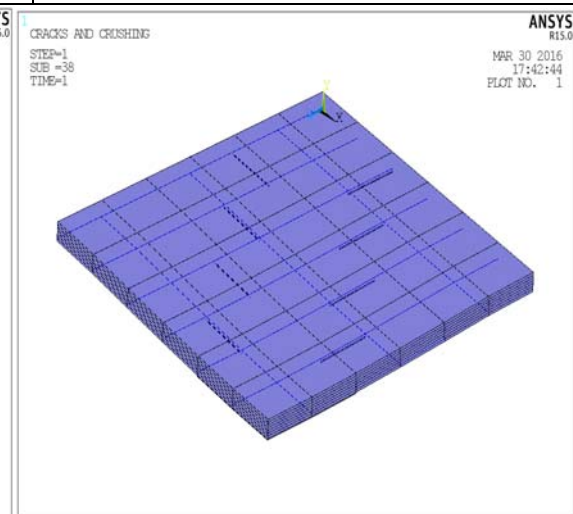


Figure 4.39d: Pattern of 3rd crack in slab FS4

d) All cracks for the slab FS1, FS2, FS3, and FS4

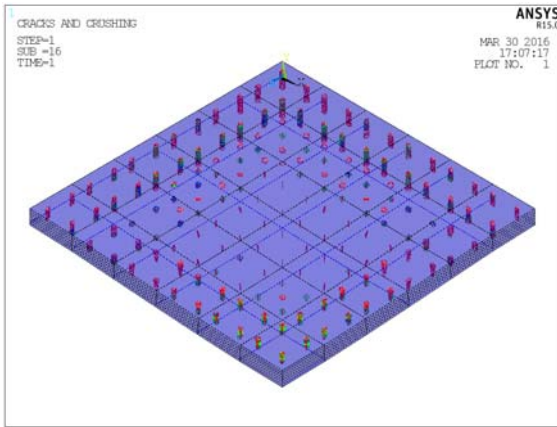


Figure 4.40a: Pattern of all cracks in slab FS1

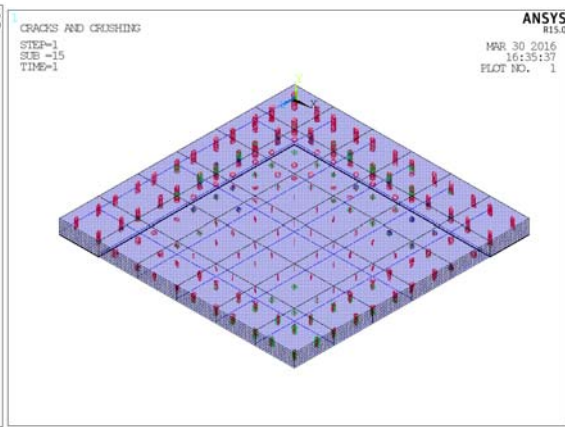


Figure 4.40b: Pattern of all cracks in slab FS2

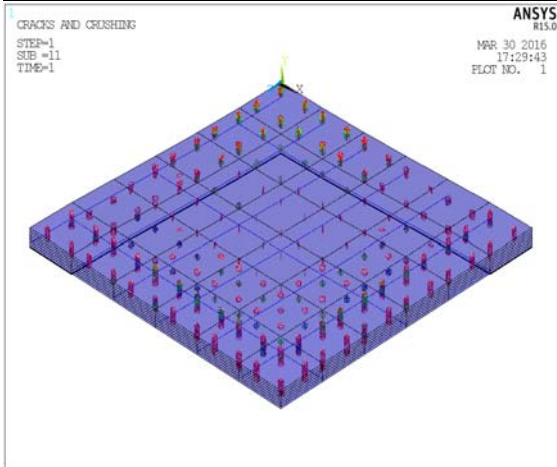


Figure 4.40c: Pattern of all cracks in slab FS3

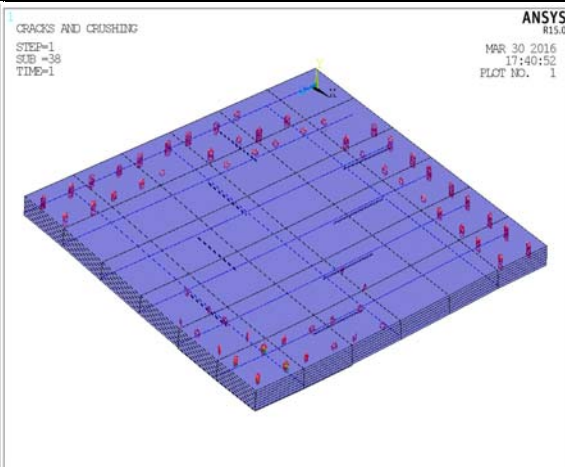


Figure 4.40d: Pattern of all cracks in slab FS4

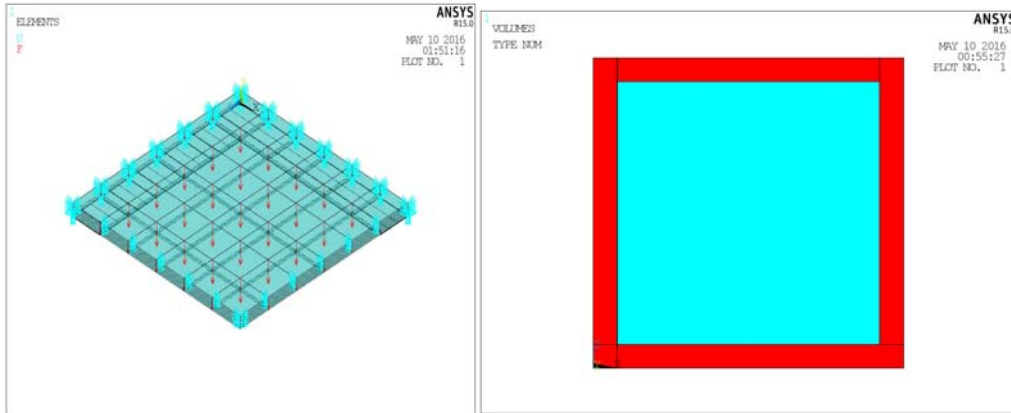
Comparing the crack patterns in different slabs, it is observed that area of cracked zone is considerably less in the slab FS4 having the FRP along the diagonal. Though the difference is not so noticeable in the 1st crack, but in the 2nd crack and mainly in the 3rd crack, the difference is prominent.

4.3.10 Width of FRP in the fixed slab

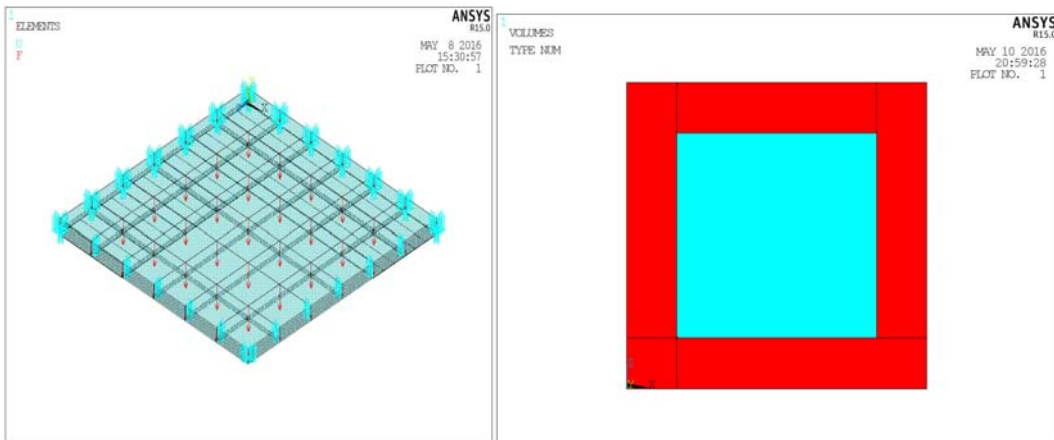
The width of FRP laminate in each of the retrofitted fixed slabs FS2, FS3 and FS4 is considered as a variable parameter in this section like simply supported slabs as this has a considerable amount of effect on the behaviour of the slab.

4.3.10.1 FRP along the support edge of the fixed slab

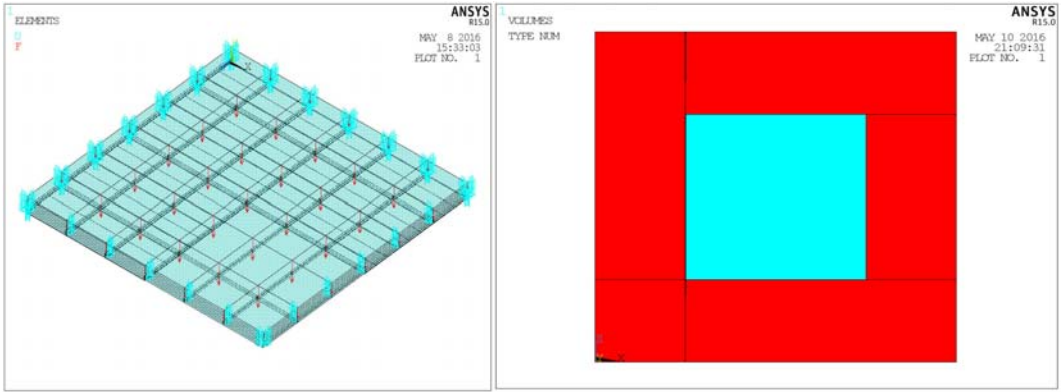
In slab FS2, the FRP has been provided along the support edge. Initially in the model, FRP elements are attached with the outermost elements of the model as shown in Figure 4.41a. Then it has been extended in the next element line as shown in Figure 4.41b. Then it is increased again in the same manner as shown in Figure 4.41c. Finally all the elements are covered with FRP elements as shown in Figure 4.41d. Thus the percentage of slab area covered with FRP are 30%, 55%, 75% and 100% respectively. All these models are analysed and the load-deflection plots coming from the analysis are compared as shown in Figure 4.42. The comparison shows that the retrofitted slabs get stiffer considerably with respect to the unretrofitted slab but the variation of the stiffness due to the increment in the area of FRP laminates are not significant. Further, the failure load increases due to the increment in the area of FRP laminates. The change is considerably high when the area is increased from 0% to 30% and 30% to 55% but after that there is very insignificant gain in terms of ultimate load beyond 55% FRP area.



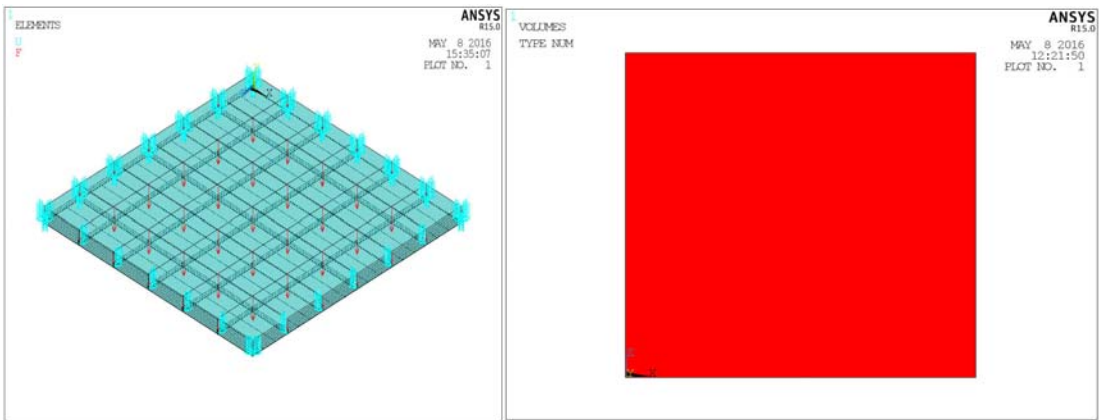
A: 30% area of Slab FS2 covered by FRP



B: 55% area of Slab FS2 covered by FRP



C: 75% area of Slab FS2 covered by FRP



D: 100% area of Slab FS2 covered by FRP

Figure 4.41: Variation of FRP width along the support edge

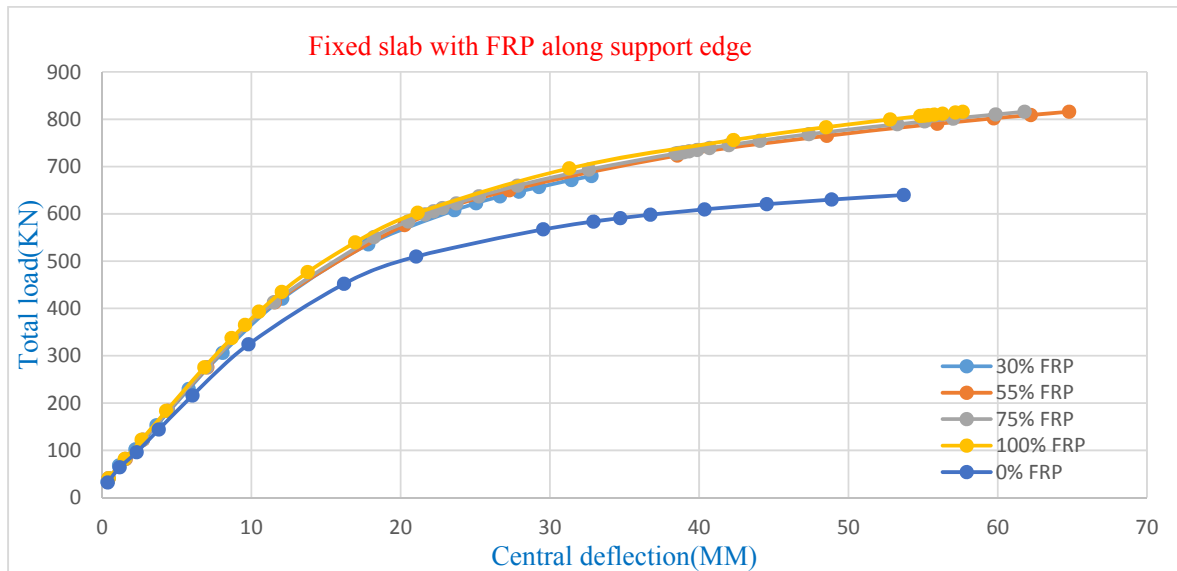
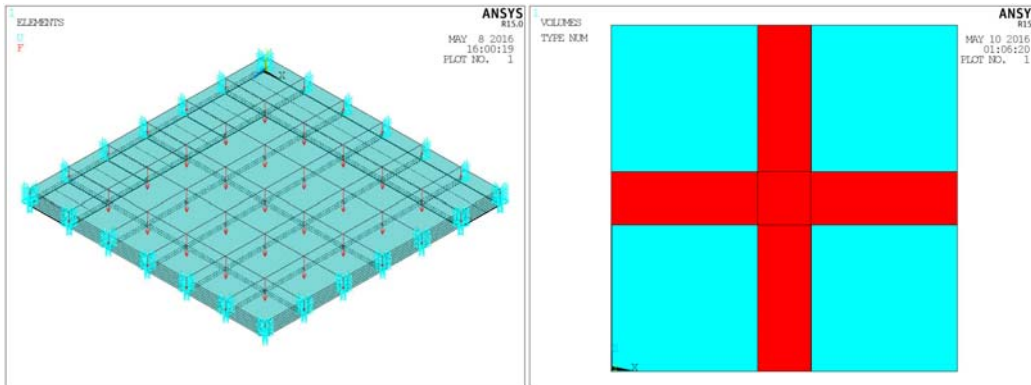


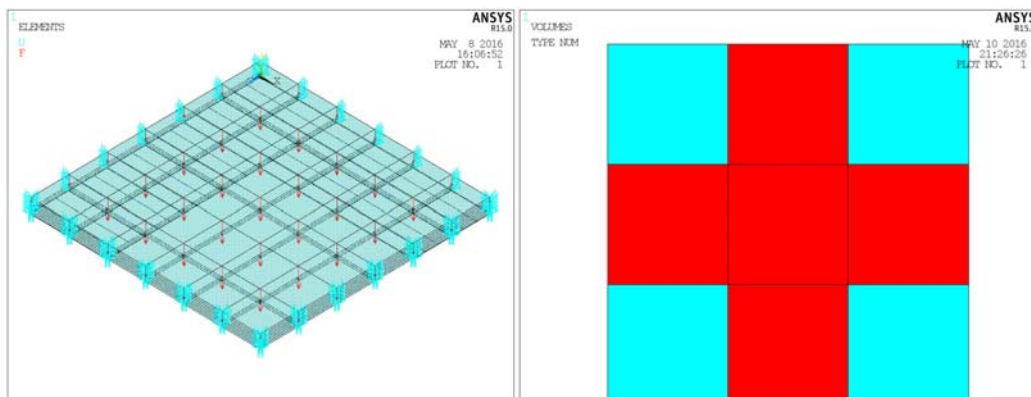
Figure 4.42: Variation of load deformation behavior of retrofitted fixed supported RC slab due to change in the area covered with FRP along support edge

4.3.10.2 FRP along the continuous edge of the fixed slab

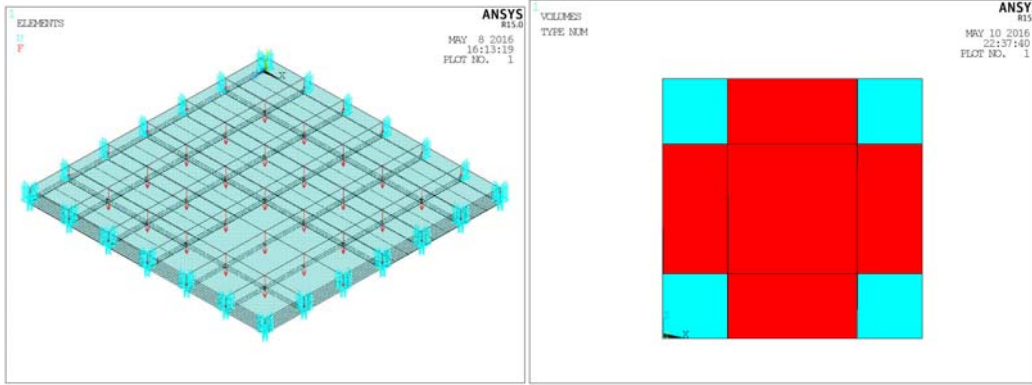
In slab FS3, the FRP has been provided along the continuous edge of the one-quarter of the slab i.e. along the middle lines (line of symmetry) of the full slab. Initially in the model, FRP elements are attached with the extreme elements of the one-quarter model i.e. FRP of two-element width along X and Z directions in full model as shown in Figure 4.43a. Then it has been extended in the next element line i.e. forming FRP of four-element width in full slab as shown in Figure 4.43b. Then it is increased again in the same manner as shown in Figure 4.43c. Finally all the elements are covered with FRP elements as shown in Figure 4.43d. Thus the percentage of slab area covered with FRP are 30%, 55%, 75% and 100% respectively. All these models are analysed and the load-deflection plots coming from the analysis are compared as shown in Figure 4.44. The comparison shows that the retrofitted slabs get stiffer considerably with respect to the unretrofitted slab but the variation of the stiffness due to the increment in the area of FRP laminates are not significant in all cases. Further, the failure load increases due to the increment in the area of FRP laminates. The change is considerably high when the area is increased from 0% to 30% and 30% to 55% but after that there is very insignificant gain in terms of ultimate load beyond 55% FRP area.



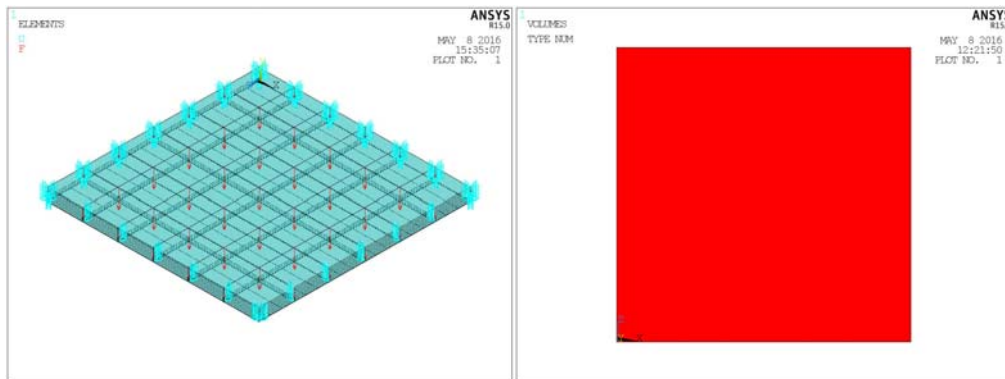
A: 30% area of Slab FS3 covered by FRP



B: 55% area of Slab FS3 covered by FRP



C: 75% area of Slab FS3 covered by FRP



D: 100% area of Slab FS3 covered by FRP

Figure 4.43: Variation of FRP width along the continuous edge

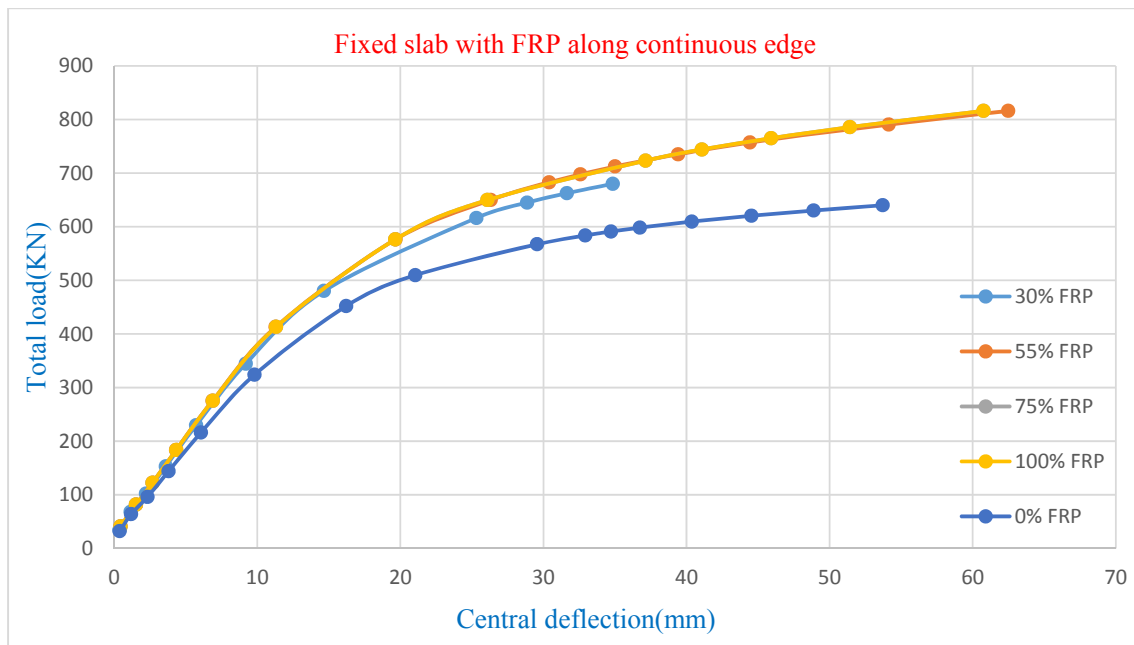
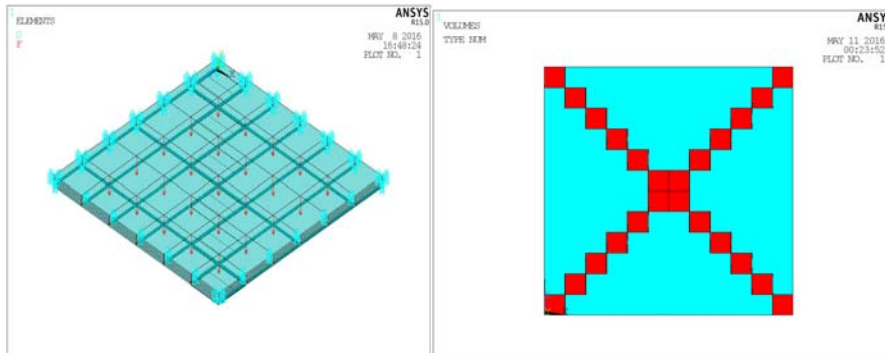


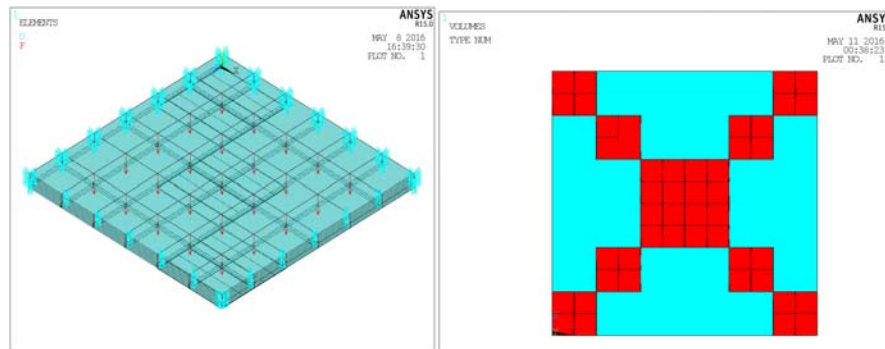
Figure 4.44: Variation of load deformation behavior of retrofitted fixed supported RC slab due to change in the area covered with FRP along continuous edge

4.3.10.3 FRP along the diagonal of the fixed slab

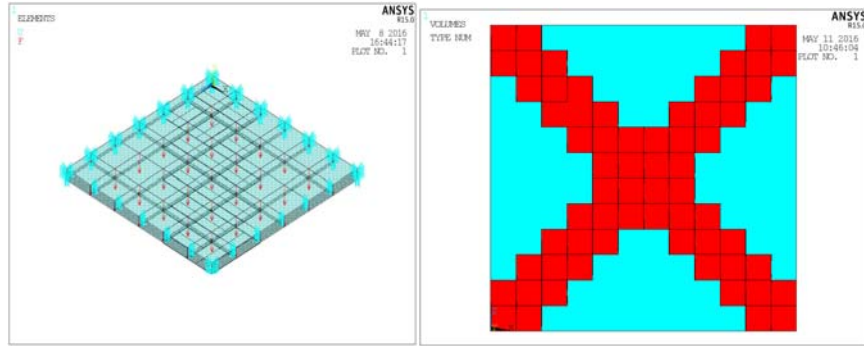
In slab FS4, the FRP has been provided along the diagonal direction of the one-quarter of the slab i.e. along both the diagonals of the full slab. Initially in the model, FRP elements are attached with twelve elements along the diagonal of the one-quarter model i.e. forty eight elements in full model giving 33% FRP area as shown in Figure 4.45b. Then it has been reduced to six elements along the diagonal of the one-quarter model i.e. twenty four elements in full model giving 16.67% FRP area as shown in Figure 4.45a. Then it is increased to cover sixteen elements along the diagonal of the one-quarter model i.e. sixty four elements in full model giving 50% FRP area as shown in Figure 4.45c. Then it is increased in the same manner to cover twenty four elements along the diagonal of the one-quarter model i.e. ninety six elements in full model giving 66.67% FRP area as shown in Figure 4.45d. Finally all the elements are covered with FRP elements as shown in the previous Figure 4.43d. All these models are analysed and the load-deflection plots coming from the analysis are compared as shown in Figure 4.46. The comparison shows that unlike the slabs having FRP along support edge and continuous edge, these slabs having FRP along diagonals get stiffer continuously with the increment in the area of FRP laminates indicating smaller deflection at the ultimate load. It is also observed that there is a prominent variation in the failure load which increases due to the increment of the width of FRP area.



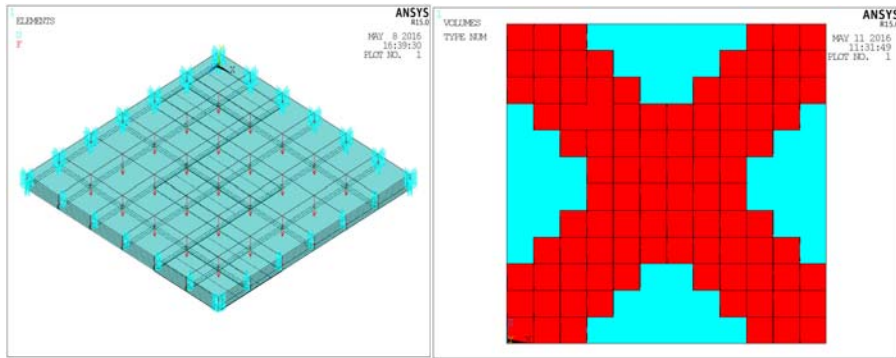
A: 16.67% area of Slab FS4 covered by FRP



B: 33% area of Slab FS4 covered by FRP



C: 50% area of Slab FS4 covered by FRP



D: 66.67% area of Slab FS4 covered by FRP

Figure 4.45: Variation of FRP width along the diagonal

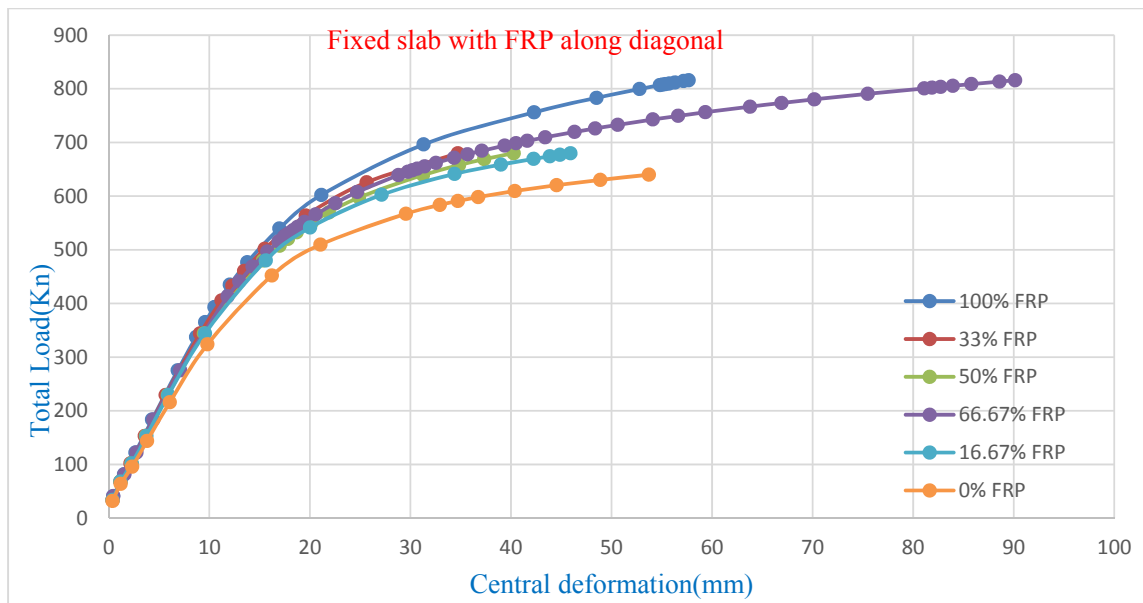


Figure 4.46: Variation of load deformation behavior of retrofitted fixed supported RC slab due to change in the area covered with FRP along diagonal

In addition to the above, the change of load carrying capacity of fixed RC slab retrofitted with FRP at different locations and having different width i.e.area of FRP are shown in the following Table 4.7 and change of deformation at ultimate load of those slab retrofitted with FRP are shown in the Table 4.8.

Table 4.7: Change of load carrying capacity of fixed RC slab retrofitted with FRP

Percentage of FRP area	Increment of load carrying capacity in percentage		
	RC slab retrofitted with Support edge FRP	RC slab retrofitted with diagonal FRP	RC slab retrofitted with Continuous edge FRP
16.67		6.25	
30 to 33.33	6.25	6.25	6.25
50 to 55	27.5	6.25	27.5
66.67 to 75	27.5	27.5	27.5
100	27.5	27.5	27.5

Table 4.8: Change of deformation at ultimate load of fixed RC slab retrofitted with FRP

Percentage of FRP area	Deformation at ultimate load(mm)		
	RC slab retrofitted with Support edge FRP	RC slab retrofitted with diagonal FRP	RC slab retrofitted with Continuous edge FRP
16.67		45.90	
30 to 33.33	32.79	34.72	34.84
50 to 55	64.78	40.26	62.48
66.67 to 75	61.80	90.13	60.57
100	57.66	57.66	57.66

It can easily be observed that to achieve maximum benefit 100% of the slab area should be covered with FRP. But in case of location of FRP along support edge or continuous edge,

coverage of 50%-55% area will give satisfactory improvement. But for the location of FRP along diagonal, the requirement of coverage with FRP is found to be 66.67%. The deformation at ultimate load has also a tendency to reduce with the increase in the area of slab covered with FRP which is realistic.

4.3.11 Layers of FRP in Fixed slab

In this section, the number of layers considered in the SOLID185 element used to model FRP has been considered as a parameter. In slab FS2, FS3 and FS4, the FRP has been provided along support edge, continuous edge and diagonal respectively of the fixed reinforced concrete slab having 3 FRP layers in it. To choose the variation like the parametric study with simply supported slab, the number of layers has been changed to 2 layers and 5 layers keeping the thickness of FRP same. As a result, the slab models FS5 (2 layers) and FS6 (5 layers) are prepared by modifying the model FS2 (FRP along support edge), the slab models FS7 (2 layers) and FS8 (5 layers) are prepared by modifying the model FS3 (FRP along continuous edge) and the slab models FS9 (2 layers) and FS10 (5 layers) are prepared by modifying the model FS4 (FRP along diagonal). All these models are analysed and the load-deflection plots coming from the analysis are compared as shown in Figure 4.47a, 4.47b, 4.47c.

Variation due to the change in layers of FRP in slab FS2, FS5 and FS6:

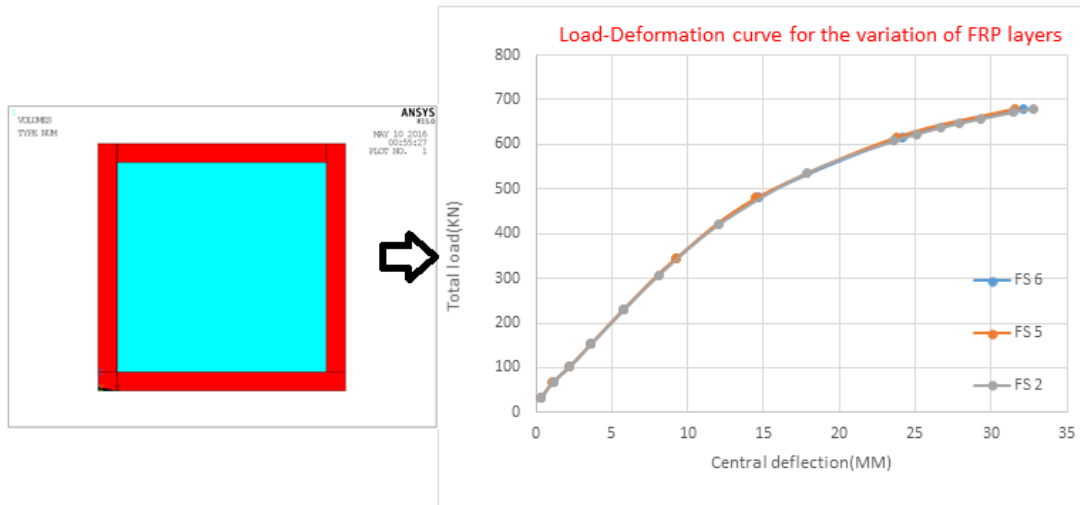


Figure 4.47a: Variation of load deformation behavior of retrofitted fixed supported RC slab due to change in number of layers in FRP along support edge

Variation due to the change in layers of FRP in slab FS3, FS7 and FS8:

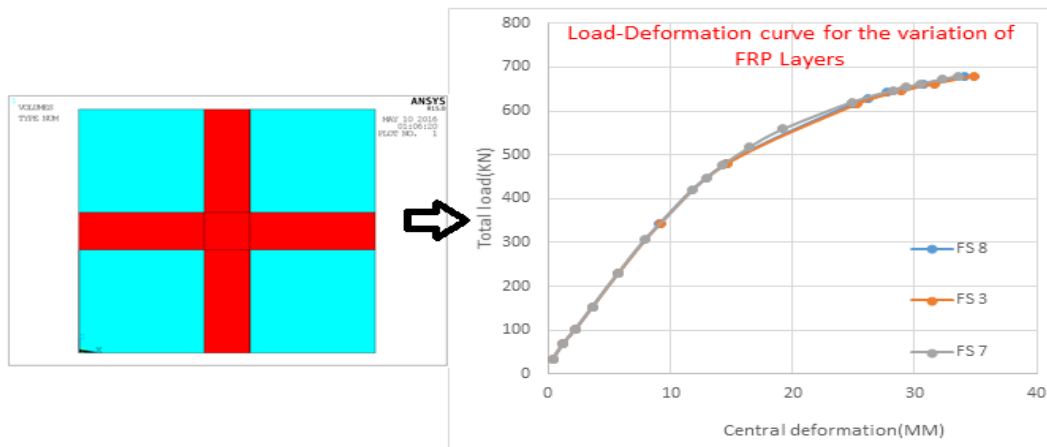


Figure 4.47b: Variation of load deformation behavior of retrofitted fixed supported RC slab due to change in number of layers in FRP along continuous edge

Variation due to the change in layers of FRP in slab FS4, FS9 and FS10:

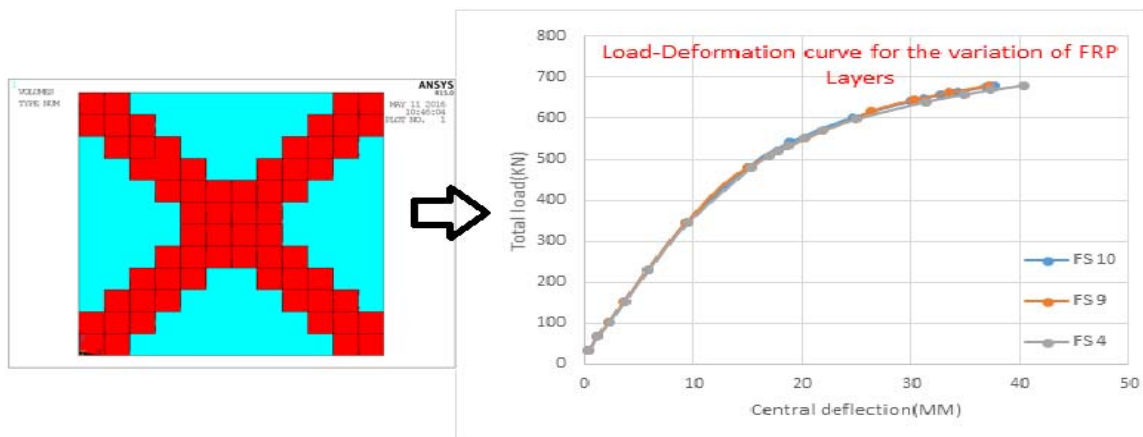


Figure 4.47c: Variation of load deformation behavior of retrofitted fixed supported RC slab due to change in number of layers in FRP along diagonal

From the comparison of Figure 4.47a and 4.47b, the load deformation curve shows that there is no considerable variation in these two curves, but some nominal variation has shown in the curve as shown Figure 4.47c i.e. the curve for the variation of FRP layers at diagonal position. It shows that the slabs gets more stiffer with the increment in the layers of FRP laminates near failure.

4.3.12 Thickness of FRP in fixed slab

In this section, the behavior of the retrofitted slab due to the change in the thickness of the FRP laminates has been studied. Initially the slab models FS2, FS3 and FS4 have been prepared considering the thickness of FRP as 3mm. Here, this thickness has been increased to 5mm. Thus FS2 (3mm thick FRP along support edge) has been changed to FS12 (5mm thick FRP along support edge), FS3 (3mm thick FRP along continuous edge) has been changed to FS13 (5mm thick FRP along continuous edge) and FS4 (3mm thick FRP along diagonal) has been changed to FS14 (5mm thick FRP along diagonal). All these models are analysed and the load-deflection plots coming from the analysis are compared as shown in Figure 4.48b, 4.49b, 4.50b for the three different location of FRP respectively.

Effect of change of thickness of FRP along support edge i.e. variation of FS2 and FS12:

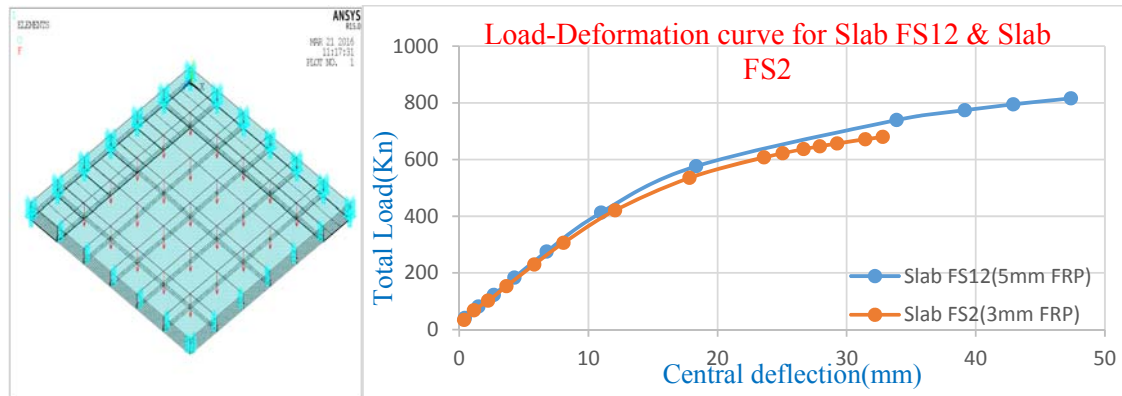


Figure 4.48a: Finite element model of slab FS12

Figure 4.48b: Variation of load deformation behavior of retrofitted fixed supported RC slab due to change in thickness of FRP along support edge

Effect of change of thickness of FRP along continuous edge i.e. variation of FS3 and FS13:

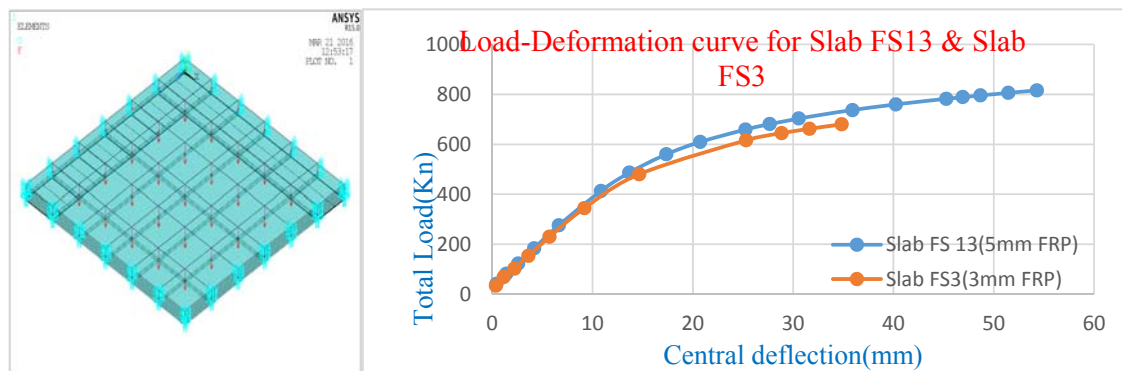
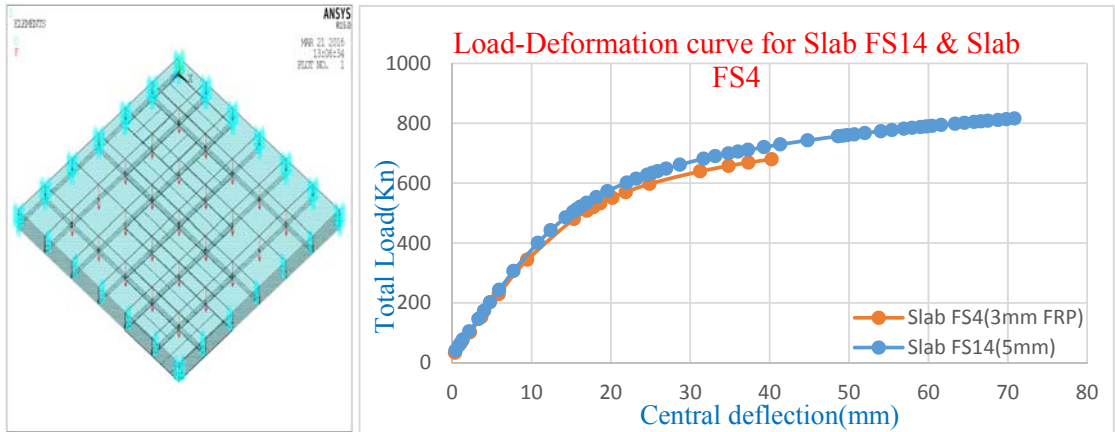


Figure 4.49a: Finite element model of slab FS13

Figure 4.49b: Variation of load deformation behavior of retrofitted fixed supported RC slab due to change in thickness of FRP along continuous edge

Effect of change of thickness of FRP along diagonal i.e. variation of FS4 and FS14:



<p>Figure 4.50a: Finite element model of slab FS14</p>	<p>Figure 4.50b: Variation of load deformation behavior of retrofitted fixed supported RC slab due to change in thickness of FRP along diagonal</p>
--	---

From the comparisons shown in Figure 4.48b, 4.49b and 4.50b, it is observed that due to the increase in the thickness of FRP, the load-deflection curve gets stiffer and gives higher ultimate load compared to that with lower thickness of FRP in all three locations of FRP i.e. along support edge, along continuous edge and along diagonal.

Effect of change of thickness of FRP on the variation of location of FRP:

To investigate further the effect of thickness of FRP on the location of FRP of retrofitted slabs, the load deflection curve of the slabs (having mm thick FRP) FS12 (FRP along support edge), FS13 (FRP along continuous edge), FS14 (FRP along diagonal) are compared in figure 4.51.

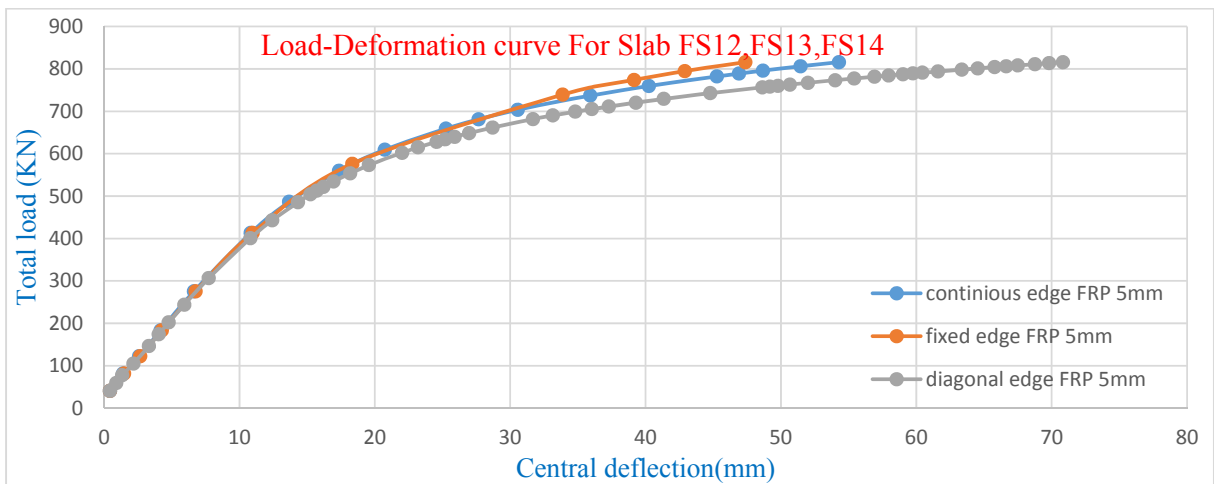


Figure 4.51: Variation of load deformation behavior of retrofitted fixed supported RC slab due to change in thickness of FRP along support edge, continuous edge and diagonal

It is found that the slab (FS12) having the location of FRP along the support edge is showing maximum stiffness and ultimate load. Compared to this, FS13 is showing lesser stiffness and ultimate load as well as FS 14 is showing the least one. It is further to be noted that this observation was not found with the slabs FS2, FS3 and FS4 in figure 4.32. Thus it can be stated that for the fixed slab if the thickness of the FRP is made more than the effect of the variation of the location of the FRP on its behavior become prominent.

4.3.13 Orientation of FRP in fixed slab

In the layers of FRP laminates, the orientation of the fibers is considered in this section as a parameter that may affect the load-displacement response of the slab retrofitted with FRP laminates. Three different sets of orientation of FRP have been considered here: $-45^{\circ}/0^{\circ}/45^{\circ}$, $-60^{\circ}/0^{\circ}/60^{\circ}$ and $-90^{\circ}/0^{\circ}/90^{\circ}$. Initially the slab models FS2 (FRP along support edge), FS3 (FRP along continuous edge) and FS4 (FRP along diagonal) have been prepared by choosing the orientation as $-45^{\circ}/0^{\circ}/45^{\circ}$. Subsequently, these have been modified by changing the orientation of the fibers of FRP. Thus FS15 ($-60^{\circ}/0^{\circ}/60^{\circ}$) and FS16 ($-90^{\circ}/0^{\circ}/90^{\circ}$) have been prepared from FS2 ($-45^{\circ}/0^{\circ}/45^{\circ}$), FS17 ($-60^{\circ}/0^{\circ}/60^{\circ}$) and FS18 ($-90^{\circ}/0^{\circ}/90^{\circ}$) have been prepared from FS3 ($-45^{\circ}/0^{\circ}/45^{\circ}$) and FS19 ($-60^{\circ}/0^{\circ}/60^{\circ}$) and FS20 ($-90^{\circ}/0^{\circ}/90^{\circ}$) have been prepared from FS4 ($-45^{\circ}/0^{\circ}/45^{\circ}$) keeping the other parameters same. All these models are analyzed and the load-deflection curves are plotted in Figure 4.52, 4.53 and 4.54 for comparison.

Effect of change of orientation of FRP provided along the support edge in FS2 ($-45^{\circ}/0^{\circ}/45^{\circ}$), FS15 ($-60^{\circ}/0^{\circ}/60^{\circ}$) and FS16 ($-90^{\circ}/0^{\circ}/90^{\circ}$):

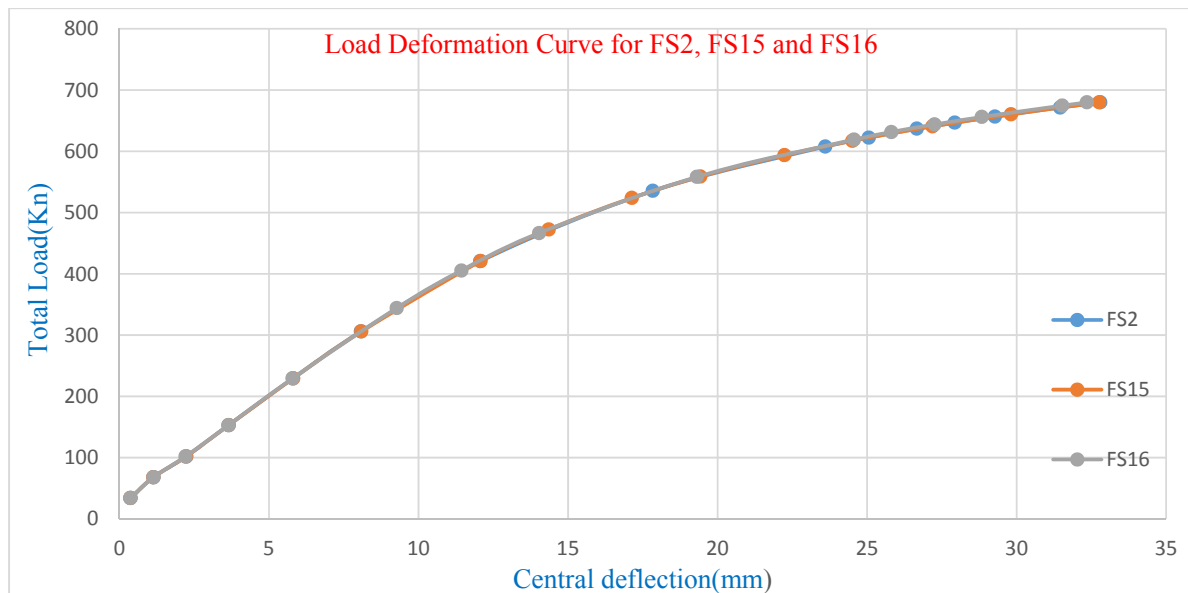


Figure 4.52: Variation of load deformation behavior of retrofitted fixed supported RC slab due to change in the orientation of FRP along support edge

Effect of change of orientation of FRP provided along the continuous edge in FS3 (-45°/0°/45°), FS17 (-60°/0°/60°) and FS18 (-90°/0°/90°):

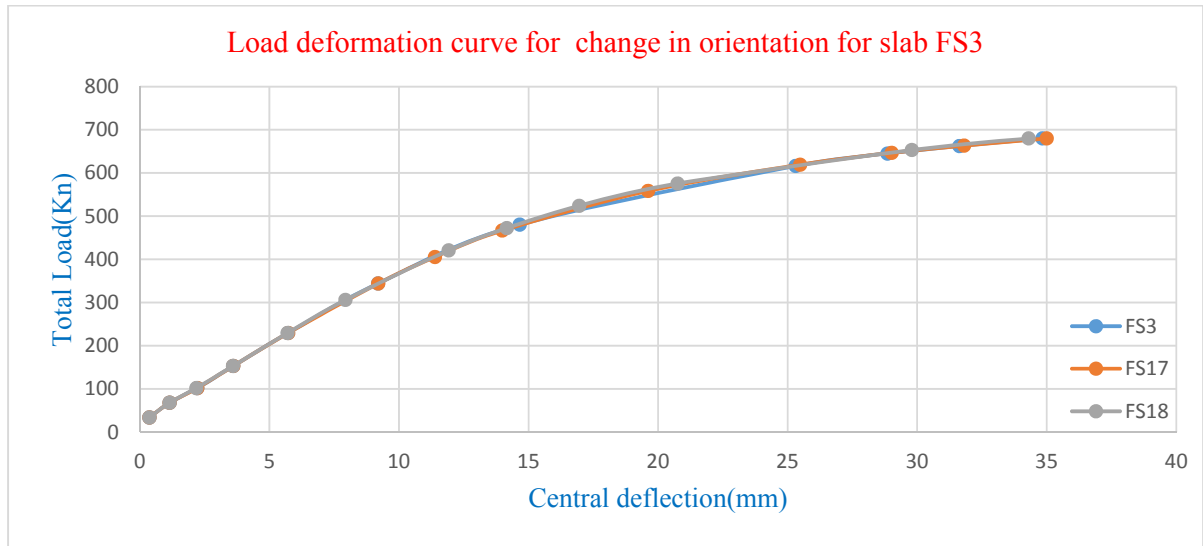


Figure 4.53: Variation of load deformation behavior of retrofitted fixed supported RC slab due to change in the orientation of FRP along continuous edge

Effect of change of orientation of FRP provided along the diagonal in FS4 (-45°/0°/45°), FS19 (-60°/0°/60°) and FS20 (-90°/0°/90°):

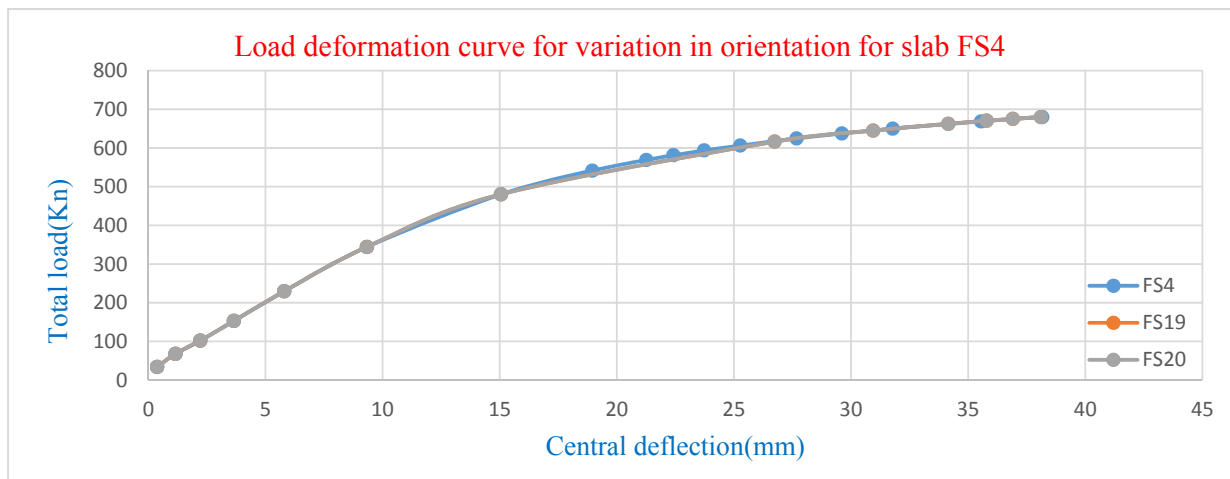


Figure 4.54: Variation of load deformation behavior of retrofitted fixed supported RC slab due to change in the orientation of FRP along diagonal

From the Figure 4.52, 4.53 and 4.54, it is seen that there no considerable difference found in the load deflection curves due to the change in the orientation of FRP for the first two cases i.e. the location of FRP along support edge and continuous edge. But there is slight differences in the curves shown in Figure 4.54 for the location of FRP along diagonal.

CHAPTER 5

CONCLUSIONS

5.1 Introduction

It has been attempted in the present work to study the behavior of reinforced concrete slab strengthened with fibre reinforced polymer (FRP) laminates following the finite element approach using the software ANSYS. Previous research work based on the experimental observation reveals the fact that use of FRP is a very good alternative for strengthening the existing reinforced concrete slab. It has also been reported that the extent of improvement in terms of the load carrying capacity or deformation under service load depends on different parameters. As the experimental study is an expensive and time-consuming approach, the numerical analysis based on finite element technique has been chosen in the present work to assess the extent of these parameters on the load deformation response of the reinforced concrete slab strengthened with FRP laminates. As ANSYS is a commonly used general purpose finite element package, it has been utilized to develop the finite element model and to analyze it in the linear as well as in the nonlinear range.

5.2 Validation

To start with this investigation, the model of an un-retrofitted reinforced concrete slab that was analyzed by previous researchers both analytically as well as experimentally has been prepared using ANSYS keeping all parameters and data same with the previous one. SOLID 65 elements are used to model 3D concrete behaviour and LINK 180 elements are used to model the same of reinforcement bars. It has been analyzed up to its ultimate collapse and the load deflection response has been compared with the same obtained by previous researchers. The present curve matches with the previous one in the elastic range and at the later part till failure. But a deviation found just after initial cracking. This may be due to the fact that the post-cracking behavior of concrete chosen for the present numerical analysis is not matching with the earlier one. But the nature of the load-deflection curve indicates that the current approach of modeling and analyzing the slab is satisfactory and may be used for the analysis of retrofitted reinforced concrete slabs.

5.3 Parametric Study

The main part of the investigation has been started with the modeling and analysis of retrofitted reinforced concrete slabs. It has been assumed that FRP strips are attached at the bottom face of the slab either on the entire area or on a part of that. Accordingly, SOLID 185 elements are attached at the bottom of the concrete SOLID 65 elements in the basic un-retrofitted model. As the behavior and ultimate load differs a lot due to the change in support conditions, two sets of models have been prepared – one for simply supported slabs and the other for fixed slabs. For

both cases, the un-retrofitted slab models (SS1 and FS1) are analyzed first and then the other retrofitted models where FRP strips are attached are developed and analyzed.

Before starting the parametric investigation, a mesh convergence study has been done for each support condition. Based on this study, discretization of the model of 1/4th slab with 6x6 mesh has been selected for further modeling of the retrofitted slabs in the parametric study. The variation with respect to the location of FRP laminate, the width of the FRP strips, thickness of the FRP, number of layers in FRP and orientation of fibers in FRP have been taken in the parametric study for both simply supported slab and fixed slab. Total 54 numbers of slabs have been modeled and analyzed using ANSYS.

5.3.1 Location of FRP

To study the effect of location of FRP strips below the slab on its overall behavior in simply supported as well as fixed end boundary conditions, three different locations of the FRP strips are considered – a) along the support edge (SS2 & FS2), b) along the continuous edge (for one quarter model) (SS3 & FS3) and c) along the diagonal (SS4 & FS4). The thickness of FRP used is 3 mm and the orientation of 3 FRP layers are (-45°, 0°, 45°). It has been observed for both support conditions that the retrofitted slab shows higher stiffness and ultimate load compared to the un-retrofitted control slab irrespective of the location of FRP. But there is a distinct difference between the behavior of simply supported slab and fixed slab. In case of simply supported boundary condition, there is a considerable amount of difference in the stiffness and ultimate load of the slabs SS2, SS3 and SS4 if the location is changed and the diagonal location of FRP giving the highest stiffness and ultimate load become the best alternative. But in the fixed condition, all retrofitted slabs FS2, FS3 and FS4 have shown more or less same stiffness. Primarily it has been understood that the location of FRP in fixed slab may not contribute any effect on the load-deflection pattern. To reinvestigate it, the thickness of FS2, FS3 and FS4 have been increased from 3mm to 5mm. Then the superposition of the results has shown the difference in the stiffness. Unlike simply supported slabs, it is observed in case of fixed slabs that the location of FRP along support edge is showing the highest stiffness and ultimate load. Thus it can be concluded that the location of FRP along diagonal makes the simply supported slab most stiff and strengthened but the location of FRP along support edge makes the fixed slab most stiff and strengthened. Moreover, the effect of the contribution of this location of FRP becomes prominent if the FRP is thicker especially in fixed slab. The comparison of the crack pattern found in these three slabs having FRP along support, continuous edge and diagonal respectively, it has been observed that amount of cracks developed is minimum in the slab where the FRP is provided along the diagonal for both boundary condition.

5.3.2 Area covered by FRP

The variation of the area of the slab covered by FRP has been considered as the second parameter whose effect on the overall performance of the slab has been tried to estimate. For each location of FRP in both simply supported and fixed slab, the width of the FRP strips has been increased to cover more area of the slab. Thus at the location of FRP along support edge and continuous edge, the percentage of slab area covered with FRP are 30%, 55%, 75% and 100% and the same in the slab with diagonal FRP are 16.67%, 33%, 50%, 66.67% and 100%. The comparison of results have shown, in general, that the stiffness of the slab increases with higher area of FRP thereby giving smaller deflection at the ultimate load irrespective of location of FRP and boundary conditions. But some exceptions are also observed ex. the variation of the stiffness due to the increment in the area of FRP laminates in fixed slab are not very significant like simply supported slab. Also the failure load increases with higher FRP area. The percentage of the area of FRP at which the change of ultimate load is huge is found different in these 6 slabs.

It can easily be observed from the above mentioned results that to achieve maximum benefit, 100% of the slab area should be covered with FRP. But in case of location of FRP along support edge or continuous edge, coverage of 50%-55% area will give satisfactory improvement for both simply supported and fixed slabs. But for the location of FRP along diagonal, the requirement of coverage with FRP is found to be 75% in case of simply supported slab and 66.67% for fixed slab.

5.3.3 Number of layers in FRP

The number of layers considered in the FRP model has also been considered as a parameter in this study. It has been varied as 2 layers, 3 layers and 5 layers keeping all other parameter including the thickness of FRP same for both simply supported and fixed slab. The comparison of results has revealed the fact that for both the boundary conditions, there is no considerable effect of these changes of number of layers of FRP on the overall load-deflection response in case of FRP along support edge and continuous edge, but some nominal variation has been observed in the curves for the FRP layers at diagonal position. It has also shown that the slabs, in general, gets more stiffer near failure with the increase in the layers of FRP laminates.

5.3.4 Thickness of FRP

The attempt has also been made to explore the extent of the effect of change of thickness of FRP on the overall response of the strengthened slab. The thickness of FRP in all locations and for both boundary conditions has been varied as 3mm and 5mm. It is observed that due to the increase in the thickness of FRP, the load-deflection curve gets stiffer and gives higher ultimate load compared to that with lower thickness of FRP in all three locations of FRP i.e. along support edge, along continuous edge and along diagonal and also for both simply supported

and fixed boundary conditions. But the change of stiffness is considerably high in case of the location of FRP along continuous edge and diagonal. It is comparatively less in the case of FRP along support edge in simply supported slabs.

5.3.5 Orientation of the fibers in FRP

In the layers of FRP laminates, the orientation of the fibers has also been varied as $-45^{\circ}/0^{\circ}/45^{\circ}$, $-60^{\circ}/0^{\circ}/60^{\circ}$ and $-90^{\circ}/0^{\circ}/90^{\circ}$ in the models of slab with 3 layers in it keeping the other parameters same. All these simply supported and fixed models are analyzed and the load-deflection curves are plotted for comparison. It is seen that there no considerable difference found in the load deflection curves due to the change in the orientation of FRP for the first two cases i.e. the location of FRP along support edge and continuous edge. But there is slight difference in the curves for the location of FRP along diagonal.

5.4 Final Remarks

In fine, it can be stated that the strengthening of reinforced concrete slab using FRP laminates is a very useful and advantageous approach. As the extent of benefit or net gain in terms of ultimate strength and deformation at service load depends on many parameters, careful observation is required to select different parameters related to the material, location, strengthening process etc. Out of three locations, the location of FRP along the diagonals of the slab gives comparatively better outcome for simply supported slab and the location of FRP along the support edge of the slab gives comparatively better outcome for the fixed slab in different respect. To get considerable difference due to the change in the parameters, the thickness of FRP is a very vital and sensitive parameter. For fixed slab the effect becomes more prominent if the FRP is thicker.

5.5 Future scope of study

The parameters considered in the present study are not exhaustive. Other parameters like different materials of FRP i.e. carbon, glass etc., the constitutive relations of the FRP materials, different solution control parameters, different mode of failures, the thermal effects etc. can be considered for the detailed investigation on the nonlinear behavior of reinforced concrete slab strengthened with FRP laminates.

REFERENCES

1. Tavarez, F.A., “**Simulation of Behavior of Composite Grid Reinforced Concrete Beams Using Explicit Finite Element Methods**,” Master’s Thesis, University of Wisconsin-Madison, Madison, Wisconsin, 2001
2. Habibulla Sheikh, “**A Finite Element Approach for the study on the behavior of RC Beam Column joint strengthened with FRP laminates**”, Master’s Thesis, Jadavpur University, Kolkata, India 2015
3. Chothani, D.G., Arora, N.K., and Dave, S.P. "**Effect of anchoring GFRP sheet on ultimate strength of slab.**" Fourth International Conference on Structural Stability and Dynamics (ICSSD 2012), 4–6 January, 2012
4. Mrinmoy Baidya, “**Numerical study on the behavior of reinforced concrete beam strengthened with FRP**”, Master’s Thesis, Jadavpur University, Kolkata, India 2015
5. Corum, J.M., Battiste, R.L., Liu, K.C. and Ruggles, M.B., **Basic Properties of Reference Crossply Carbon-Fiber Composite**, Oak Ridge National Laboratory, Tennessee 3783 1-6285, February 2000.
6. A. Mehta, (2011), “**Effect of initial stress levels on strength of beams retrofitted using pre-stressed fibre composites**” M.E. Thesis, Thapar University, Patiala.
7. A.K. Tiwary, and M.Mohan, “**A review paper on strengthening of beam column joint upgraded with CFRP sheets**”, IOSR Journal of Mechanical and Civil Engineering (IOSR-JMCE), PP 20-26
8. S. Roychowdhury, “**Behavioural study of thick reinforced concrete slab subjected to thermal gradient using layered finite element**”, Phd. Thesis, Jadavpur University, Kolkata, India 2007
9. U. Ebead, H. Marzouk, and L. M. Lye, “**Strengthening of two-way Slabs using FRP materials: a simplified analysis based on response surface methodology**” 2nd World Engineering Congress, Sarawak, Malaysia, 22-25 July 2002
10. Mosallam S. Ayman, Mosalam M. Khalid. “**Strengthening of two-way concrete slabs with FRP composite laminates**”, Construction and Building Materials 17, 43–54, 2003

11. Usama Ebead, Hesham Marzouk, “**ACI code verification for FRP externally reinforced slab**”, ACI-440F. 2002
12. J. Yao, J.G. Teng, J.F. Chen, “**Experimental study on FRP-to-concrete bonded joints**”, Composites: Part B 36, 99–113, 2005
13. S.T. Smith, R.J. Gravina, “**Critical debonding length in FRP flexurally strengthened RC member**”, International Institute for FRP in Construction, 2005
14. Khalil Belakhdar , “**Nonlinear Finite Element Analysis of reinforced concrete slab strengthened with shear bolts**”, Jordan Journal of Civil Engineering, Volume 2, No. 1, 2008
15. Kwak, H.G., Fillipou, C.F. “**Finite Element Analysis of Reinforced Concrete Structures Under Monotonic Loading**” Structural Engineering Mechanics and Materials, (1990) Report no. UCB/ SEMM-90/14.
16. K.W. Neale, “**Assesment of numerical models for FRP-strengthened concrete structure**”, International Institute for FRP in Construction, 2007
17. Ravikant Shrivastava, Uttamasha Gupta, U B Choubey , “**FRP: Research, education and application in India and China in Civil Engineering**”, Int. J. of Recent Trends in Engineering and Technology, Vol. 1, No. 6, Nov 2009
18. A. Napoli, F. Matta, E. Martinelli, A. Nanni and R. Realfonzo, “**Modelling and verification of response of RC slabs strengthened in flexure with mechanically fastened FRP laminates**”, Magazine of Concrete Research, 62, No. 8, 593–605, August 2010
19. Kenneth W. Neale, Ahmed Godat, Hussien M. Abdel Baky, Walid E. Elsayed and Usama A. Ebead , “**Approaches for Finite Element simulation of FRP-strengthened concrete beam and slabs**” Architecture Civil Engineering Environment , No. 4/2011
20. Lakshmikandhan K. N, Sivakumar P, Ravichandran R, “**Damage assessment and strengthening of reinforced concrete beams**”, International Journal of Material and Mechanical Engineering (IJMME) Volume 2 Issue 2, May 2013
21. Mustafa Basheer Mahmood, V. C. Agarwal, “**Non-Linear Finite Element Analysis of RC slabs strengthened with CFRP laminates**”, International Journal of Engineering Trends and Technology (IJETT) – volume 5 number 3- Nov 2013

22. M.B.S Alferjani, A.A. Abdul Samad, Blkasem. S Elrawaff , N. Mohamad, M.Hilton and Abdalla Ab Sinusi Saiah , **“Use of Carbon Fiber Reinforced Polymer Laminate for strengthening reinforced concrete beams in shear: A review”**, International Refereed Journal of Engineering and Science (IRJES), Volume 2, Issue 2, PP.45-53 February 2013
23. K.J. Willam, and E.P.Warneke, **“Constitutive Model for Triaxial Behaviour of Concrete.”**Seminar on Concrete Structures Subjected to Triaxial Stresses, International Association of Bridge and Structural Engineering Conference, Bergamo, Italy, p.174, 1974.
24. Mahmood M. Idrees and Yousif Ramadhan Ali , **“Strengthening by CFRP strips of two-way reinforced concrete slabs supported on bearing walls”**, Zanco Journal of Pure and Applied Sciences Vol.26, No.1, 2014
25. Fahmy A. Fathelbab, Mostafa S. Ramadan, Ayman Al-Tantawy, **“Strengthening of RC bridge slabs using CFRP sheets”**, Alexandria Engineering Journal (2014) 53, 843–854, Received 7 October 2013; revised 30 August 2014; accepted 16 September 2014 Available online 18 October 2014
26. Sheetal Gawas, Dr. S.V.Itti, **“Study on two way RC slab using ANSYS with and without central opening”**, International Journal of Scientific Engineering and Technology (ISSN: 2277-1581) Volume No.3 Issue No.8, pp : 1108-1110 1 Aug 2014
27. **ANSYS User’s Manual**, Release 15.0. (2015)
28. **IS 456: 2000 (Fourth Revision)**, “Indian Standard: Plain and Reinforced Concrete- Code of Practice”, Bureau of Indian Standards, New Delhi, July 2000.
29. Owen, D.R.J., J.A.Figueiras, and Damjanic, F., **“Finite element analysis of reinforced and prestressed concrete structure including thermal loading”**, Computer Methods in Applied Mechanics and Engineering, v.41, pp.323-366, 1983
30. Taylor, R., Maher, D.R.H. and Hayes, B., **“Effect of arrangement of reinforcement on the behavior of reinforced concrete slab”**, Magazine of concrete research, 18(55), 1966